INTERNATIONAL ATOMIC ENERGY AGENCY
UNITED NATIONS EDUCATIONAL, SCIENTIFIC AND CULTURAL ORGANIZATION
INTERNATIONAL CENTRE FOR THEORETICAL PHYSICS
I.C.T.P., P.O. BOX 586, 34100 TRIESTE, ITALY, CABLE: CENTRATOM TRIESTE

ICFA INTERNATIONAL COMMITTEE FOR FUTURE ACCELERATORS

ISTITUTO NAZIONALE DI FISICA NUCLEARE INFN

H4.SMR. 394/12

SECOND ICFA SCHOOL ON INSTRUMENTATION IN ELEMENTARY PARTICLE PHYSICS

12 - 23 JUNE 1989

Fundamental and Experimental Aspects of Calorimetry

P. JENNI

CERN, EP Division, Geneva, Switzerland

FUNDAMENTAL AND EXPERIMENTAL ASPECTS OF CALORIMETRY

I Role of calorimetry in modern collider experiments

II How does a calorimeter work ?

III Examples of signal detection

IV Purely electromagnetic showers and calorimeters

V Hadron showers and calorimeters

VI Calibration issues

VII Jet calorimetry and missing transverse energy measurements

VIII Calorimeters in present and future collider detectors

P. Jenni CERN EP, Lectures at the 2nd ICFA School on Instrumentation in Elementary Particle Physics, ICTP Trieste, June 12-23, 1989.

REFERENCES TO REVIEWS AND LECTURES

USED AS BASIS MATERIAL :

- U. Amaldi, Fluctuations in Calorimetry Measurements; Phys. Scripta 23 (1981) 409.

- C.W. Fabjan and T. Ludlam, Calorimetry in High-Energy Physics; Ann. Rev. Nucl. Part. Sci. 32 (1982) 335.

- R. Wigmans, Energy Loss of Particles in Dense Matter, Calorimetry; Proc. ICFA School on Instrumentation in Elementary Particle Physics, Trieste 1987, p. 41.

- K. Kleinknecht, Detectors for Particle Radiation; Cambridge University Press.

- C.W. Fabjan and R. Wigmans Energy Measurement of Elementary Particles CERN - EP/89-64

I ROLE OF CALORIMETRY IN MODERN COLLIDER EXPERIMENTS

The calorimetry plays a major role in :

. measurements of electrons (example $Z \rightarrow e^+e^-$)

. measurements of jets, the final state particle bundles from quarks or gluons, containing both charged and neutral particles (example $W/Z \rightarrow q\bar{q} \rightarrow$ jet + jet)

. measurements of neutrinos or other non-interacting particles causing an apparent transverse energy imbalance (example $W \rightarrow e\nu$)

. electron - hadron separation

. fast trigger for interesting events

Calorimetric measurements of electrons (positrons, photons) exploit

. characteristic differences between electromagnetic and hadronic showers

. good, and improving resolution for high energy electrons ($\sigma E/E \propto k/\sqrt{E}$) compared to magnetic spectrometers ($\sigma p/p \propto kp$)

electrons measured with a calorimeter

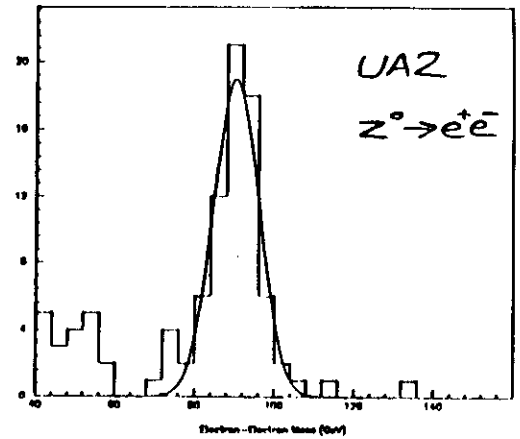

muons measured with a spectro-meter

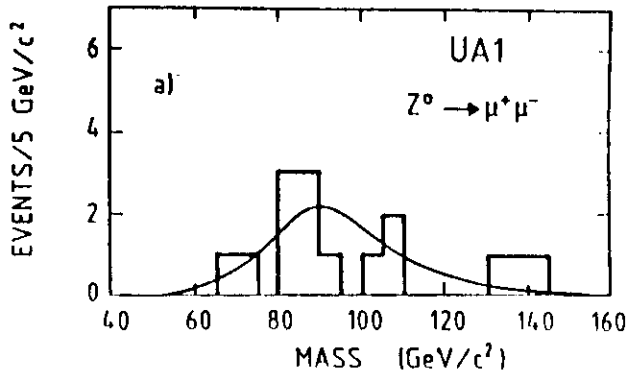

"LEGO" plot

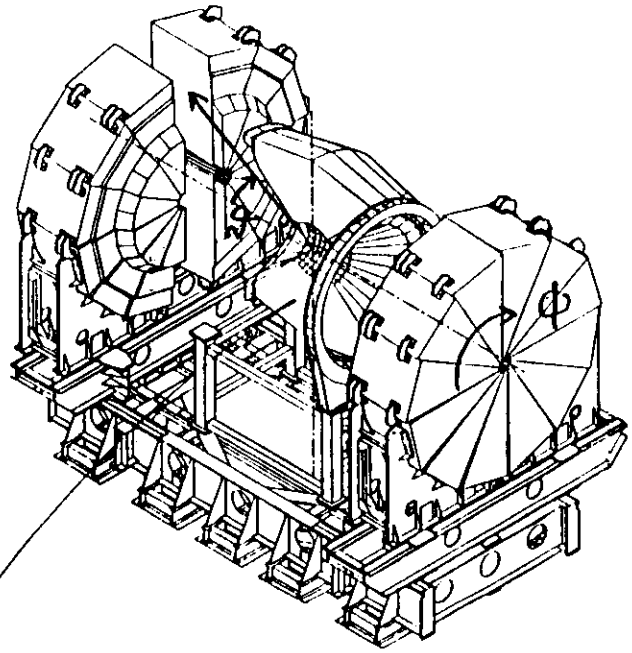

unfold calorimeter cell map

tower height ∝ transverse energy in the cell

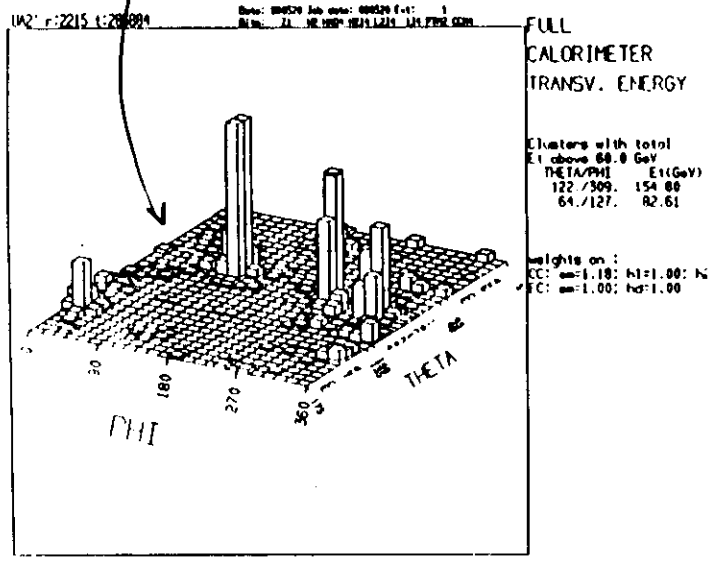

Candidate for a $Z \to ee$

transverse energy map for all UA2 calorimeter cells

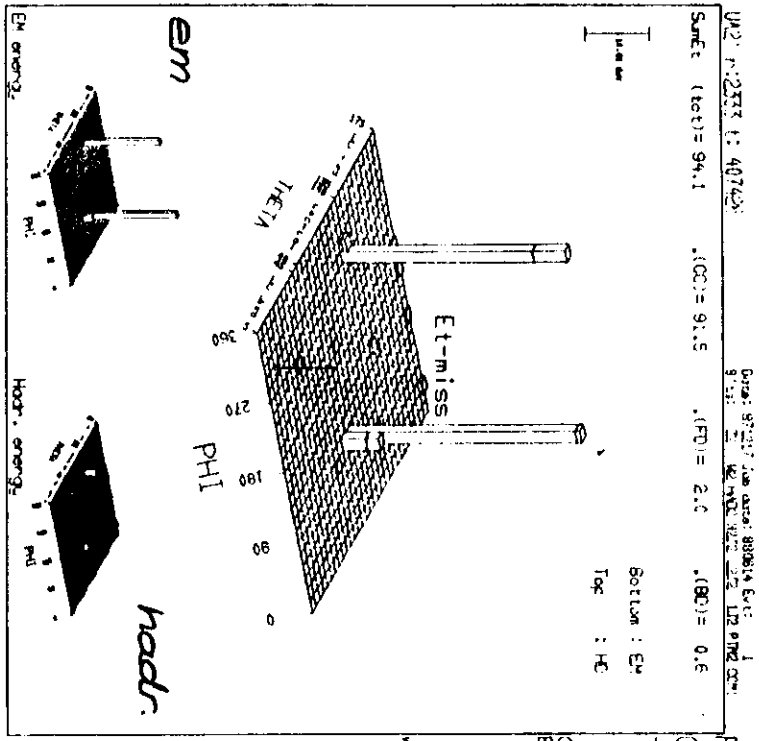

Measurements of jets

study interactions between quarks and gluons

example $qg \rightarrow qg$

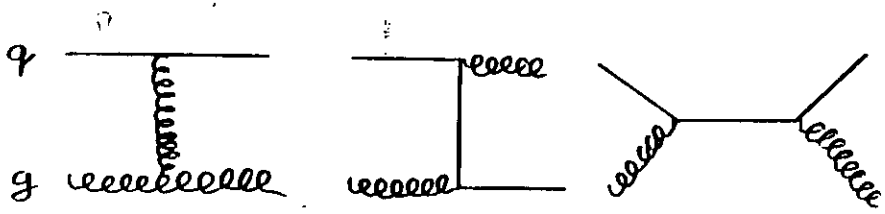

or the decays of new particles into quarks (or gluons)

example IVB (W, Z) $\rightarrow q\bar{q}$

- the 4-vectors of the q, g cannot be measured directly (confinement)
- q, g fragment (hadronize) into jets of final state particles ($\pi^{\pm}$, π^{0}, K, D ... p, n ...)
- a hadron calorimeter is needed to measure the jets

a high p_T 2-jet event

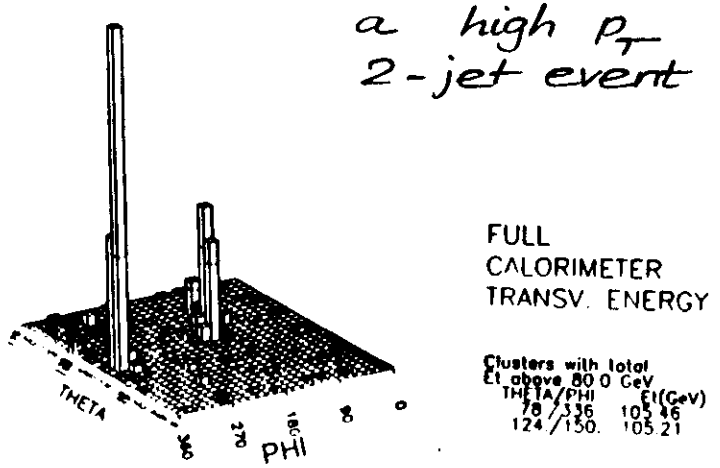

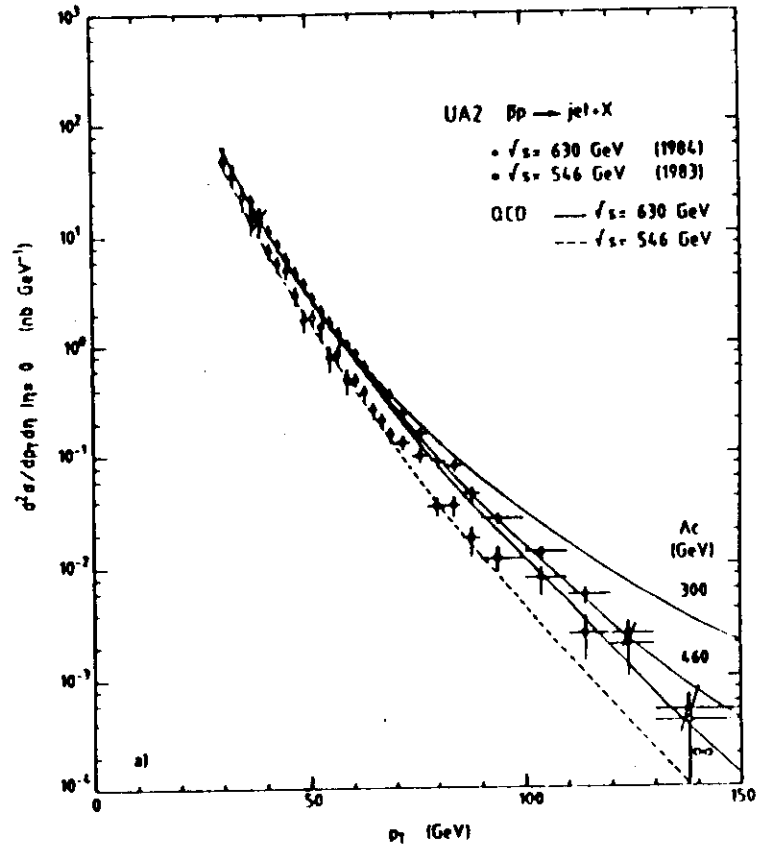

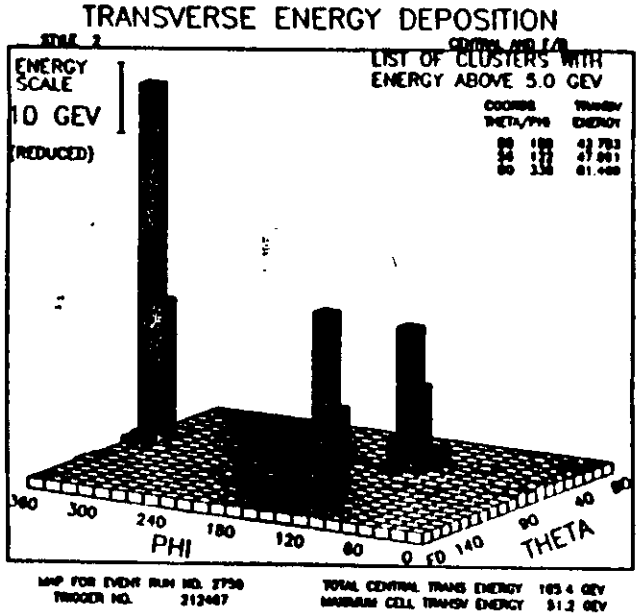

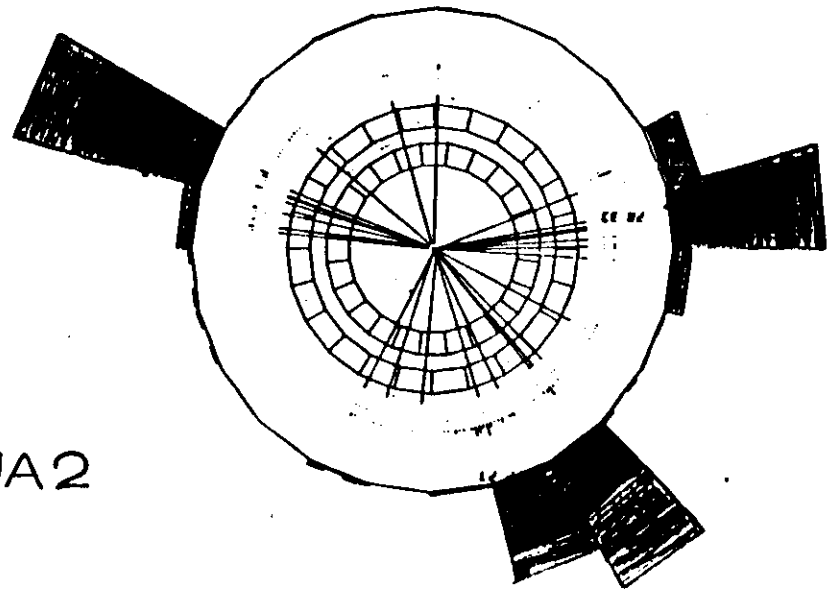

UA2

Jet spectroscopy

$W, Z \rightarrow q\bar{q} \rightarrow$ jet + jet

A good mass resolution is needed to find a signal

⇒ requires best possible energy resolution for hadrons (jets)

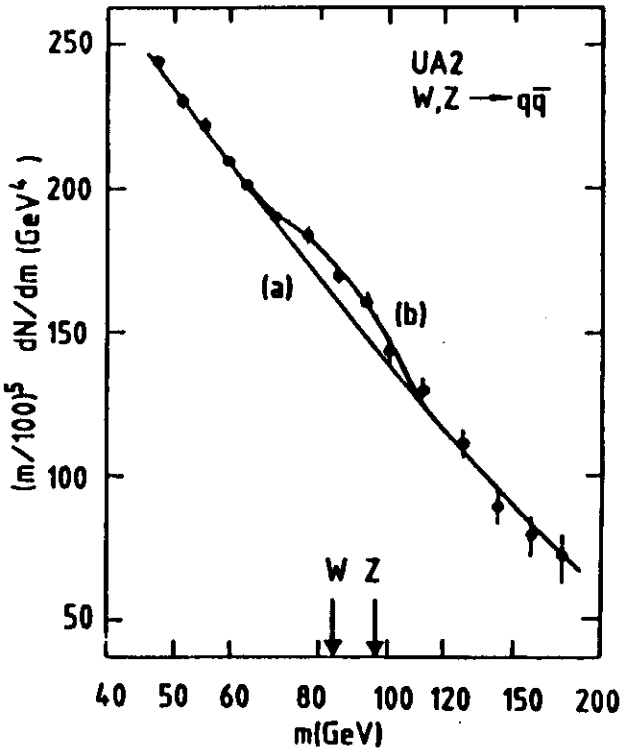

$m_{jet-jet}$

Measurement of neutrinos or other particles leaving the detector without interactions

Indirect detection by calorimetric measurement of all the other particles from the reaction.

The appartent (transverse) energy imbalance is used as signature.

Examples

- $\bar{p}p \rightarrow W + X$
  $\qquad \rightarrow e\nu$

  the missing transverse energy corresponds to E_T^{ν}

- signature for SUSY
  $\bar{p}p \rightarrow \tilde{g}\tilde{q} + X$
  $\tilde{q} \rightarrow q\tilde{\gamma}$
  $\tilde{g} \rightarrow q\bar{q}\tilde{\gamma}$

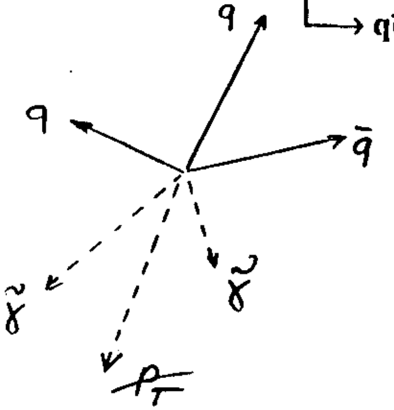

the missing transverse energy corresponds to the two photinos

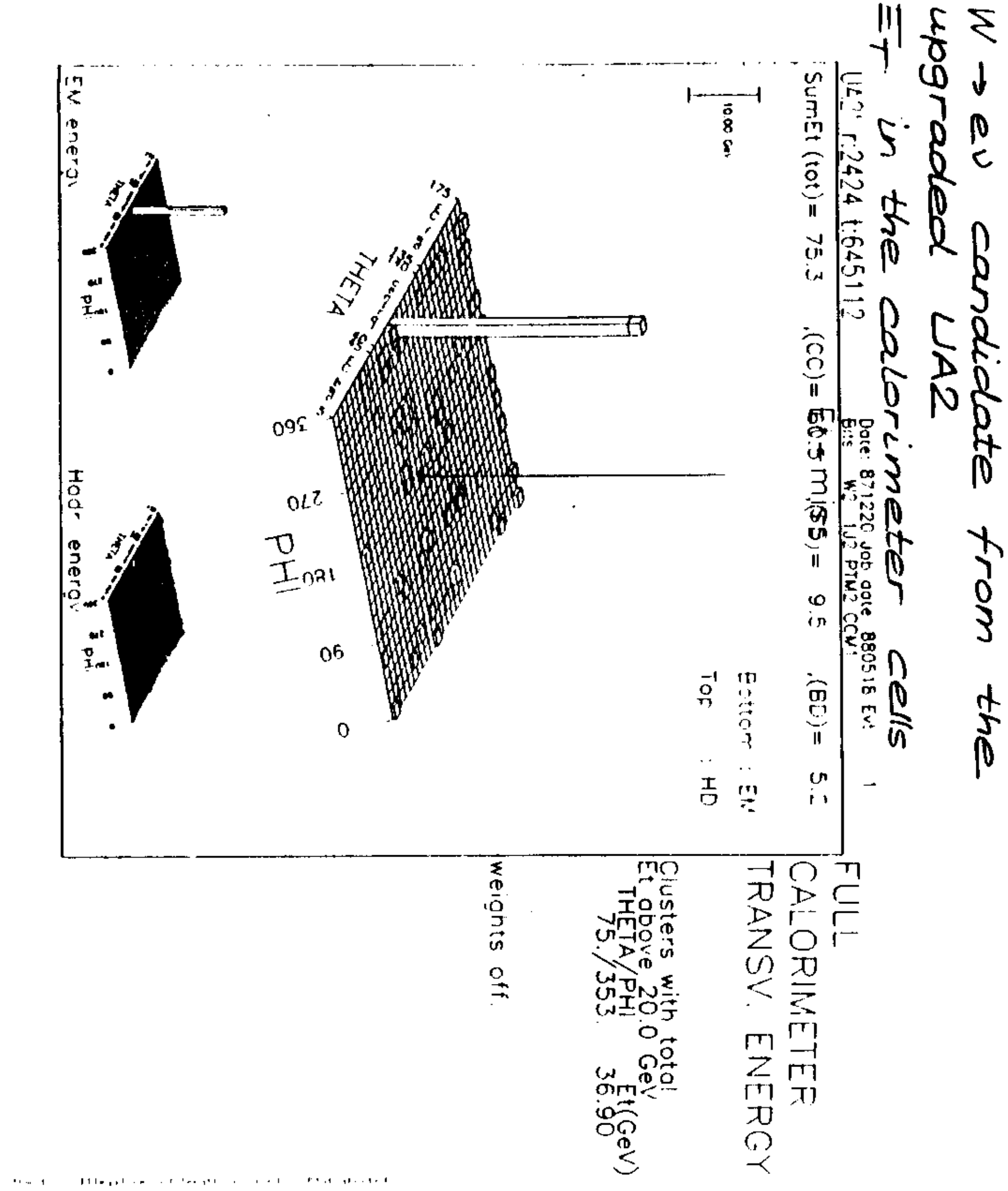

Neutrino Jacobian peak for

$\bar{p}p \rightarrow W + X$ events.

$\hookrightarrow e\nu$

The E_T^ν is inferred from all other particles measured in the calorimeter.

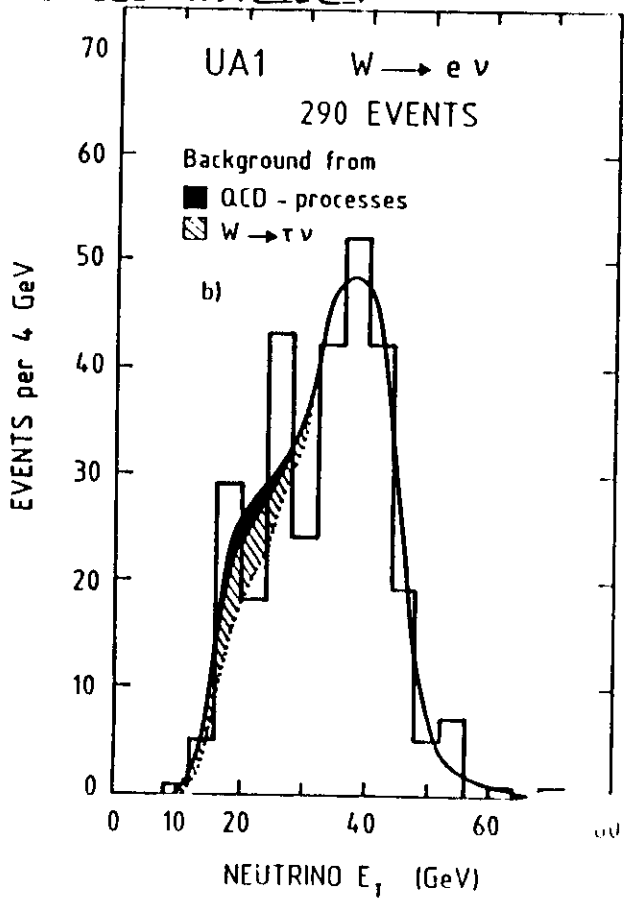

Electron - hadron separation

This is a very important aspect of calorimetry particularly at hadron colliders.

Leptons (electrons, muons, eventually also taus) are used to select interesting physics processes out of very large backgrounds of ordinary hadronic events.

Very topical examples are the present searches for the t quark at the CERN and FNAL $\bar{p}p$ Colliders.

very large jet background

but about 10 % of t are expected to decay

$t \rightarrow e\nu b$

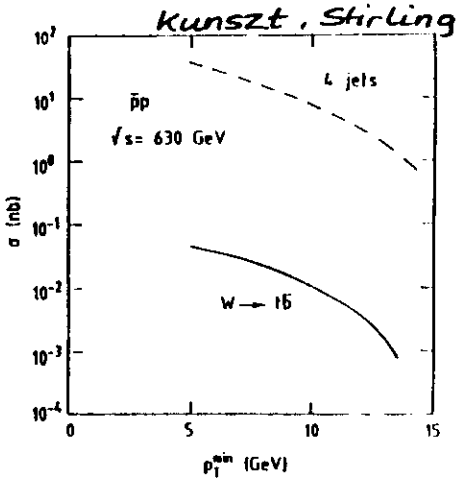

jet threshold

Fast trigger for interesting events

At hadron colliders the interesting event rates are typically 10^{-8} (or even smaller) of all collisions.

example $\bar{p}p \rightarrow W + X$
$\hookrightarrow e\nu$

at $\sqrt{s} = 630$ GeV $\quad \sigma \sim 0.6$ nb
compared to 60 mb for σ_{tot}.

Calorimeters offer fast and localized measurements of energy depositions. It is possible to make very fast (order 100 ns) decisions on potentially interesting event topologies (electrons, clustered hadronic energy for jets, missing transverse energy ...)

II HOW DOES A CALORIMETER WORK ?

Calorimeters are blocks of matter in which the primary particle interacts and deposits all its energy in a cascade (shower) of increasingly lower energy particles.

A fraction of the initial energy goes into a measurable signal (for example scintillation light or ionization charge) which is (more or less...) proportional to the initial energy.

Fluctuations in the shower process and in the measured signal determine the energy resolution.

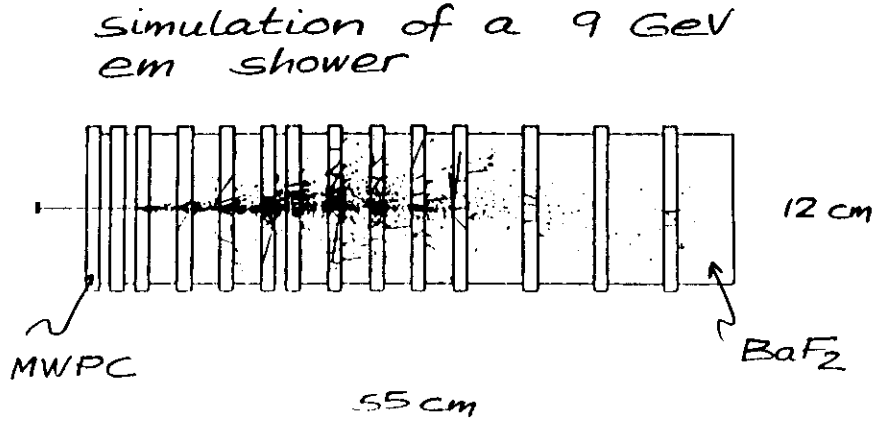

- basic processes of energy loss of particles in matter
- shower development
- a first comparison between electromagnetic and hadronic showers
- total absorption vs. sampling calorimeters.

The basic processes of energy loss of particles in matter :

neutral particles

γ electromagnetic interactions
- e^+e^- pair creation
- Compton effect
- photoelectric effect

n strong interaction with nuclei

ν only weak interaction
→ escapes most of the time
normal detectors

charged particles

$e^\pm$ electromagnetic interactions
- bremsstrahlung
- ionization of atoms
- Cherenkov radiation
- transition radiation

hadrons$^\pm$ as above plus

- strong interactions with nuclei

Passage of γ through matter

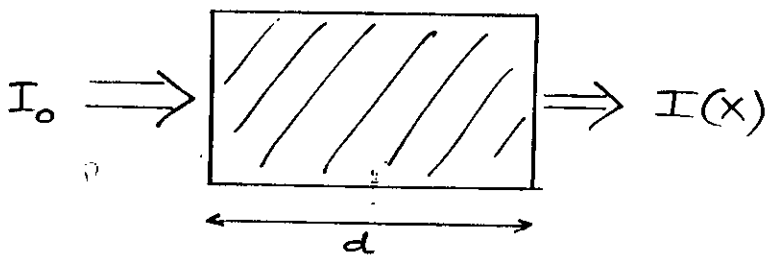

$I(X) = I_o\, e^{-\mu d} = I_o\, e^{-(\mu/\rho)X}$

- d thickness [cm]
- X mass thickness $X = \rho d$
- μ linear absorption coefficient
- μ/ρ mass absorption coefficient
- ρ density

μ is related to the photon absorption cross-section σ

- $\mu = \sigma N_o \rho / A$
- N_o Avogadro's constant
- A mass of a mole of the material

example Pb

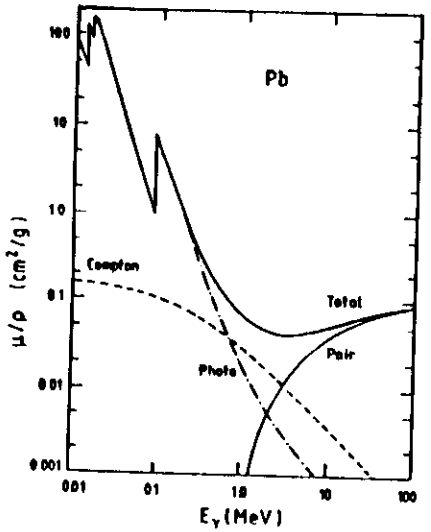

Cross-section approximations as a function of the reduced photon energy $\varepsilon = E\gamma/m_e$:

- **Photoelectric effect**

  γ + atom → ion + e^-

  $\varepsilon > 1$: $\sigma_{pe} = 4\,\pi\, r_e^2\, Z^5\, \alpha^4 / \varepsilon$

  $r_e = 2.8$ fm classical electron radius

  $\varepsilon < 1$: depends on L-, K- ... shells

. Compton effect

$$\gamma + e^- \rightarrow \gamma + e^-$$

at very low $E\gamma$

$$\sigma Th = \frac{8\pi}{3} r_e^2 = 0.67 \text{ barn}$$

(classical Thomson formula)

at high $E\gamma$

Klein-Nishina cross-section
(see text books)

for $\varepsilon >> 1$:

$$\sigma_c = \frac{3}{8} \sigma Th \frac{1}{\varepsilon} \left(\frac{1}{2} + \ln 2\varepsilon \right)$$

. Pair production

$$\gamma + \text{nucleus} \rightarrow e^+e^- + \text{nucleus}$$

$1 < \varepsilon < \frac{137}{Z^{1/3}}$:

$$\sigma_p = 4\alpha r_e^2 Z^2 \left(\frac{7}{9} \ln 2\varepsilon - \frac{109}{54} \right)$$

$\varepsilon > \frac{137}{Z^{1/3}}$:

$$\sigma_p = 4\sigma r_e^2 Z^2 \left[\frac{7}{9} \ln \left(\frac{183}{Z^{1/3}} \right) - \frac{1}{54} \right]$$

at high $E\gamma$ one has

$$\mu_p = 4\alpha r_e^2 Z^2 \frac{N_o}{A} \frac{7}{9} \ln \frac{183}{Z^{1/3}} = \frac{7}{9} \frac{1}{X_o}$$

where X_o is the so-called radiation length

(pair creation happens at high $E\gamma$ with a probability $P = 1 - e^{-7/9} \approx 54$ % within one X_o)

PARTICLE DETECTORS, ABSORBERS, AND RANGES (Cont'd)

Atomic and Nuclear Properties of Materials*

Material	Z	A	Nuclear[a] total cross section σ_T [barn]	Nuclear[b] inelastic cross section σ_I [barn]	Nuclear[c] collision length λ_T [g/cm²]	Nuclear[c] interaction length λ_I [g/cm²]	dE/dx min[d] $\overline{\Delta E}$ [MeV/g/cm²]	dE/dx min[d] E_{mp} t cm [MeV] () is for gas [keV]	Radiation length[e] L_{rad} [g/cm²]	Radiation length[e] L_{rad} [cm] () is for gas	Density[f] [g/cm³] () is for gas [g/ℓ]	Refractive index n[f] () is (n − 1)×10⁶ for gas
H_2	1	1.01	0.0387	0.0155	43.3	50.8	4.12	(0.19)	61.28	865	0.0708(0.090)	1.112(140)
D_2	1	2.01	0.073	0.061	45.7	53.7	2.07	(0.17)	122.6	757	0.167(0.177)	1.128
He	2	4.00	0.133	0.102	49.9	65.1	1.94	(0.16)	94.32	755	0.125(0.178)	1.024(35)
Li	3	6.940	0.211	0.157	54.6	73.4	3.58	0.70	82.76	155	0.534	—
Be	4	9.01	0.268	0.199	55.8	75.2	1.61	2.61	65.19	35.3	1.848	—
C	6	12.01	0.331	0.231	60.3	86.3	1.78	3.57	42.70	18.8	2.265[g]	—
N_2	7	14.01	0.379	0.265	61.4	87.8	1.82	(0.93)	37.99	44.5	0.808(1.25)	1.205(300)
O_2	8	16.00	0.420	0.292	63.2	91.0	1.82	(1.31)	34.24	28.7	1.14(1.43)	1.22(266)
Ne	10	20.18	0.507	0.347	66.1	94.6	1.73	(0.75)	28.94	24.0	1.207(0.90)	1.092(67)
Al	13	26.98	0.634	0.421	70.6	106.4	1.62	3.81	24.01	8.9	2.70	—
Si	14	28.09	0.660	0.440	70.6	106.0	1.66	3.36	21.82	9.36	2.33	—
Ar	18	39.95	0.868	0.566	76.4	117.2	1.51	(1.30)	19.55	14.0	1.40(1.78)	1.233(281)
Fe	26	55.85	1.120	0.703	82.8	131.9	1.48	10.7	13.84	1.76	7.87	—
Cu	29	63.54	1.232	0.782	85.6	134.9	1.44	11.85	12.86	1.43	8.96	—
Sn	50	118.69	1.967	1.21	100.2	163	1.26	8.3	8.82	1.21	7.31	—
Xe	54	131.30	2.120	1.29	102.8	169	1.24	(3.57)	8.48	2.77	3.057(5.89)	(705)
W	74	183.85	2.767	1.69	110.3	185	1.16	21.1	6.76	0.35	19.3	—
Pb	82	207.19	2.960	1.77	116.2	194	1.13	11.7	6.37	0.56	11.35	—
U	92	238.03	3.378	1.98	117.0	199	1.09	19.3	6.00	≈0.32	≈18.95	—
Air, 20°C, 1 atm (STP in parens.)					62.0	90.0	1.82	(1.12)	36.66	(30420)	0.001205(1.29)	1.000273(293)
H_2O					60.1	84.9	2.03	1.72	36.08	36.1	1.00	1.33
Shielding concrete[h]					67.4	99.9	1.70	3.68	26.7	10.7	2.5	—
SiO_2 (quartz)					67.0	99.2	1.72	3.28	27.05	12.3	2.2	1.458
H_2 (bubble chamber 26°K)					43.3	50.8	4.12	0.20	61.28	≈1000	≈0.063[i]	1.100
D_2 (bubble chamber 31°K)					45.7	53.7	2.07	0.22	122.6	≈900	≈0.140[i]	1.110
H-Ne mixture (50 mole percent)[j]					63.0	94.9	1.84	0.59	29.70	73.0	0.607	1.092
Ilford emulsion G5					82.0	134	1.44	4.79	11.0	2.89	3.819	—
NaI					94.8	152	1.32	4.13	9.49	2.59	3.67	1.775
BeF_2					92.1	146	1.35	3.78	9.91	2.05	4.01	1.56
BGO ($Bi_4Ge_3O_{12}$)					97.4	156	1.27	8.07	7.98	1.12	7.1	2.15
Polystyrene, scintillator (CH)[k]					58.4	82.0	1.93	1.72	43.8	42.4	1.032	1.581
Lucite, Plexiglas ($C_5H_8O_2$)					59.2	83.6	1.95	1.98	40.55	≈34.4	1.16-1.20	≈1.49
Polyethylene (CH_2)					56.9	78.8	2.09	1.68	44.8	≈47.9	0.92-0.95	—
Mylar ($C_5H_8O_2$)					60.2	85.7	1.86	2.24	39.95	28.7	1.39	—
Borosilicate glass (Pyrex)[l]					66.3	97.6	1.72	3.32	28.3	12.7	2.23	1.474
CO_2					62.6	90.5	1.82	(1.92)	36.2	(18310)	(1.977)	(410)
Methane CH_4					54.7	74.0	2.41	(0.91)	46.5	(64890)	0.423(0.717)	(444)
Isobutane C_4H_{10}					56.3	77.4	2.22	(3.43)	45.2	(16930)	(2.67)	(1270)
Freon 12 (CCl_2F_2) gas, 26°C, 1 atm.[m]					70.6	106	1.62	4.49	23.7	4810	4.95	1.001080
Silica Aerogel[n]					65.5	95.7	1.83	0.28	29.85	≈150	0.1-0.3	1.0+0.25ρ
G10 plate[o]					62.6	90.2	1.87	2.7	33.0	19.4	1.7	—

* Table revised April 1984 by Joachim Engler. For details, see Report KfK 3346B, Kernforschungszentrum, D 7500 Karlsruhe, P.O. Box 3640, FRG.

a. σ_{total} at 60-240 GeV for neutrons (≈ σ for protons) from Murthy et al., Nucl. Phys. B92, 269 (1975).

b. $\sigma_{inelastic} = \sigma_{total} - \sigma_{elastic} - \sigma_{quasielastic}$; for neutrons at 60-375 GeV from Roberts et al., Nucl. Phys., B159, 56 (1979). For protons and other particles, see Carroll et al., Phys. Lett. 80B, 319 (1979); note that $\sigma_I(p) \approx \sigma_I(n)$.

c. Mean free path between collisions (λ_T) or inelastic interactions (λ_I), calculated from $\lambda = A/(N\times\sigma)$.

d. For minimum ionizing protons and muons. $\overline{\Delta E}$ is energy loss per g/cm² from Barkas and Berger, *Tables of Energy Losses and Ranges of Heavy Charged Particles*, NASA-SP-3013 (1964). For electrons and positrons see: M.J. Berger and S.M. Seltzer, *Stopping Powers and Ranges of Electrons and Positrons* (2nd Ed.), U.S. National Bureau of Standards report NBSIR 82-2550-A (1982). E_{mp} is the most probable deposited energy in one cm, in MeV for solids and liquids, in keV for gases. E_{mp} varies with depth in a nonproportional manner. (See Sec. C.1 preceding.) Parentheses refer to gaseous form at STP (0°C, 1 atm.)

e. From Y.S. Tsai, Rev. Mod. Phys. 46, 815 (1974). Corrections for molecular binding applied for H_2 and D_2. Parentheses refer to gaseous form at STP (0°C, 1 atm.)

f. Values for solids, or the liquid phase at boiling point, except as noted. Values in parentheses for gaseous phase at STP (0°C, 1 atm.). Refractive index given for sodium D line.

g. For pure graphite; industrial graphite density may vary 2.1 - 2.3 g/cm³.

h. Standard shielding blocks, typical composition O_2 52%, Si 32.5%, Ca 6%, Na 1.5%, Fe 2%, Al 4%, plus reinforcing iron bars. The attenuation length, $\ell = 115 \pm 5$ g/cm², is also valid for earth (typical $\rho = 2.15$), from CERN-LRL-RHEL Shielding esp., UCRL-17841 (1968).

i. Density may vary about ± 3%, depending on operating conditions.

j. Values for typical working conditions with H_2 target: 50 mole percent, 29°K, 7 atm.

k. Typical scintillator, e.g., PILOT B and NE 102A have an atomic ratio H/C = 1.10.

l. Main components: 80% SiO_2 + 12% B_2O_3 + 5% Na_2O.

m. Used in Cerenkov counters. Values at 26°C and 1 atm. Indices of refraction from F.R. Hayes, R.A. Schluter, and A. Tamosaitis, ANL-6916 (1964).

n. $n(SiO_2) + 2n(H_2O)$ used in Cerenkov counters, ρ = density in g/cm³. From M. Cantin et al., Nucl. Instr. Meth. 118, 177 (1974).

o. G10 plate, typical 60% SiO_2 and 40% Epoxy.

Photon cross-sections in C, Fe and U as a function of E_γ

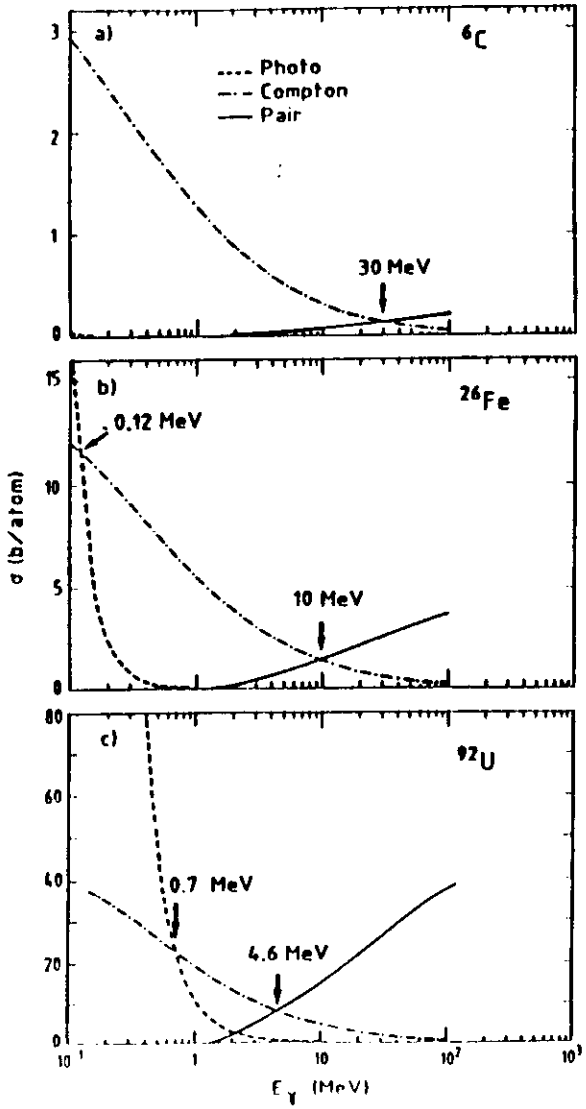

Energy loss of electrons (charged particles) in matter

Bremsstrahlung

radiation of photons in the Coulomb field of a nucleus

energy loss for electrons

$$-\left(\frac{dE}{dx}\right)_{brems} = 4\alpha N_o \frac{Z^2}{A} r_e^2 E \ln \frac{183}{Z^{1/3}}$$

$$= \frac{E}{X_o}$$

Ionization energy loss for fast electrons ($\beta \sim 1$)

$$-\left(\frac{dE}{dx}\right)_{ion} = 4\pi N_o \frac{Z}{A} r_e^2 m_e \left[\ln \frac{2mv^2\gamma^2}{I} - 1\right]$$

(see text books for more complete formulae and the famous Bethe-Bloch formula)

typical $\frac{dE}{dx}$ behaviour

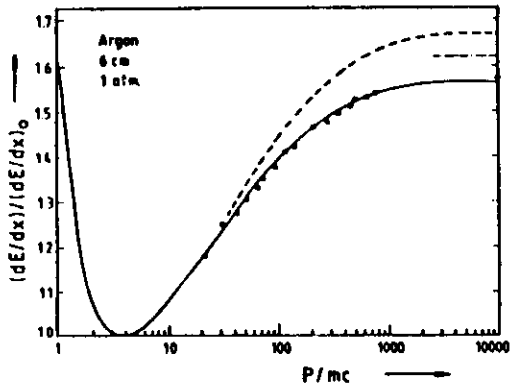

At very high electron energy $\left(\frac{dE}{dx}\right)_{ion}$ can be neglected :

$$\frac{dE}{E} = -\frac{dx}{X_o}$$

and $\langle E \rangle = E_0 e^{-x/X_o}$. After 1 X_o an electron loses $1 - 1/e \approx 63$ % of its energy.

At low energies $\left(\frac{dE}{dx}\right)_{ion}$ becomes dominant.

The energy where

$$\left(\frac{dE}{dx}\right)_{ion} = \left(\frac{dE}{dx}\right)_{brems}$$

is called the critical energy ε_c

Convinient approximations :

$$X_o = 180\ \frac{A}{Z^2}\ \left[\frac{g}{cm^2}\right]$$

$$\varepsilon_c = \frac{550}{Z} \qquad [\text{MeV}]$$

or $$\varepsilon_c = 2.66\ \left(\frac{Z\ X_o}{A}\right)^{1.11}$$

$e^{\pm}$ energy loss in C, Fe and U as a function of E_e

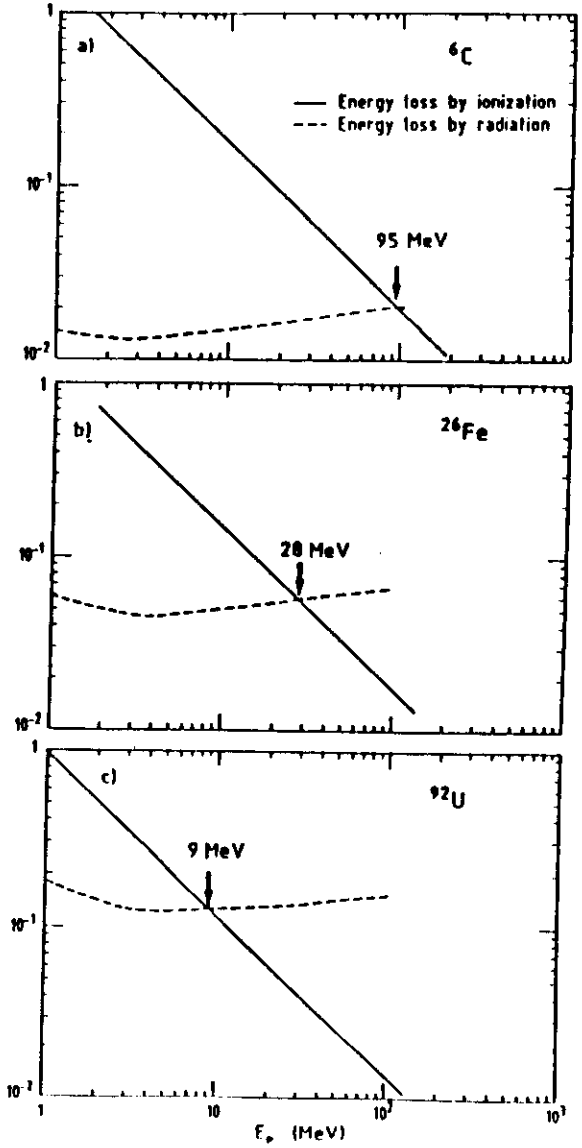

Other energy loss effects are generally less important for calorimetry

Cherenkov effect :

emission of photons if the particle velocity > phase velocity $c' = c/\sqrt{\text{dielectric constant}}$ of light in the material

(the Cherenkov light is used in lead glass em calorimeters)

Transition radiation :

emission of photons when the particle traverses discontinuities of material layers

The development of showers

All the basic tools to understand electromagnetic showers are now available. In practice they can be simulated very accurately by Monte Carlo techniques (EGS4 code).

Longitudinal development :

- rather steep rise of the shower profile due to the multiplication

  bremsstrahlung → pair-production

- no further particle multiplication occurs when the average particle energy equals ε_c

- more and more electrons stop
  → slow decrease of particle multiplicity.

longitudinal em shower profiles

EGS4 10 GeV e^-

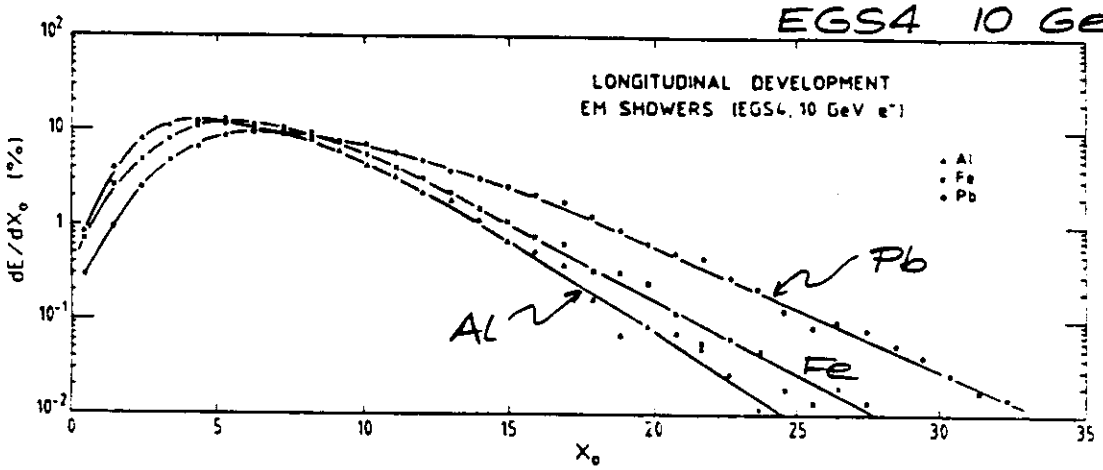

The energy loss depends mainly on the electron density in the medium.

 # atoms / volume is about constant → longitudinal em shower profile depends on Z. It scales approximately with Xo

The lateral shower profile is dominated by two effects :

- multiple scattering of electrons (early phase of the shower)
- long free paths for low energy photons (late phase of the shower)

The radial spread is characterized by the Molière radius ρ_M :

$$\rho_M = \frac{X_0}{\varepsilon_c} \cdot 21 \text{ MeV} \approx 7 \frac{A}{Z} \left[\frac{g}{cm^2} \right]$$

(multiple scattering lateral spread of an electron beam with energy ε_c after 1 X_0)

About 95% energy is contained in a cylinder with $R = 2 \rho_M$.

Generally em showers are narrow → good position resolution is possible

Lateral em shower profil

1 GeV e^- in Lead

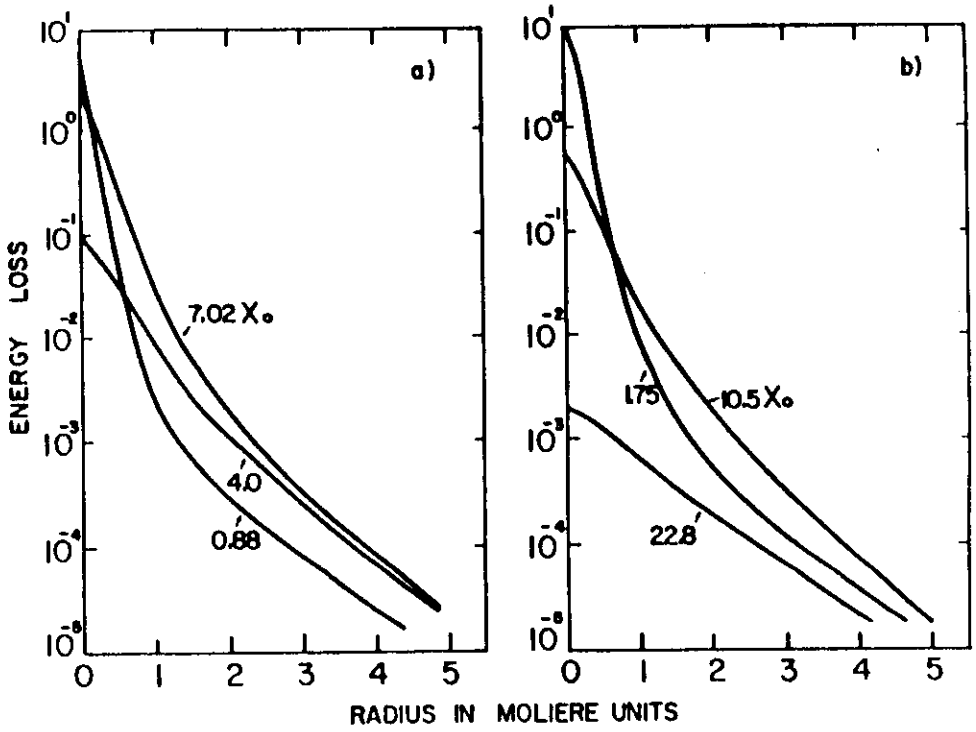

The development of hadronic showers is much more complex because of the strong interactions with a very large variety of reactions :

- meson production

- nuclear physics reactions (break-up of nuclei with release of p, n, α, γ..., energy loss due to binding energies...)

The γ's (from π^o, η ... or from the nuclear reactions) create local em showers.

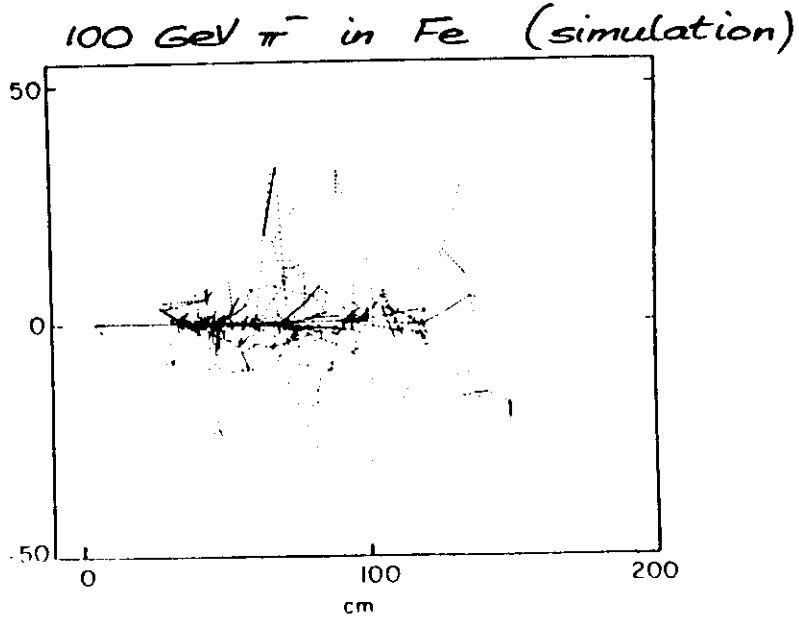

Monte Carlo simulations of hadronic showers are therefore much more difficult and also less reliable than electromagnetic showers.

A classical calculation for the relative contributions is

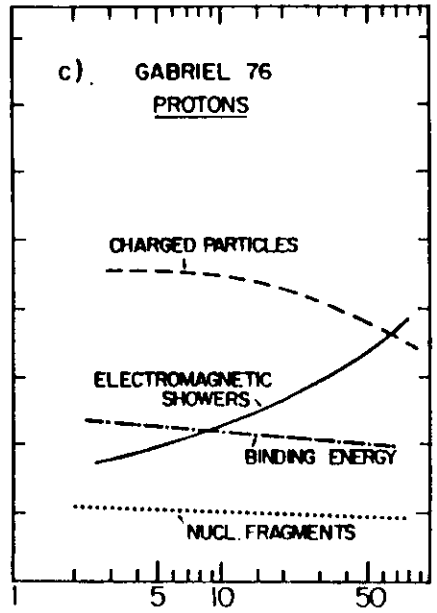

More recent progress in understanding ($\rightarrow$ simulation) of hadron showers will be discussed later.

The profile of hadronic showers is governed by the nuclear interaction length λ which is related to the inelastic cross-section σ_i by

$$\lambda = A / \sigma_i \, N_0 \, \rho$$

As an approximation one can use

$$\lambda \approx 35 \, A^{1/3} \quad [g/cm^2]$$

very rough shower size :

radial containment for 95%

$$R \approx \lambda$$

longitudinal containment for 95%

$$L/\lambda \approx 0.6 \ln E - 0.2 + 4 \, E^{0.15} \quad (E \text{ in GeV})$$

Typical hadronic shower developments in different materials

→ approximate scaling with λ

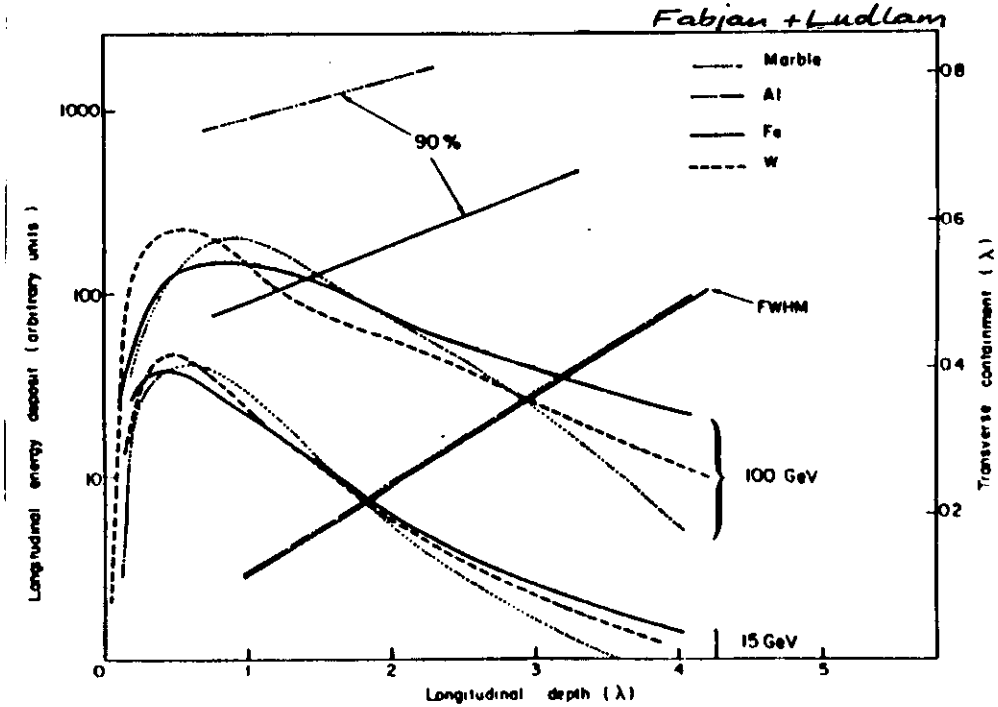

(measured w.r. to interaction vertex)

Experimental study of the contribution of nuclear fission with a method based on the analysis of induced radioactivity

(Leroy, Sirois and Wigmans, 1986)

identify radioactive fission and capture products with high resolution γ-ray spectroscopy scanning each calorimeter plate after exposure to π or p beam

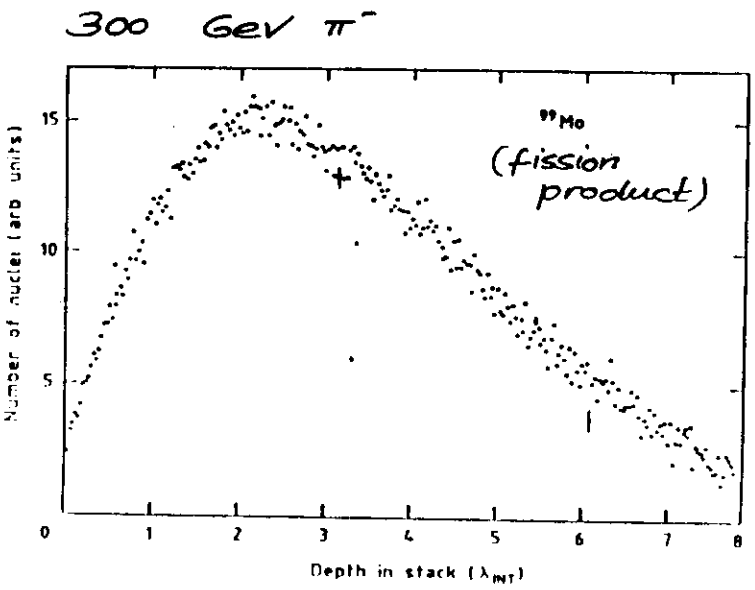

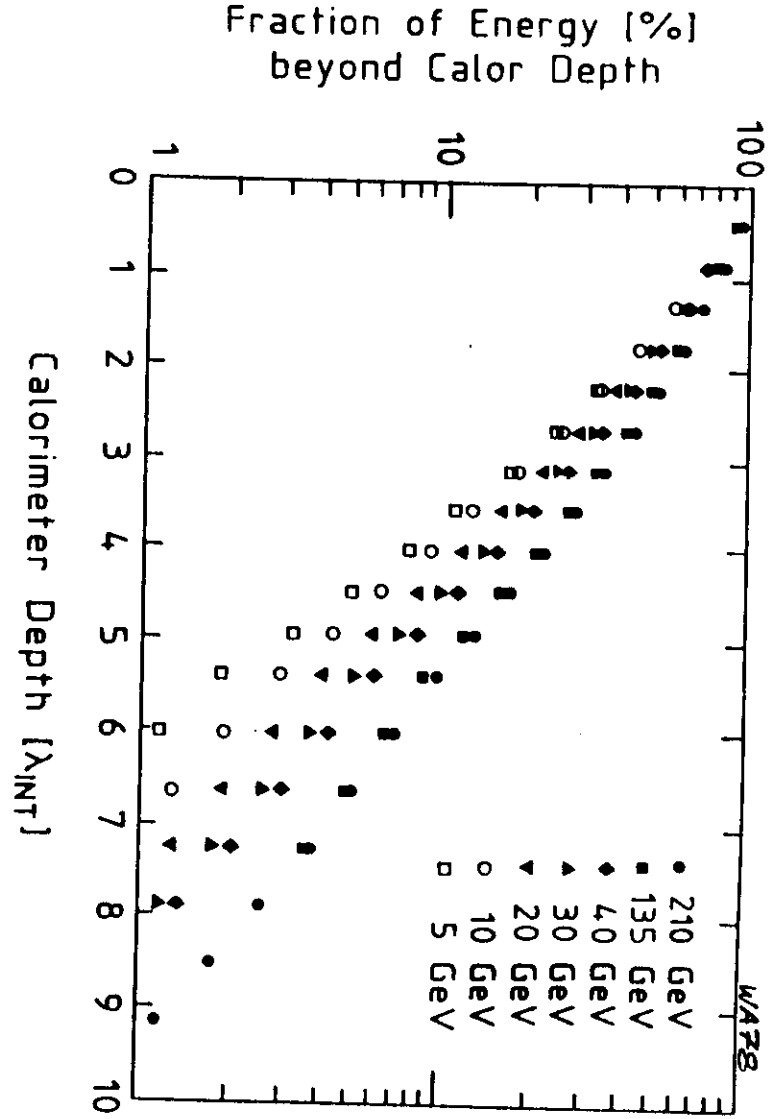

Examples of simulated showers
(UA2 end cap calorimeters)

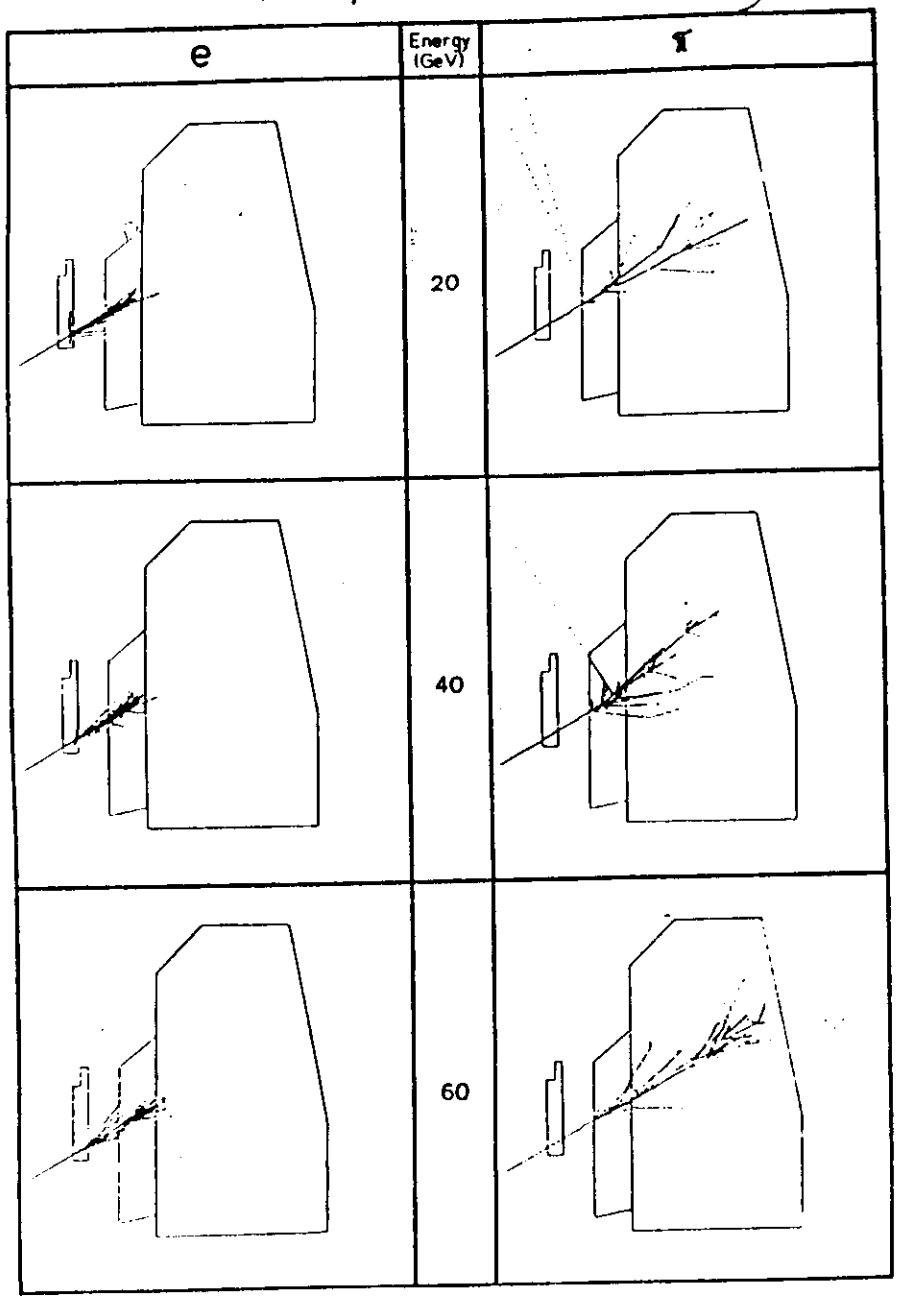

Homogeneous and sampling calorimeter

One would obviously achieve the best energy resolution if all the energy lost by the particle of interest could be measured. Then the ultimate limit of a homogeneously sensitive calorimeter would be determined by the fluctuations intrinsic to the shower development.

Statistical processes, intrinsic fluctuations grow with $\sqrt{E}$ → resolution σ_E/E improves with $1/\sqrt{E}$.

In practice homogeneous calorimeters are only possible for em showers (small dimensions !)

Hadron calorimeters are "sampling" the shower development by signal detectors alternating (or interspersed) with inactive absorber material.

III EXAMPLES OF SIGNAL DETECTION

Homogeneous fully sensitive calorimeters which are used in particle physics experiments are based on the detection of light.

These are either crystals like Sodium iodide [NaI (TL)],
Bismuth germanate [$Bi_4 Ge_3 O_{16}$, called BGO], Ba F_2 ... or glasses like scintillating glass or lead glass [mixture PbO and Si O_2].

The light is produced mainly by scintillation except for the the case of lead glass counters which are based on the detection of the Cherenkov light produced by the $e^{\pm}$ from the shower.

Readout for sampling calorimeters

- photon collection
  usually by light guides followed by conversion into charge by photomultipliers (or photodiodes etc)

- charge collection
  measuring the ionization charge in active calorimeter layers (solids, liquids, or gases)

In all cases the charge has to be amplified (internally or externally) for measurements with analog-to-digital converters (ADCs).

The choice of a particular readout technique depends on many factors and requirements :

- energy resolution
- signal linearity and uniformity
- granularity
- hermeticity (no dead space)
- signal stability (calibration)
- rate dependence
- radiation hardness
- costs

Signal response can be non-linear with respect to the ionization density. Saturation effects can occur.

Birk's law :

$$dL/dx = \frac{dE/dx}{1 + kB\ dE/dx}$$

L signal output

kB Birk's parameter

typically 0.01 g/MeV cm² scint.

0.005 LAr

0.003 gas

important effect for slow heavily ionizing particles in the shower

Brückmann et al.

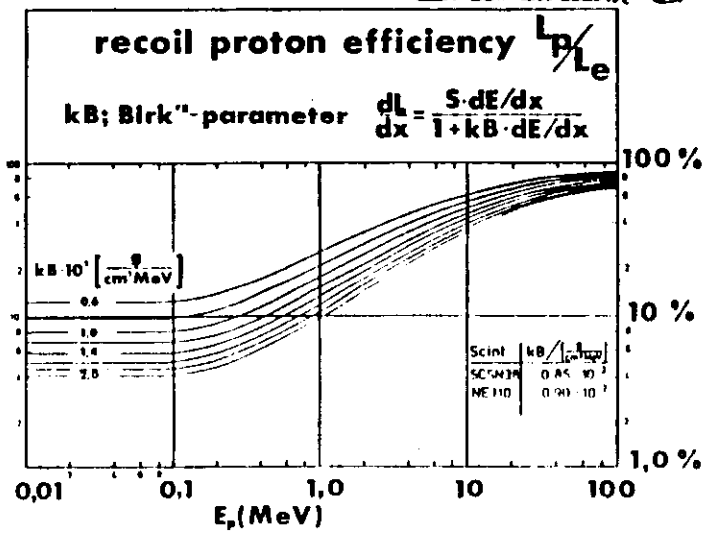

Plastic scintillators

Used (with WLS) in several large scale collider experiments (examples: UA1, UA2, CDF, ZEUS ....)

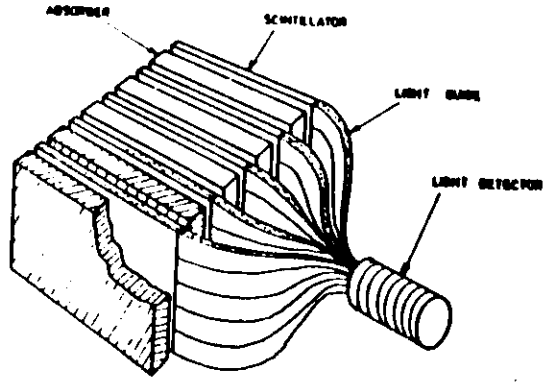

direct light collection

(large dead space)

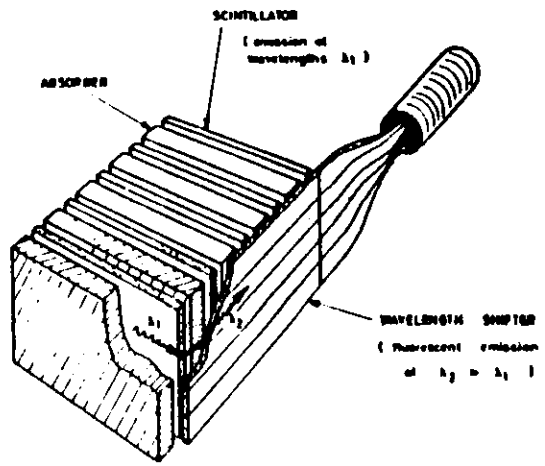

standard technique: light collection with wave-length-shifter (WLS) plates

Some properties of scintillating crystals

Table 14. *Properties of scintillating inorganic crystals*

Scintillator	NaI(Tl)	LiI(Tl)	CsI(Tl)	$Bi_4Ge_3O_{12}$	BaF_2	
Density (g/cm³)	3.67	4.06	4.51	7.13	4.9	
Melting point (°C)	650	450	620			
Decay time (μs)	0.23	1.3	1.0	0.35	0.62	6×10^{-4}
λ_{max}(emission) (nm)	410	470	590	480	310	225
Light yield (photons/MeV)	4×10^4	1.4×10^4	1.1×10^4	2.8×10^3	6.5×10^3	2×10^3
Radiation length λ_0 (cm)	2.59			1.12	2.1	
Refractive index n	1.85			2.15	1.56	
$(dE/dx)_{min}$ (MeV/cm)	4.8			8	6	
Temperature coefficient of light output (%/°C)	0.22–0.9			1.7		
Radiation damage	yes			yes		
Hygroscopic	yes			no		

Some properties of plastic scintillators and WLS.

Table 15. *Organic fluorescent materials and wavelength shifters*

Structure	λ_{max} emission (nm)	Decay time (ns)	Yield/ yield (NaI)
Primary fluorescent material			
Naphthalene 	348	96	0.12
Anthracene 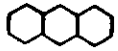	440	30	0.5
p-Terphenyl 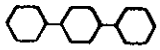	440	5	0.25
PBD 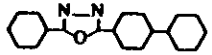	360	1.2	
Wavelength shifter			
POPOP 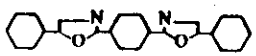	420	1.6	
bis-MSB 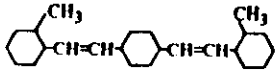	420	1.2	

Typical example of a calorimeter module with several cells read out by WLS.

The scintillator plates are read out on two opposite sides of the cell

HELIOS

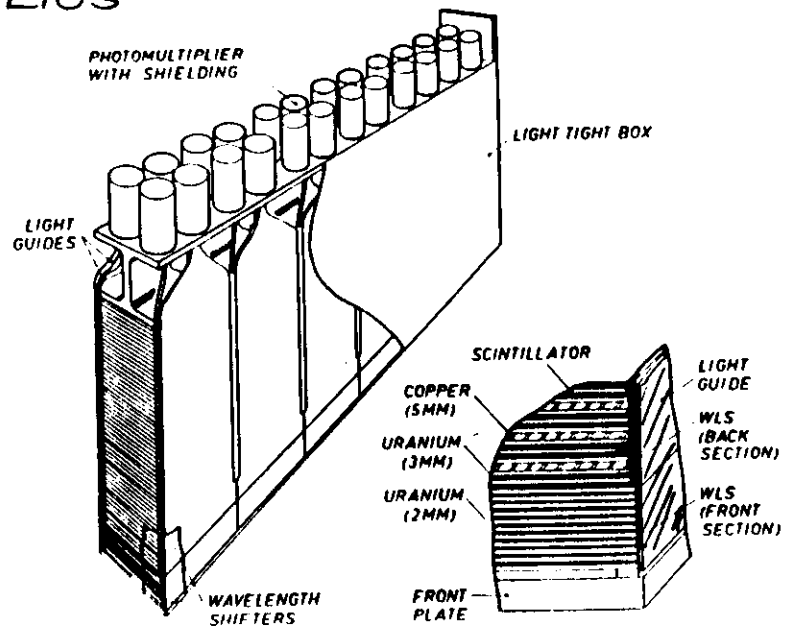

two longitudinal sections are read out separately for each cell

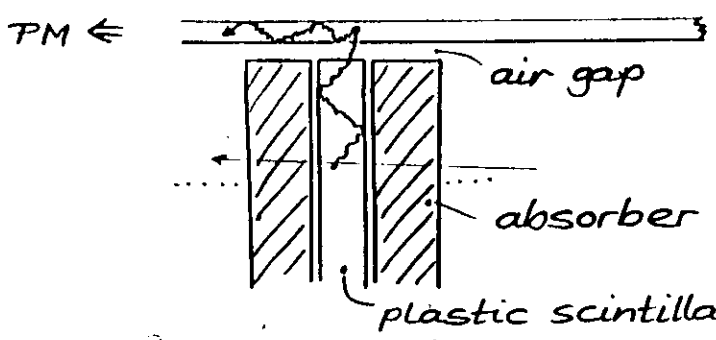

UA2

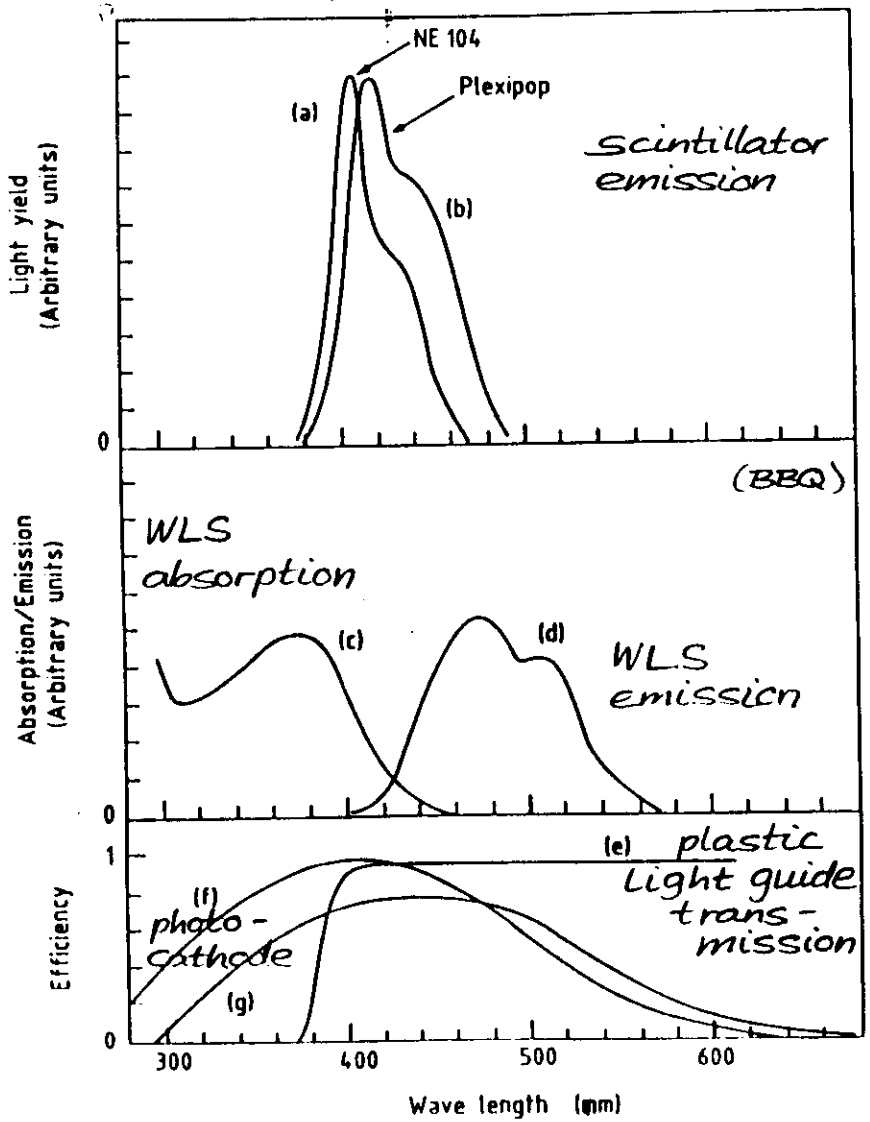

Main problem: light attenuation

λ_{att} → non-uniform response within a cell

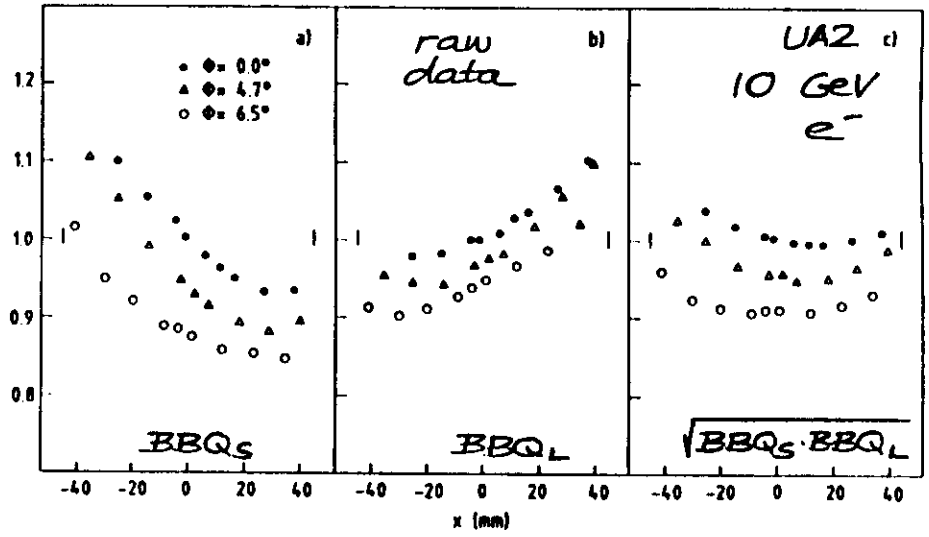

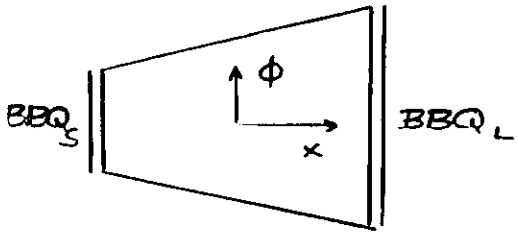

after offline corrections for λ_{att} effects all within 1%

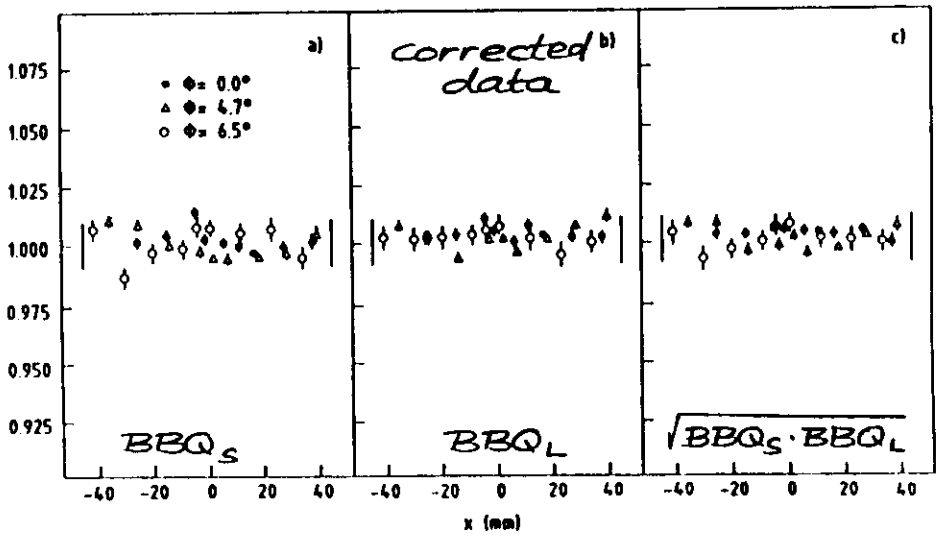

ZEUS prototype studies

ZEUS prototype studies

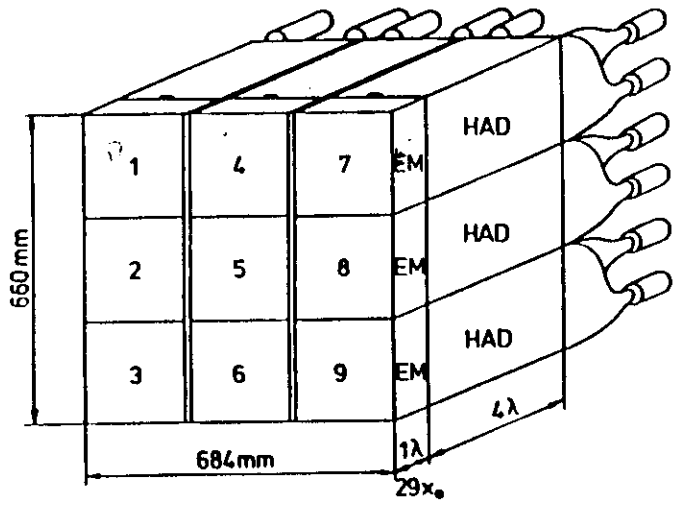

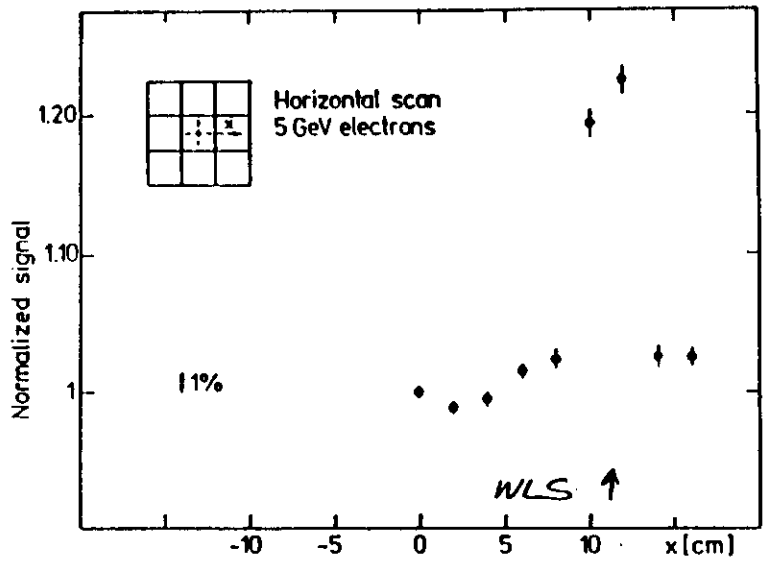

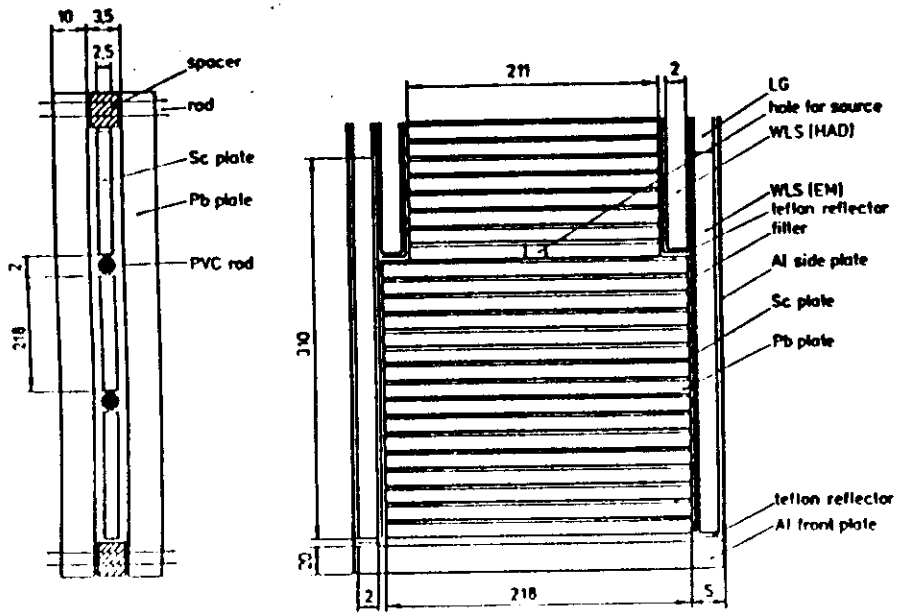

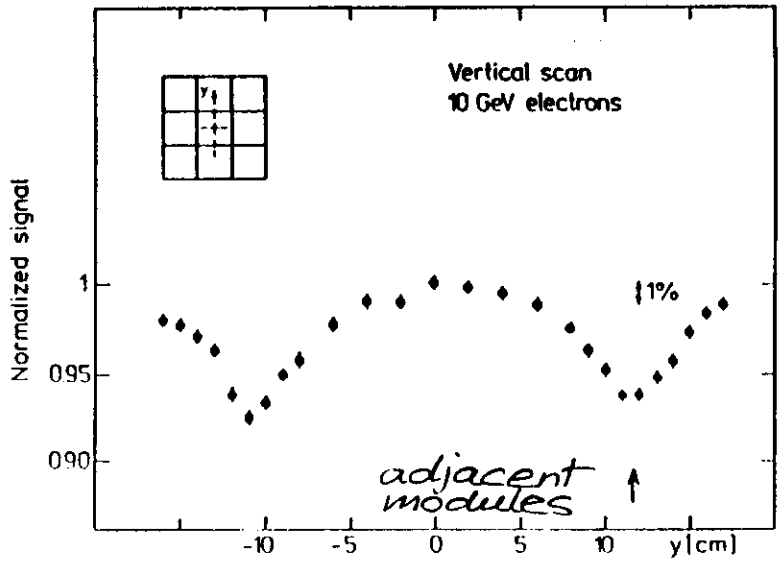

Non-uniformities affect directly the resolution of calorimeters.

Recent developments in scintillator calorimeters :

ZEUS :

Very careful studies to eliminate non-uniformities
(materials with large λ_{att}, absorption masks to make the light yields and transmissions uniform)

Scintillating fibre calorimeters
(known as em for example in Ω, DELPHI luminosity ...)
R + D for hadron calorimeter, see later.

ZEUS prototype studies

non-uniform response from the WLS plates

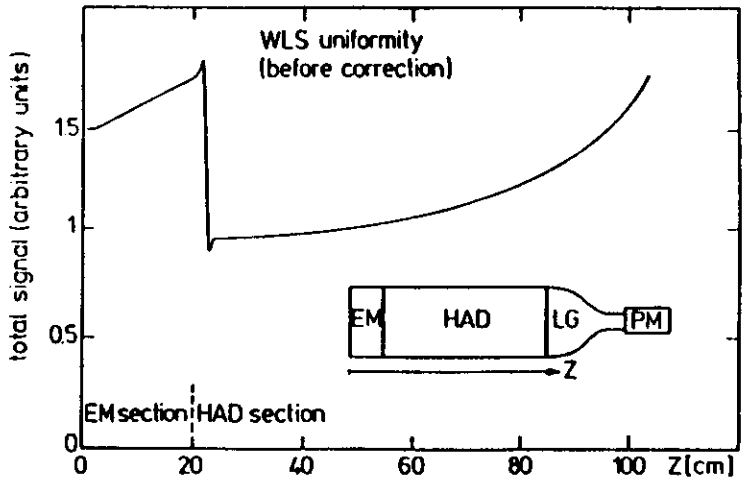

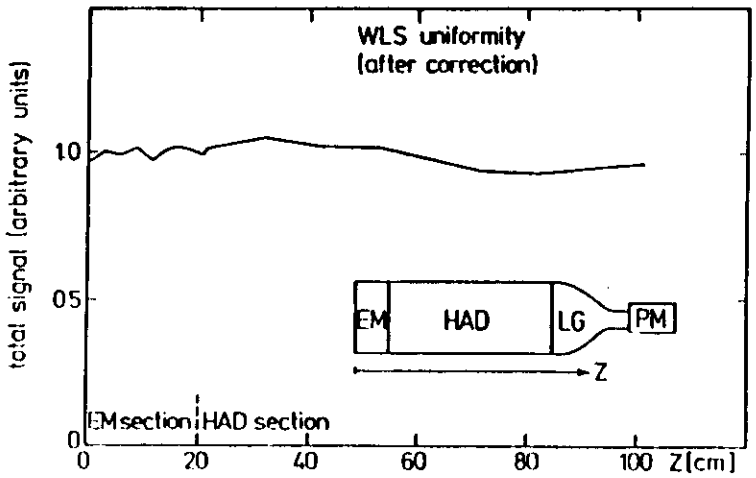

Charge collection (examples)

. Silicon layers

electron-hole pairs are created in the semiconductor with charges separated by the electric field
→ direct electrical signal
(see lectures by C. Damarell)

Only small em Si calorimeters have been used so far in experiments, but interesting R + D work is going on also for hadron Silicon calorimeters (SICAPO).

. Liquid ionization chambers

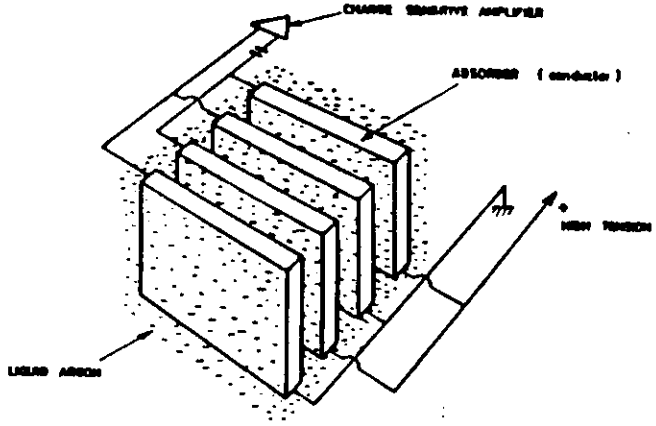

used (or will be used) in large detectors are

Liquid Argon (LAr)

at ~ 80° K → needs cryogenics

examples : Mark II, Tasso, Cello, D0, H1 ...

TMP

at room temperature

will be used in UA1

In liquids the charge is collected without internal amplification. Electrons must be able to drift over sufficient long gap distances → purity essential
(LAr < 1 ppm O_2, TMP ≤ 1 ppb O_2 !)

Some properties of room temperature calorimeter liquids

Table 1

Structure formulae

a) TMS

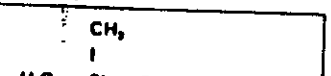

b) TMP

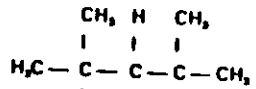

c) HEDS

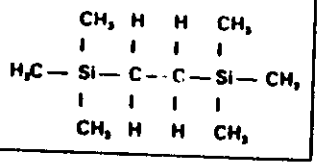

Table 2

Properties of room temperature calorimeter liquids

	TMS	TMP	HEDS
Density (g/cm³)	0.645	0.72	~ 0.75
dE/dx (MeV/cm)	1.36	1.58	~ 1.60
Mobility (cm²/V · s)	100	30	45
Flashpoint (°C)	−18	+7	~ 10
Boiling point (°C)	26.5	122	150
Dielectric const.	1.84	1.98	-
Vapour pressure at 20 °C (Torr)	650	15	< 10
Free electron yield at E = 15 kV/cm (10^3/mm)	1.93	2.16	~ 1.2

electron yield for LAr and TMP

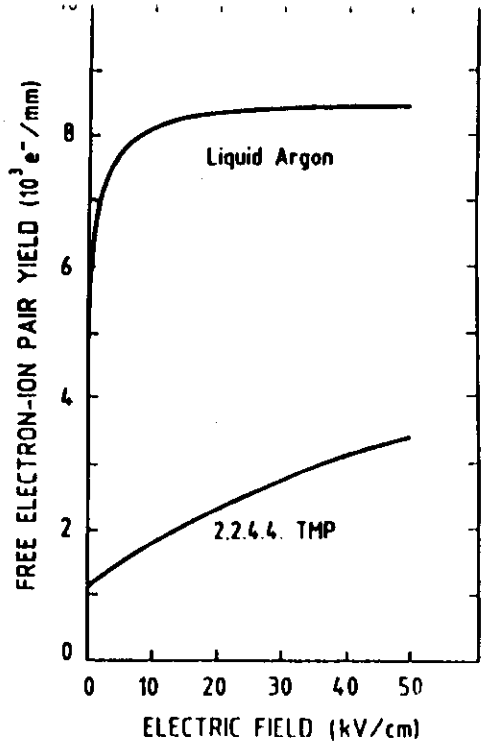

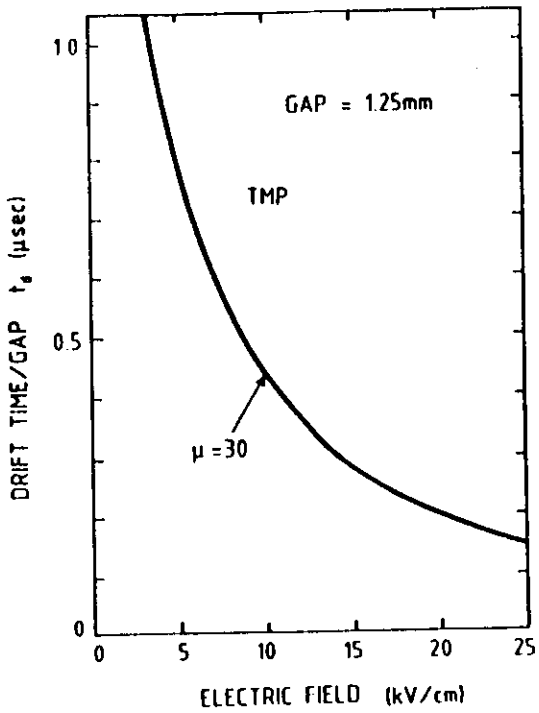

drift time of the electrons in a 1.25 mm TMP gap

(similar times for LAr)

(from UA1)

example : UA1 TMP - Uranium calorimeter

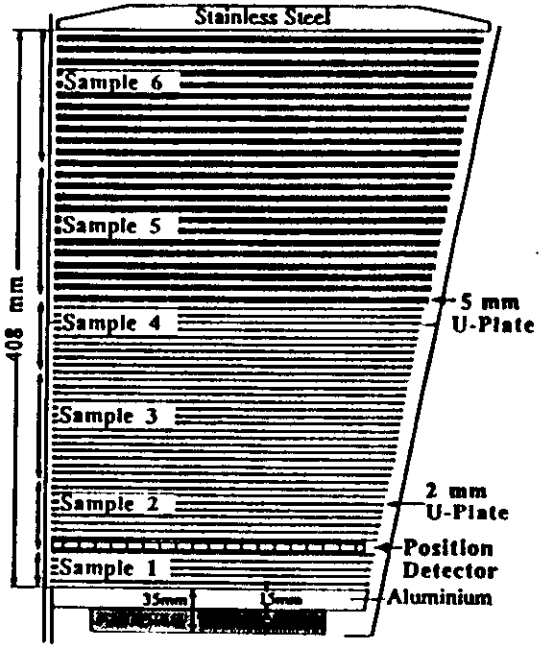

the TMP is contained in sealed boxes which slide between the U-plates

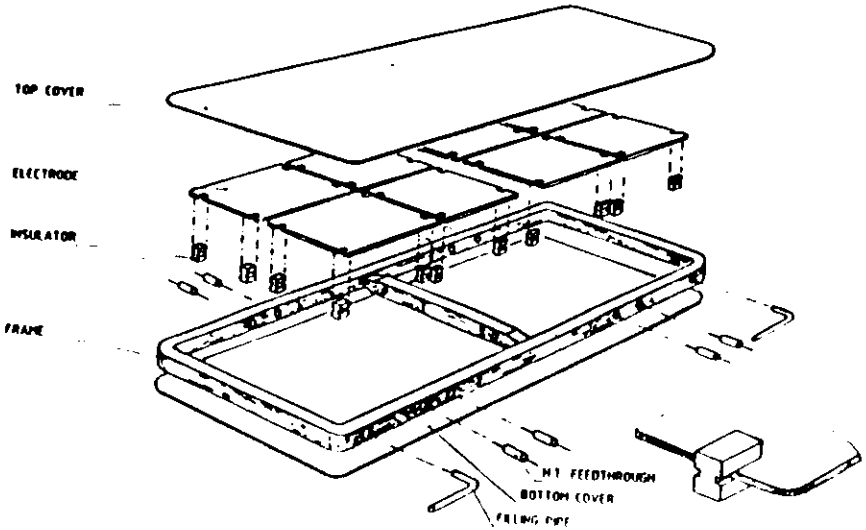

- **gas chamber read-out (wire chambers or tubes)**

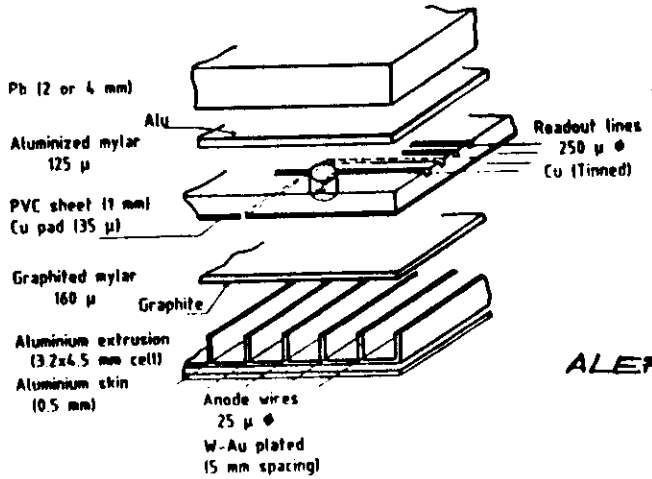

the internal amplification (avalanche) is exploited

- **proportinal mode**
  → signal proportional to the energy loss
- **saturated mode (Geiger, streamer)**
  → signal proportional to the # of wires hit (non-linear effects)

This read-out is used for example in LEP experiments and in future calorimeters (H1, ZEUS) to catch in an economic way the tail of hadron showers leaking out at the back of the main calorimeters.

Comparison of some read-out techniques
(such a table is arbitrary and needs comments !)

	scintillator	Si	liquids	gas
sampling active/passive	1-10%	<1%	1-10%	10^{-4}
dead space hermeticity	G	G	G (cryogenis LAr)	G
granularity	B	G	G	G
signal uniformity	B (fibres ok)	G	G	~G
stability	B	G	G	B
signal/noise	G	G	B	B
radiation resistance	B-G	B (neutrons)	G	G
speed/rate	G	G	B	B
costs	G	B	G	G

G means can be good
B means bad or very difficult

As we will see next good or adequate resolutions can be achieved for all except for gas calorimeters.

IV PURELY ELECTROMAGNETIC SHOWERS AND CALORIMETERS

The best energy resolutions are obtained in fully sensitive homogeneous calorimeters.

The intrinsic resolution depends on the fluctuations in the measurable total track length L_m in the shower (sum over all measurable charged track segments). L_m depends on the minimal detectable energy E_m. The total track length is about $L/X_o \sim E/\varepsilon_c$.

The intrinsic shower fluctuations are typically

$$\sigma_E/E \sim 0.005/\sqrt{E} \qquad (E \text{ in GeV})$$

NaI (Tl) crystals have reached $\sigma_E/E = 0.9\%$ at 1 GeV (for 24 X_o long crystals which contain the showers fully).
example : Crystal Ball Detector.

L3 BGO prototype performance

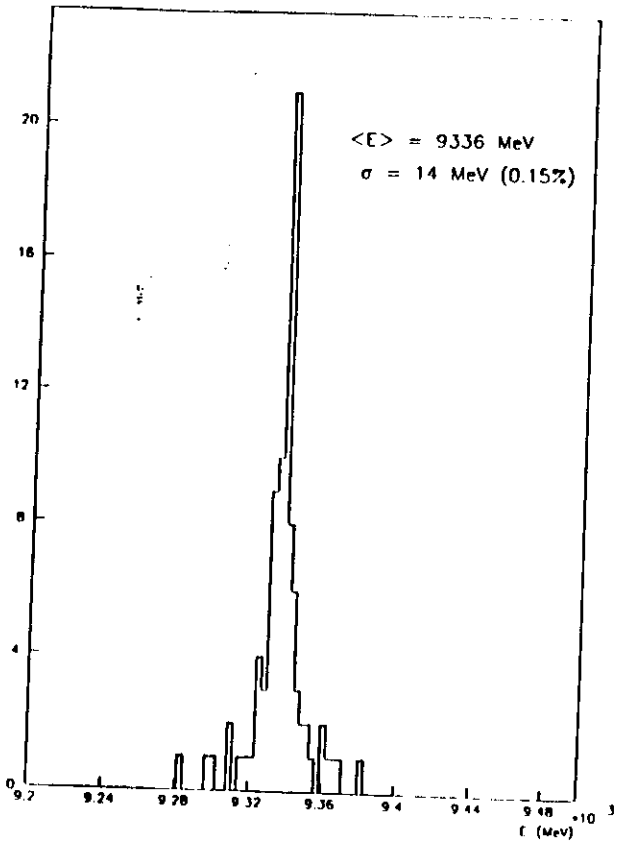

resolution

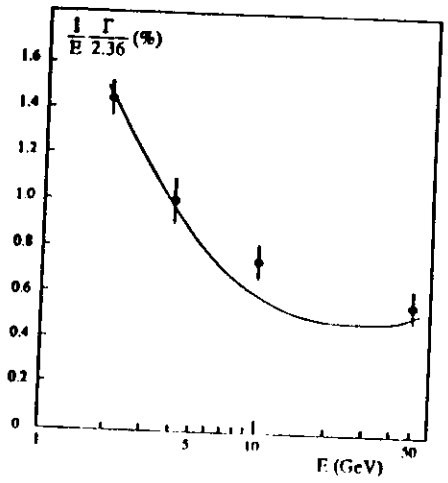

An other example for a homogeneous em calorimeter is the BGO ($Bi_4 Ge_3 O_{12}$) crystal with X_o = 1.1 cm as used for example in the L3 experiment at LEP.

In both cases the intrinsic resolution limit is not quite reached

→ fluctuations in the light collection dominate

In Lead Glass counters (examples OPAL and DELPHI end caps at LEP) one detects the Cherenkov radiation of the $e^{\pm}$ in the shower. The Cherenkov threshold in LG implies that $E_m \geq 0.7$ MeV.

→ intrinsic resolution is of the order 3 - 5 % / $\sqrt{E}$, corresponding to the resolution reached in LG counters.

The energy resolution is degraded if the shower is not fully contained due to

- longitudinal leakage
- lateral leakage

In general the longitudinal loss is more dangerous than the lateral loss.

approximations

$$l(95\%)/X_o \leq \ln E/\varepsilon_C - \left\{ \begin{matrix} 1 & \text{electrons} \\ 0.5 & \text{photons} \end{matrix} \right\} + 0.08\ Z \pm 9.6$$

$$r\ (95\%) \leq 2\ \rho_M$$

example
15 GeV e^-
in marble
(CHARM)

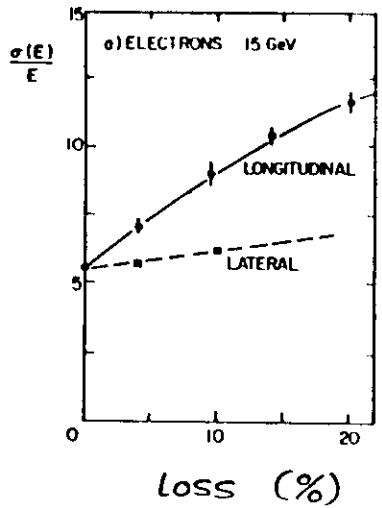

For sampling calorimeter further, and generally more important, statistical fluctuations occur in the sampling procedure.

Only a fraction of the charged shower particles (tracks) are in the active layers, and their fluctuations are called sampling fluctuations.

Intuitively it is clear, that the smaller the thickness of the passive absorber plates, the smaller are the sampling fluctuations :

$$\sigma_E/E = \sqrt{\varepsilon_C \cdot t/E}$$

t absorber thickness in units of X_o

The detected particles (mainly electrons, only in the beginning of the shower $\gamma \rightarrow e^+e^-$, Sect. II) are either :

- created in the absorber and reaching the active layer
- created in the active layer

The fraction of soft electrons reaching the active layer depends on the absorber Z.

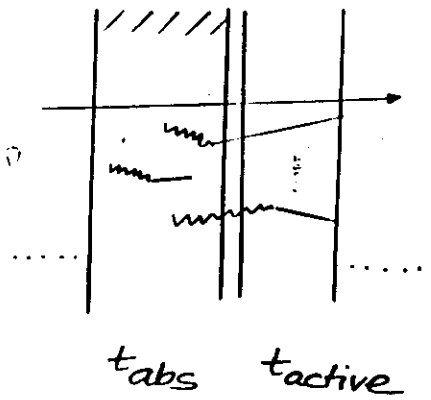

- number of soft e^- created in the absorber which reach the active layer $\propto 1/t_{abs}$
- number of soft e^- created in the active layer $\propto 1/t_{abs}$ and also $\propto t_{active}$ (sampling fraction)
- fast electrons from $\gamma \rightarrow e^+e^-$ fluctuations proportional to $\sqrt{N/2}$, may traverse several active layers

The relative contributions depend on the calorimeter type, the Z of the absorber and active layers.

10 GeV e^- shower

EGS4 calculations for the energy deposited by ionization from $e^\pm$

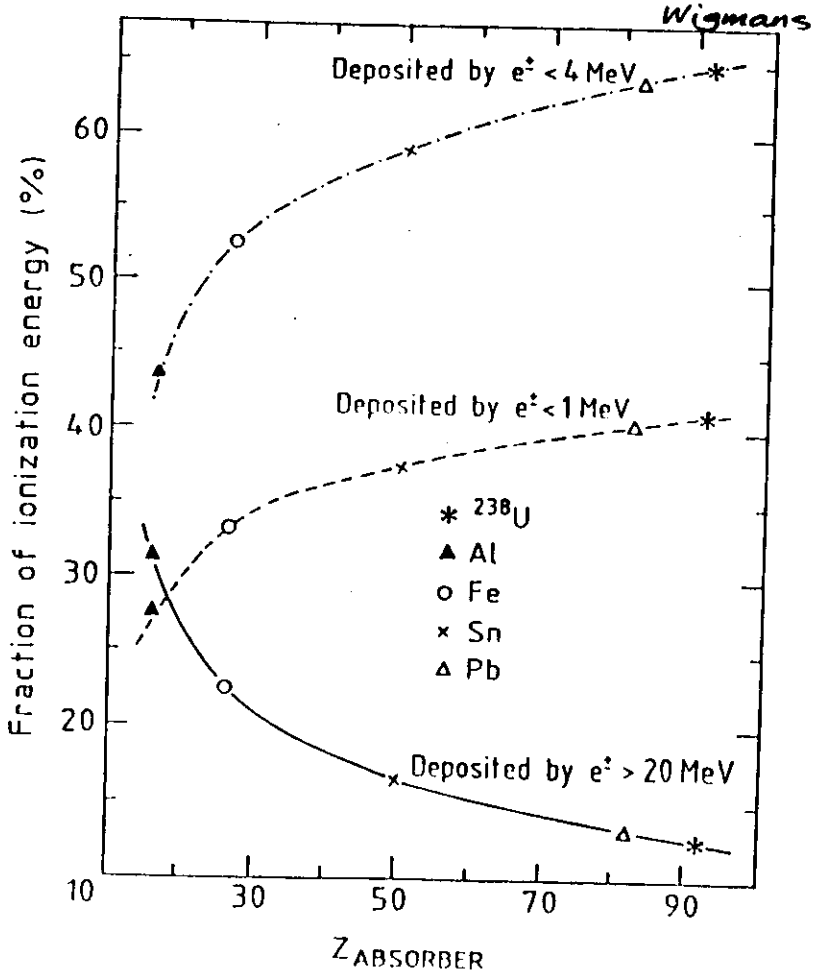

example Fe / LAr

soft electrons created in the LAr dominate as σ_E/E improves with increasing LAr gap for constant Fe absorber plates.

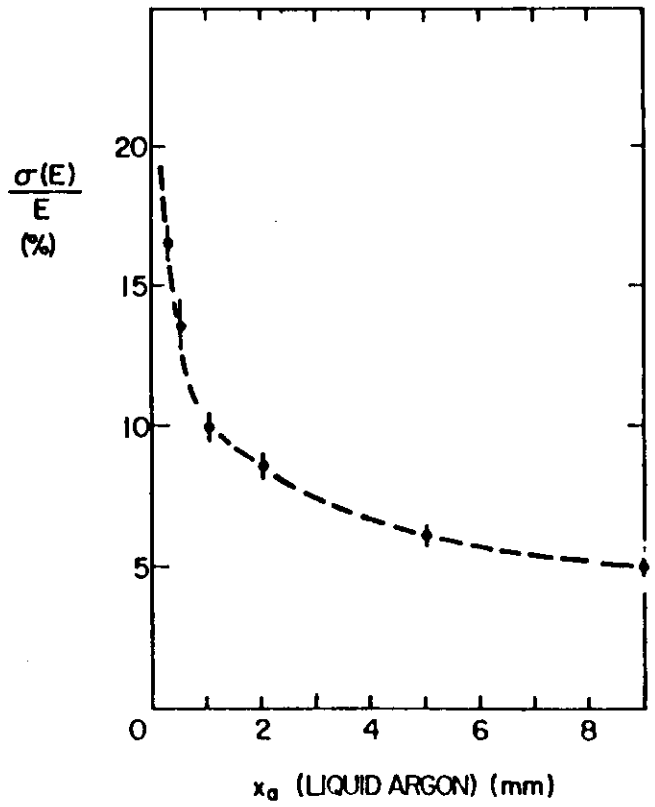

And of course instrumental effects can contribute to make the resolution worse ...

- **scintillators : light collection and photocathode efficiencies (usually less than 1000 photo-electrons / GeV → ≥ 3 % / √E from photon statistics)**

- **wire chambers : shower sampling statistics is dominated by**
  - **path length variations (very soft electrons at large angles can traverse a long path in the active gas layer)**
  - **Landau fluctuations (long tails in the dE/dx ionization per thin layer)**

To the extend that the intrinsic, sampling, and instrumental fluctuations are uncorrelated their contributions to the resolution have to be added in quadrature :

$$\sigma^2 = \sigma^2_{intr} + \sigma^2_{samp} + \sigma^2_{detector}.$$

example:

Calculated contributions to a Pb - gas em sampling calorimeter

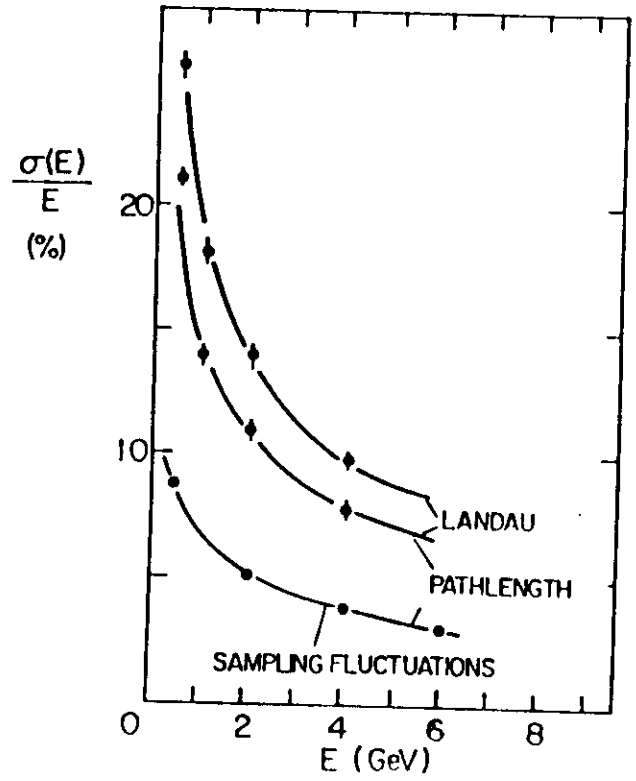

Some typical em energy resolutions σ_E/E which have been reached for E > 1 GeV.

homogeneous detectors

NaI (Tl) and BGO	**$0.015\ E^{-1/4}$**
Lead glass	**$0.04\ E^{-1/2}$**

sampling calorimeters

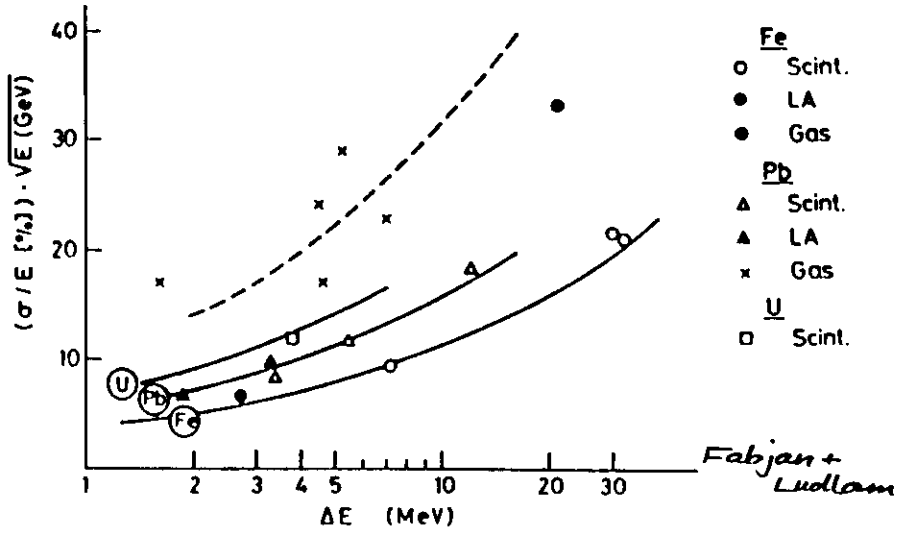

$\Delta E = \varepsilon_c \cdot t$ **energy lost in one single sampling layer for a m.i.p.**

An interesting development

BaF_2 scintillator read out with photosensitive MWPC.

BaF_2

BaF_2: $\rho = 4.9\ g/cm^2$ $\quad X_0 = 2.05\ cm$

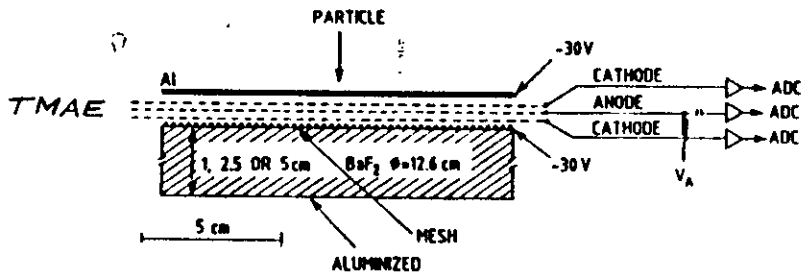

R. Bouclier et al.

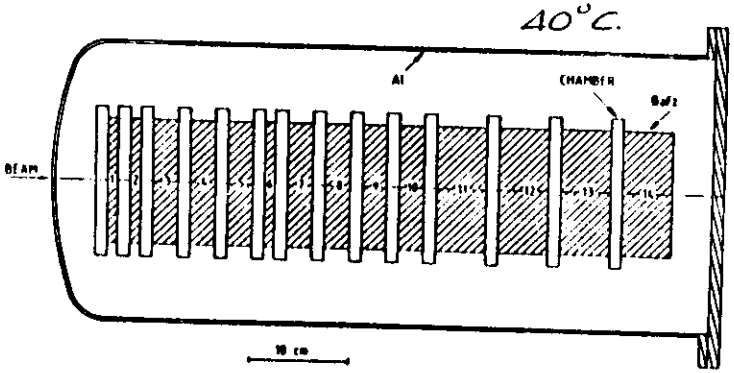

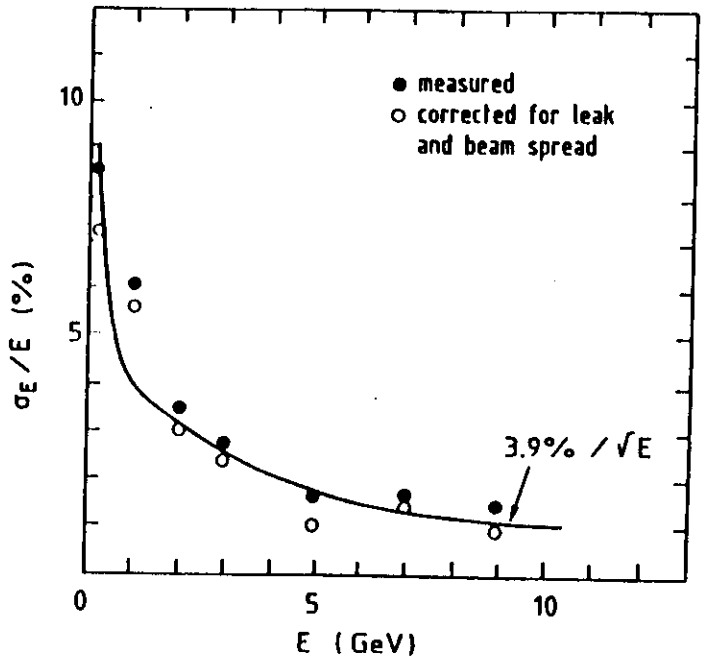

9 GeV e^- simulation

R. Bouclier et al.

V HADRON SHOWERS AND CALORIMETERS

The energy resolution for hadronic calorimetry is much more complex to describe.

Remember : A very large variety of strong interaction processes with meson production and nuclear reactions which release p, n, α, γ ... are occuring. Intrinsic shower fluctuations are an important contribution to the final calorimeter performance.

An important fraction of the incident hadron energy goes into local electromagnetic showers initiated by the γ's.

On the other hand not all the energy deposited in the nuclear processes can be detected due to the energy lost due to nuclear binding effects.

As a consequence the signals from electrons/ photons and hadrons of the same energy are not the same in general.

H1 test beam result

50 GeV π^- and e^-

(Pb and Fe / LAr)

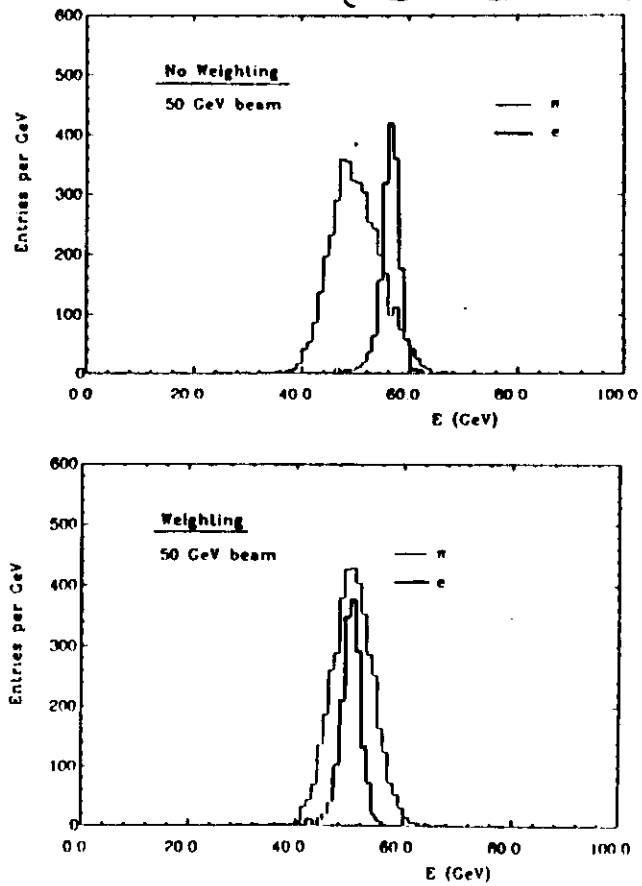

Fig.40 Pulse height distributions for 50 GeV electrons and pions before (a) and after (b) weighting measured with a liquid argon calorimeter (from H1)

ZEUS test beam result

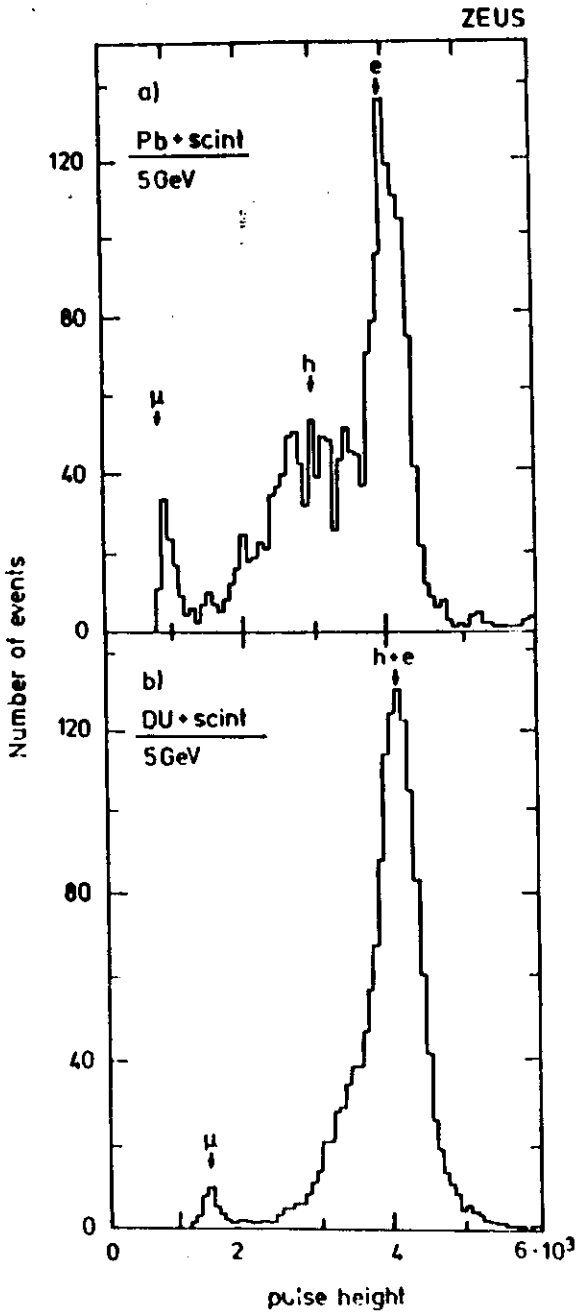

A few early ($\lesssim$ 1985) e/h response ratios measured for various calorimeter configurations.

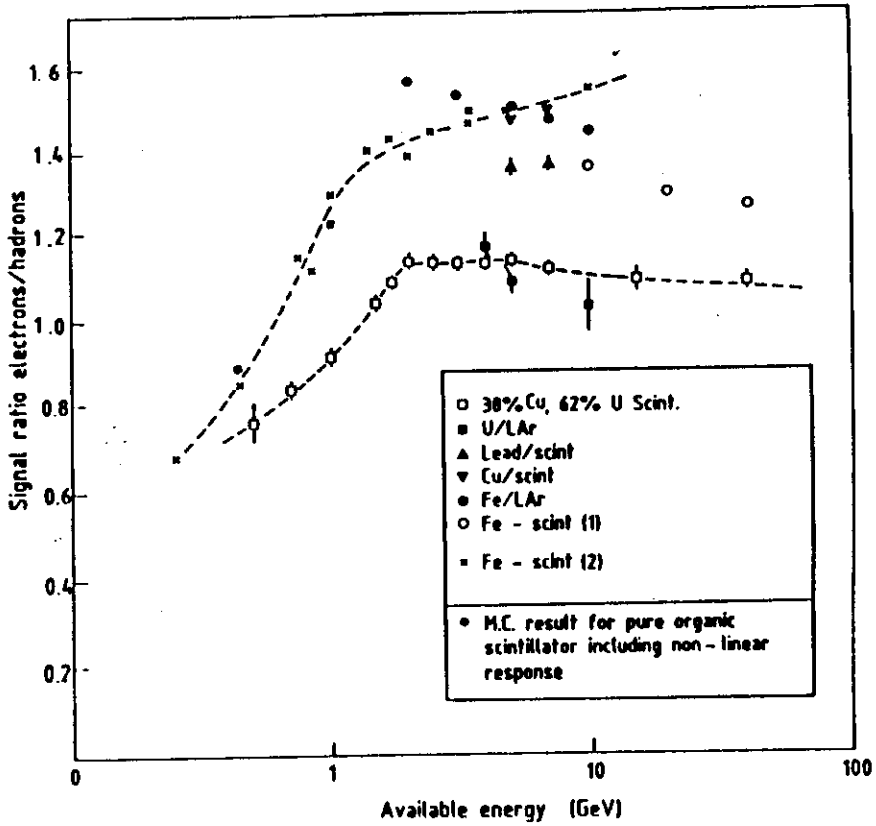

e/h plays a crucial role for the hadron calorimeter resolution.

$e/h \simeq 1$ is a necessary condition to achieve:

- good resolution which scales like $1/\sqrt{E}$
- no constant term in the resolution
- Gaussian signal distributions
- linear signal response as a function of the energy

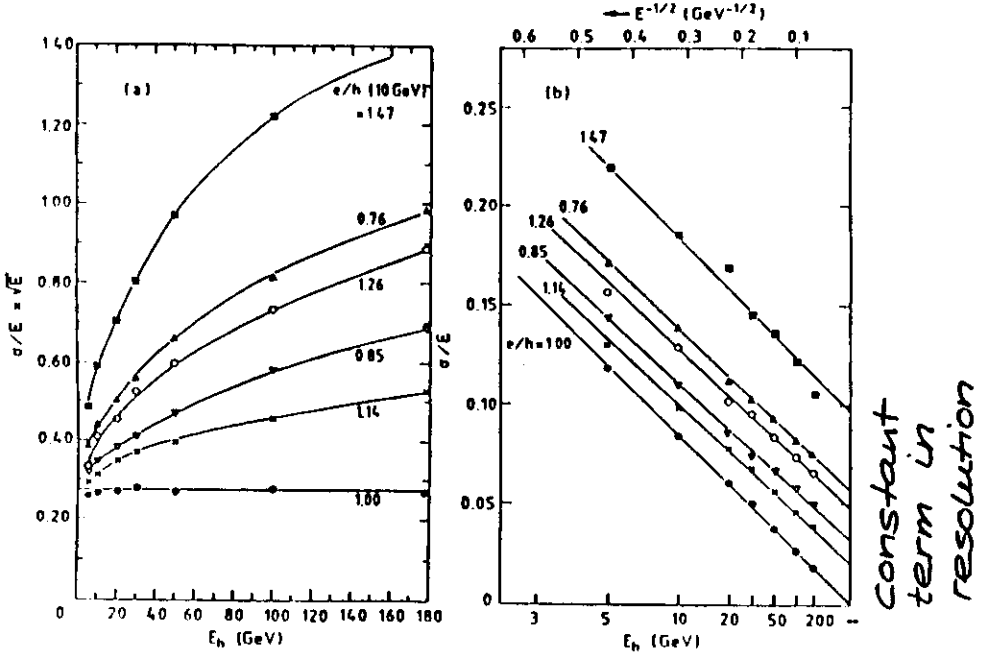

constant term in resolution

hadron energy

(MC model Wigmans)

effects of e/h = { 1.4 CDHS; 1.05 HELIOS; 0.80 WA78

resolution

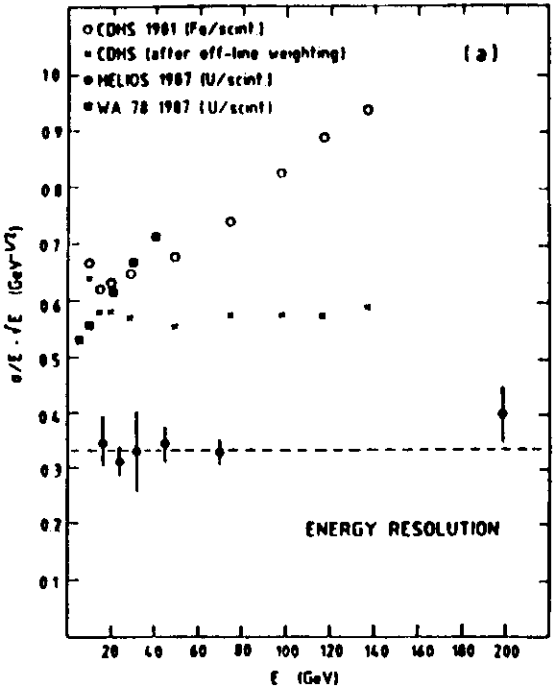

signal shape

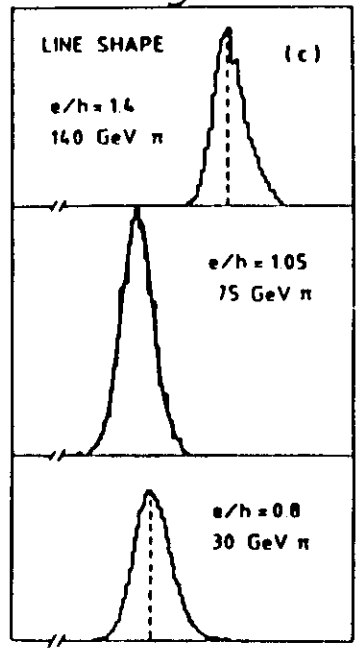

linearity

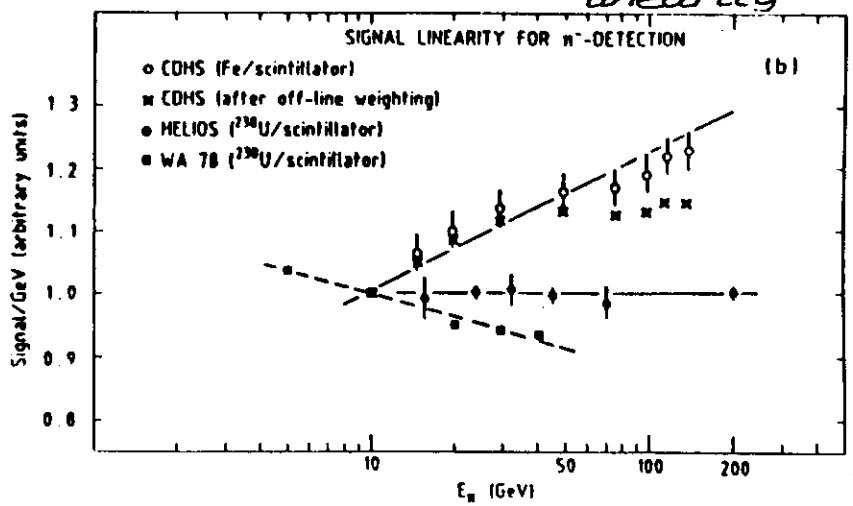

The fraction f_{π^0} of the hadron energy going into π^0's is not constant. An approximation is

$$f_{\pi^0} \simeq 0.1 \ln E \quad (E \text{ in GeV})$$

$$e/h^{meas}(E) = e/h^{intr.} \Big/ [1 - f_{\pi^0}(1 - e/h^{intr.})]$$

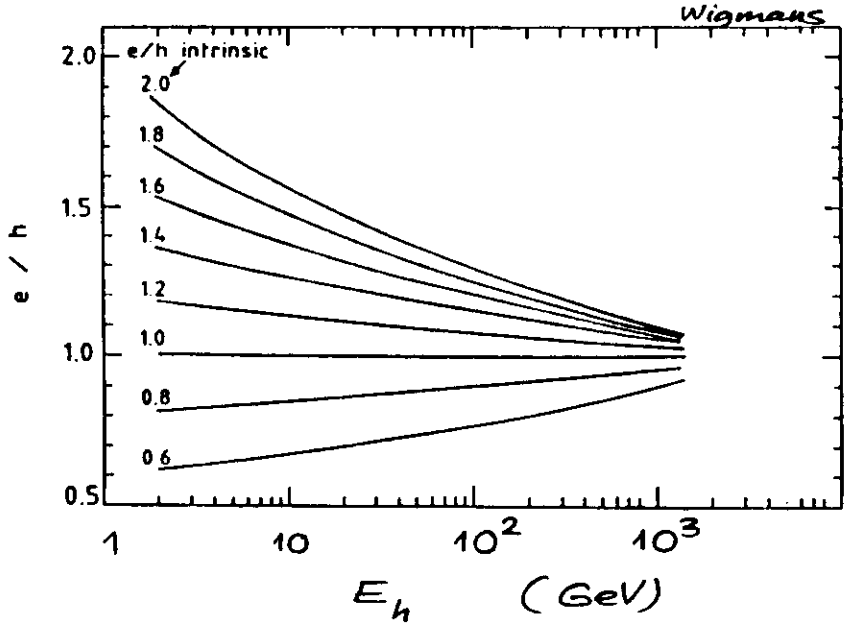

The crucial question is then :

how can one obtain e/h = 1 ?

There are two approaches.

Weighting method

- **the shower is sampled longitudinally and weights are applied to each sample such as to eliminate event-by-event fluctuations in f_{π^0}.**
- **does not correct for fluctuations in the energy lost in nuclear physics processes**
- **non-linearities are not completely removed**

Compensating calorimeters

- **the absorber and detection media are chosen such that the same response is obtained for the em and hadronic component of the showers**
- **best resolution can be obtained if fluctuations in the nuclear physics processes can be observed (for example neutrons)**

The weighting method was pioneered by CDHS (1980).

This technique will be used at HERA by the H1 experiment (Pb and Fe / LAr)

CDHS

$$\sum_i E_i' = E_i (1 - c' E_i)$$

$$c' = c / \sqrt{E_{tot}}$$

$c' E_i < 30\ \%$

E_i unweighted energy

The CDHS set-up:
16 modules (samples)
(5 × 2.5 cm Fe + 5 × 0.5 cm scint.)
e/h ~ 1.4

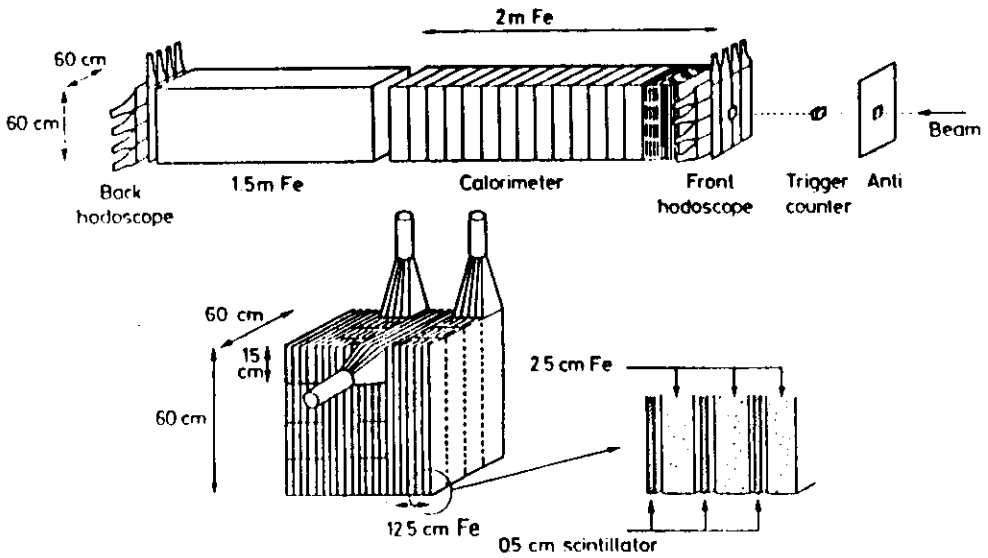

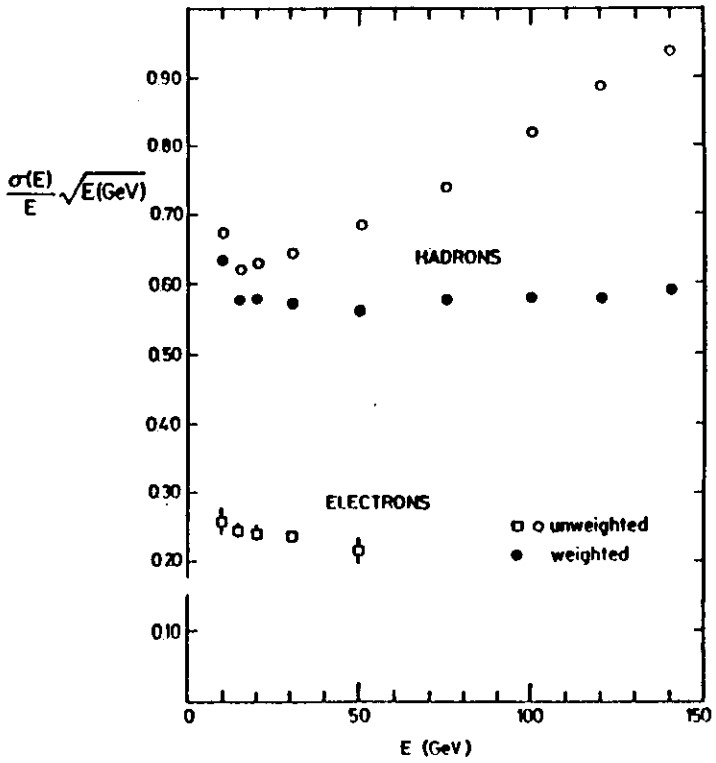

correlation between the maximum energy in a single sample vs total energy

CDHS π^- 140 GeV

raw data

after weights

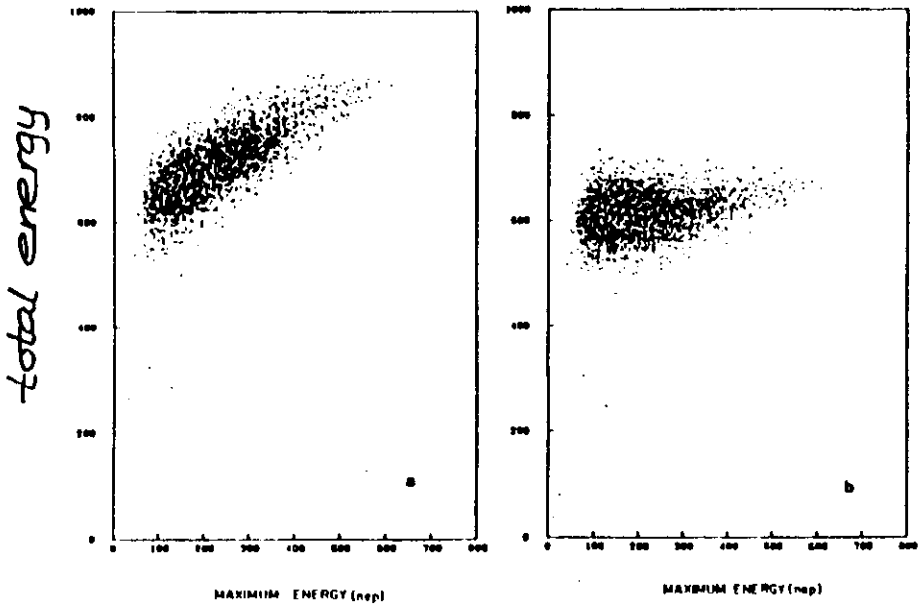

maximum energy

an other example

WA 78

U/scint.

with

e/h ~ 0.8

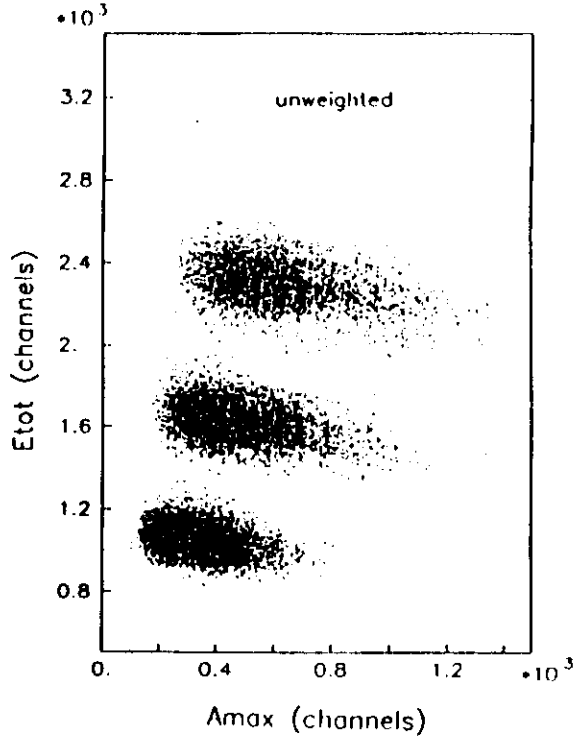

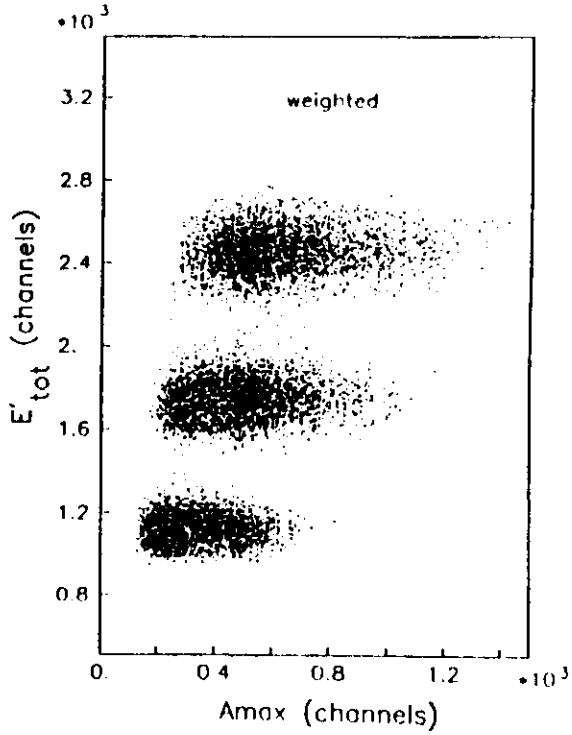

Compensating sampling calorimetry

The main methods to achieve $e/h \approx 1$ are

- reduce em (π^0) response, can be done by using the knowledge of em shower physics (mainly photoelectric effect)
  - → high Z absorber plates
  - → low Z active material

- boost ("amplify") hadron response by detecting the released neutrons from the nuclear processes
  - → slow recoil protons in the active layer (needs hydrogen in the active material)
  - → this signal can be tuned through the sampling fraction

As a scale one uses often the response to a minimum ionizing particle (mip).

Sampling fraction

$$f_{samp} = \frac{dE/dx \text{ (read out)}}{dE/dx \text{ (read out + absorber)}}$$

$$e/h \text{ intr} = \frac{e/mip}{f_{ion} \cdot {}^{ion}/mip + f_n \, {}^{n}/mip + f_\gamma \, {}^{\gamma}/mip}$$

f_{ion} average hadron energy fraction deposited in form of ionization by hadrons in the cascade.

f_n neutrons

f_γ nuclear γ's

$e/mip < 1$ for high Z absorber (soft γ's are absorbed due to Z^5 in photoelectric cross-section)

e/mip signal calculations (EGS4) for U calorimeters

active layer fixed to 2.5 mm

absorber fixed to 3 mm layers

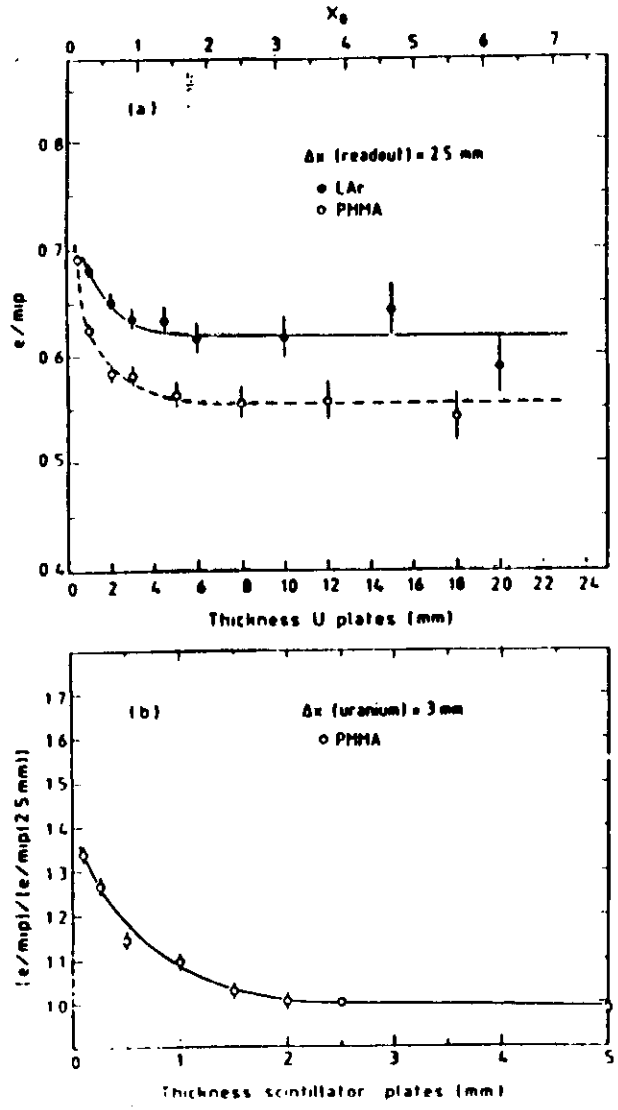

wigmans

e/mip calculations (EGS4)

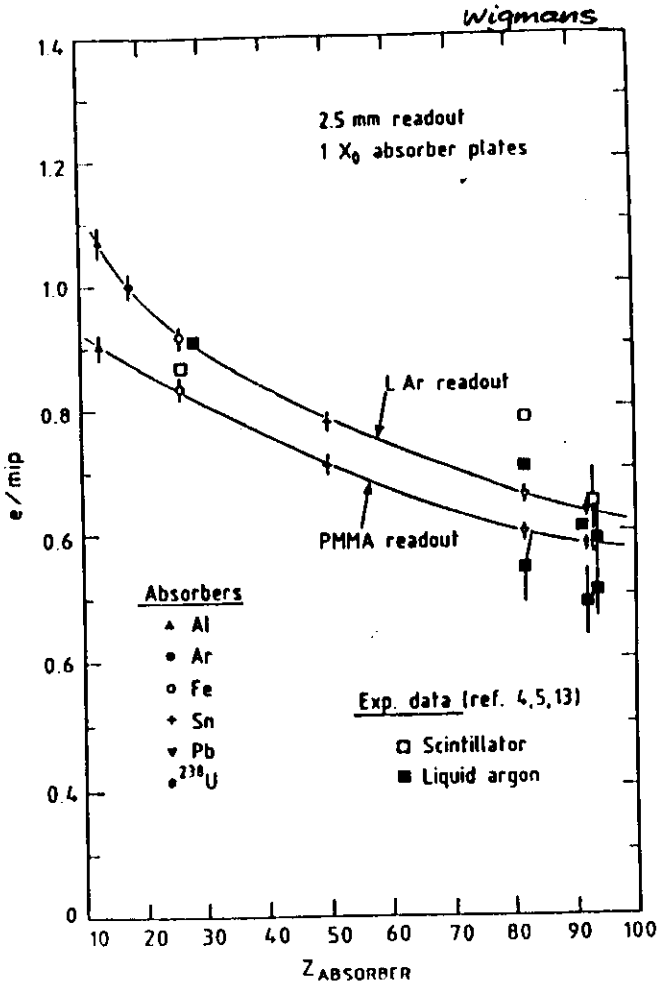

e/mip signal in case of stainless steel wrapping of the U plates (EGS4)

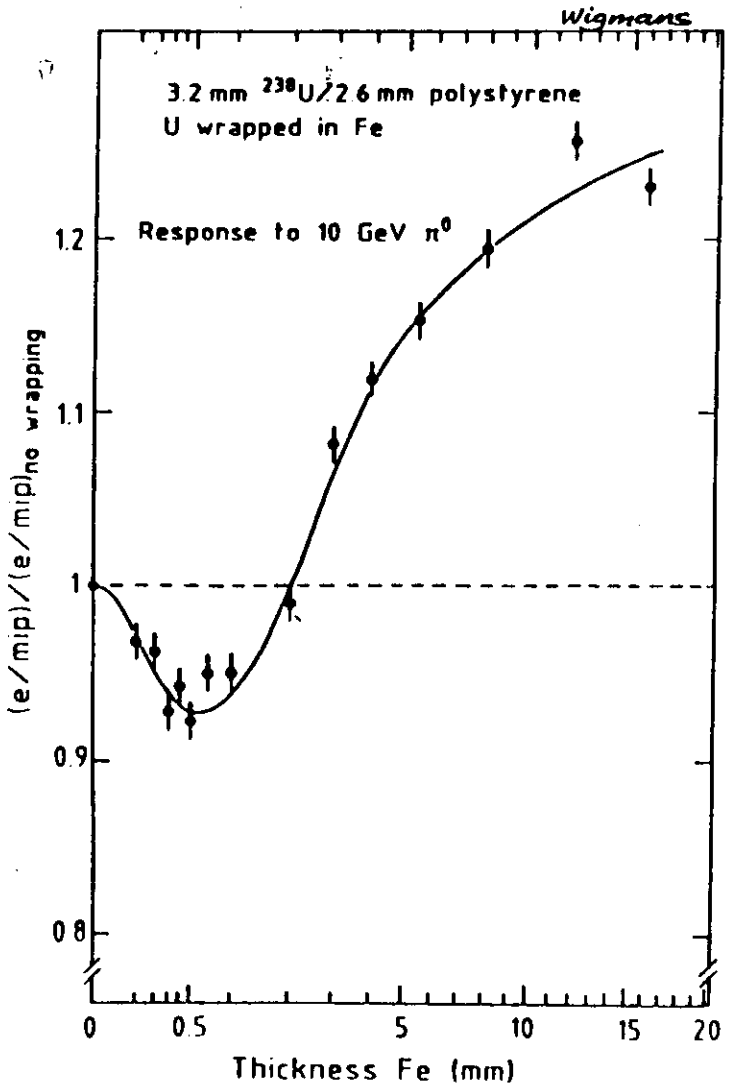

γ/mip - **large # γ from nuclear de-exitation**

- **in U^{238} there is an important contribution from nuclear fission (~ 10 fissions / GeV, each releasing ~ 7.4 MeV in form of γ's)**
- **typical response γ/mip ~ 0.4**

f_{ion} - **the contribution of charged pions from the cascade is small (10 - 15% of non-em shower part)**

- **major component comes from protons**

ion/mip

- **$\pi^{\pm}$, $K^{\pm}$ ... behave like mip**
- **low energy p behave different (saturation effects etc)**

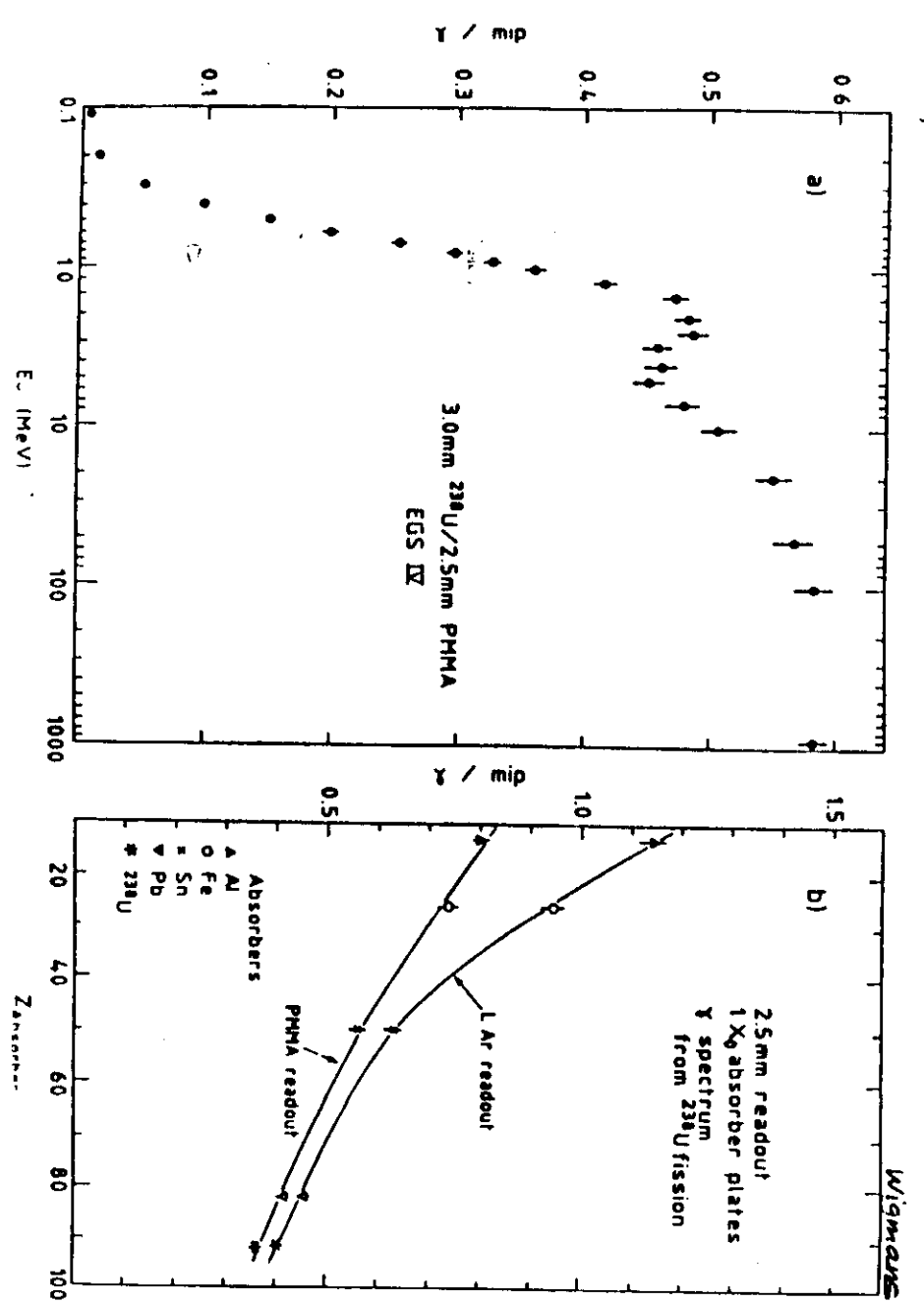

γ / mip values

f_n - varies from ~8% for Fe to ~ 15% for U

n/mip

- soft neutrons are the most important component to "tune" the compensation by detection of recoil protons
- depends on the sampling fraction
- depends on the signal integration time

cross-sections for neutron-induced reactions

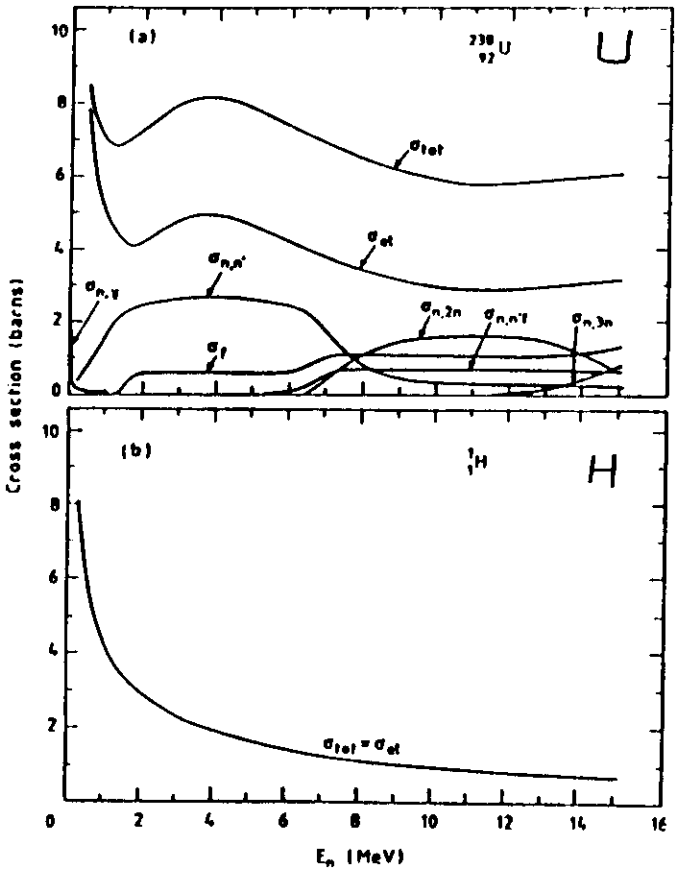

n/mip

different contributions for the U/scintillator case

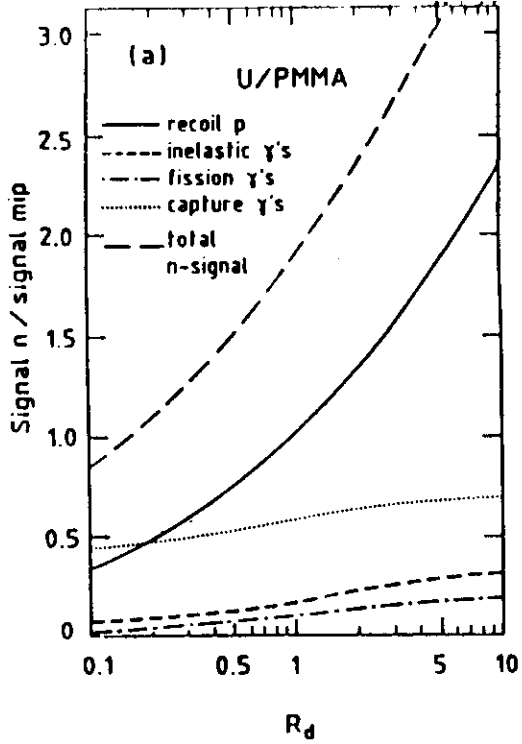

e/h ratio for different contributions from the γ's released in thermal n capture in a U/scint. calorimeter

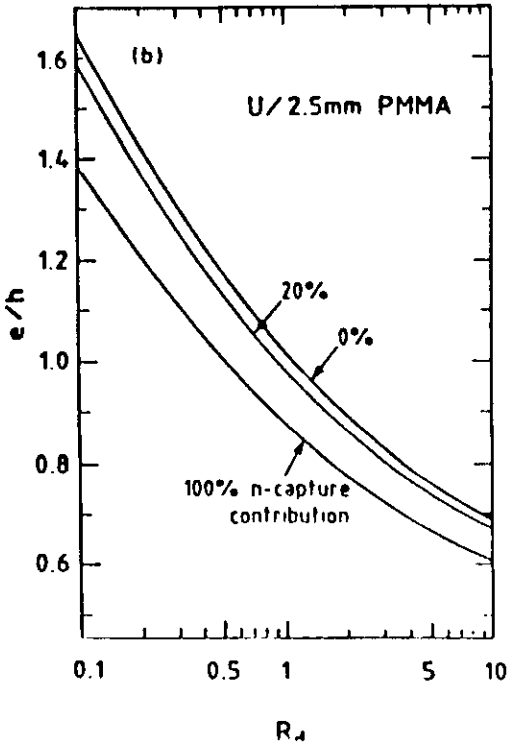

R_d : passive over active layer thickness ratio

effect of the low-energy neutrons in a U / gas calorimeter (L3)

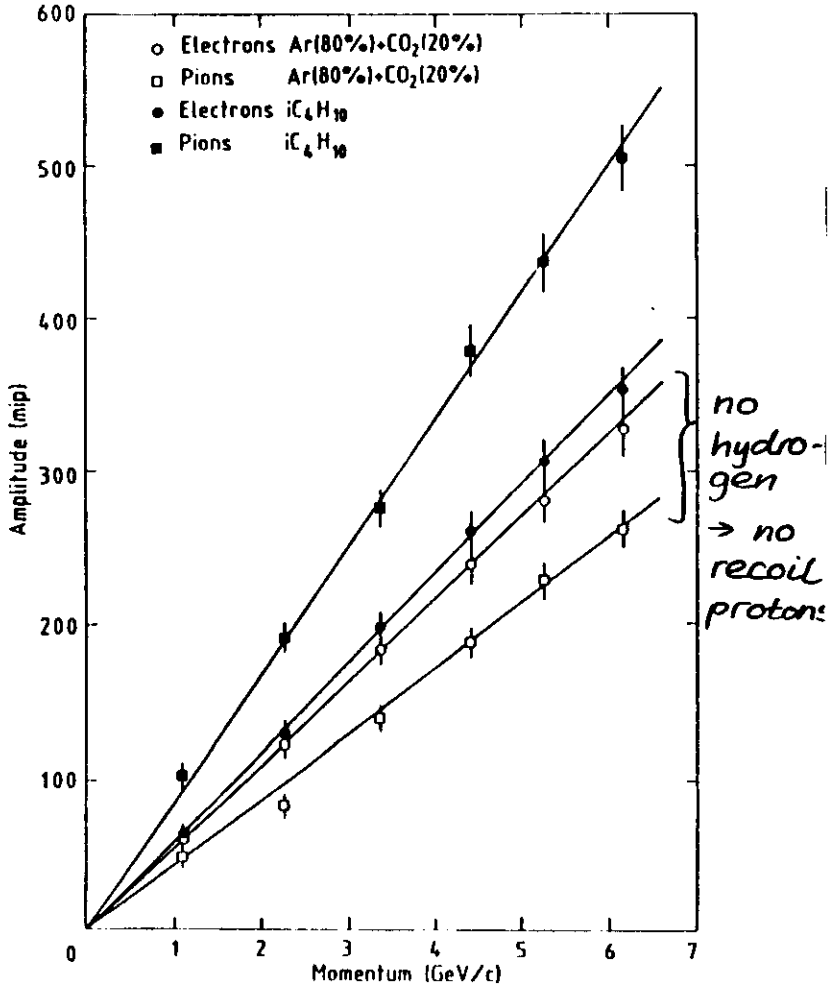

neutron response in a U / gas calorimeter (L3)

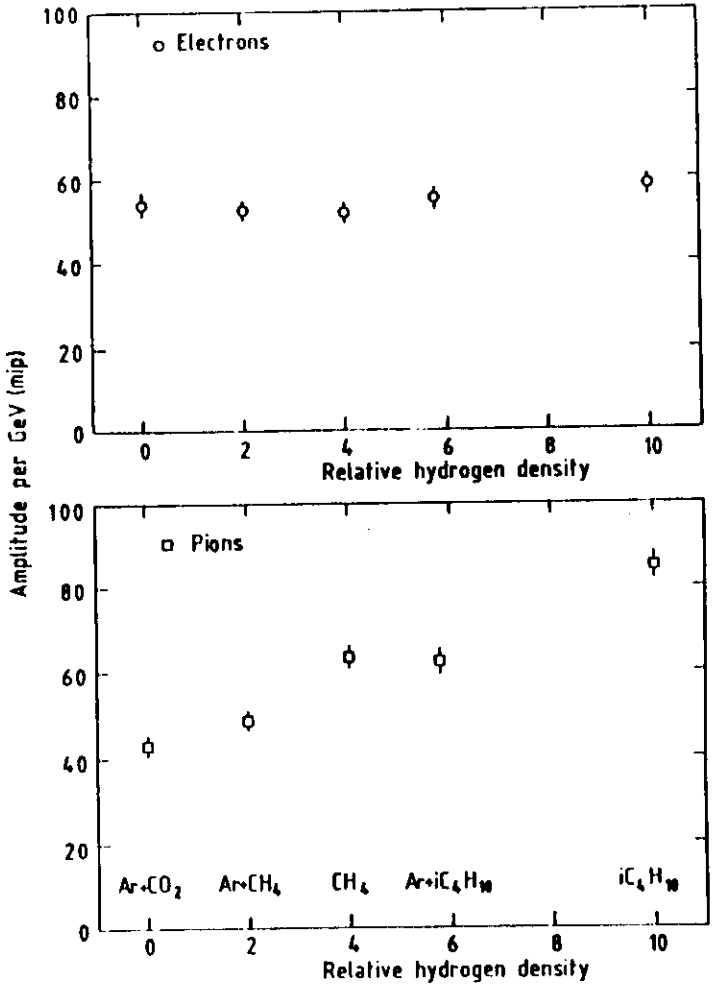

Uranium/copper scintillator

AFS Collaborations (1985)
HELIOS

3mm U 5mm
2 : 1
2.5 mm sc.

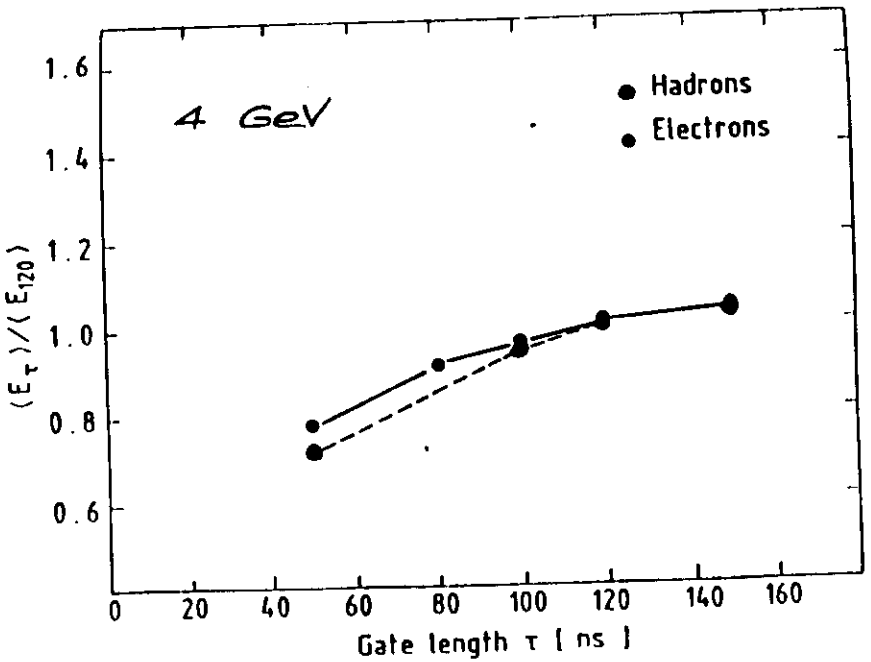

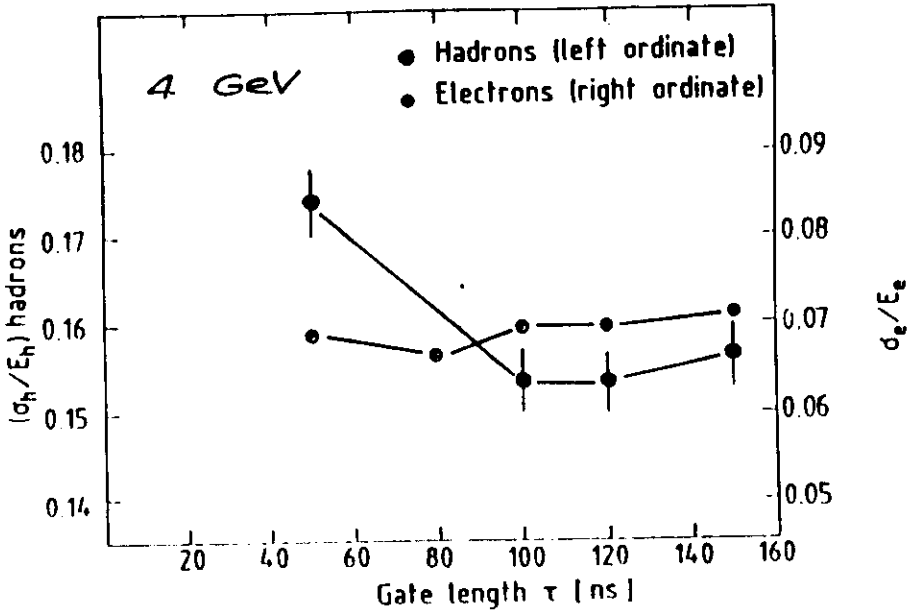

Time evolution of the effects contributing to the compensation

H. Brückmann, HERMES MC simulation (1986)

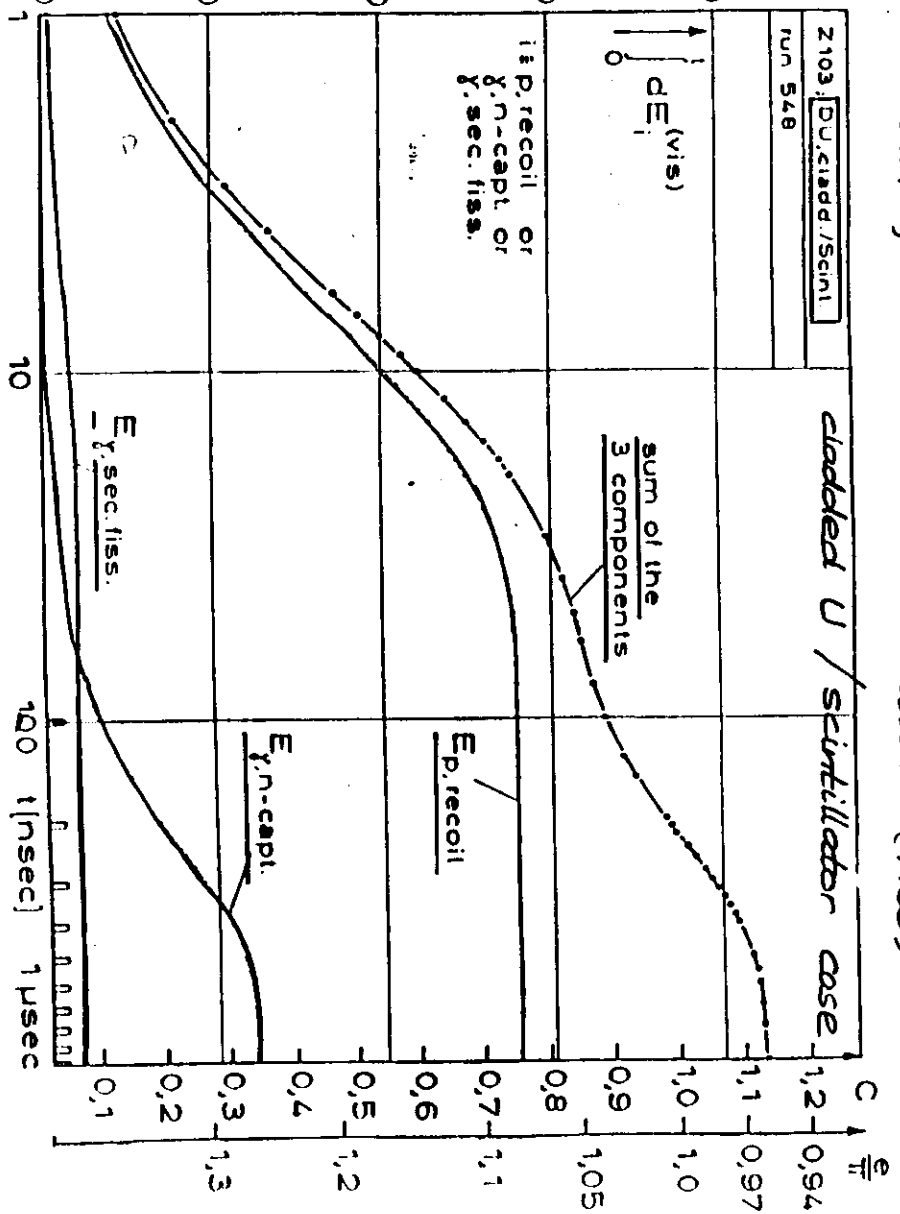

Direct observation of the difference in time structure of the signals from em and hadronic showers at 150 GeV. (Pb / sintillating fibre R+D LAA)

two effects:

- em showers more localized
  → no spread in light travel time
- slow components in hadronic shower

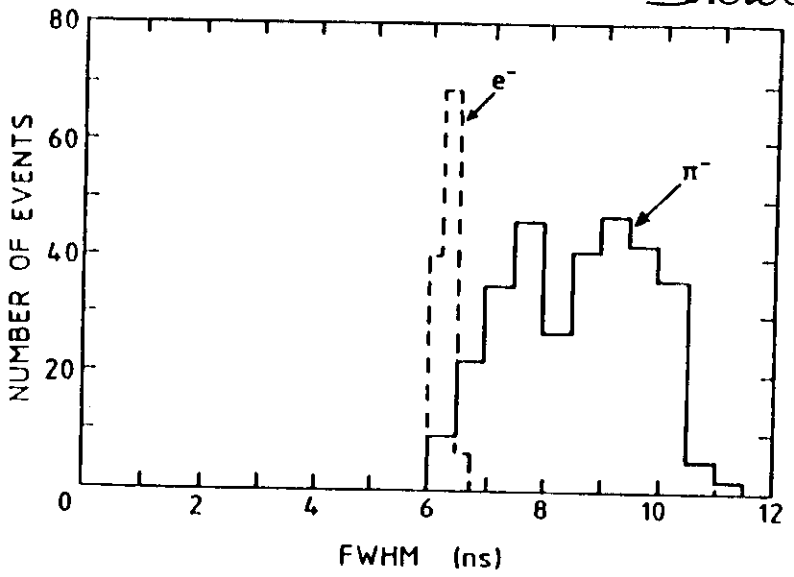

In summary many effects contribute to e/h and have to be considered to achieve e/h ≈ 1 :

- **Z of the absorber and active media**
- **hydrogen content of active medium**
- **saturation (kB) active medium**
- **nuclear physics properties of absorber**
- **signal integration time**
- **thickness of passive and active layers**
- **sampling fraction**

e/h ≈ 1 cannot be achieved for all absorber and read out combinations :

The calculations are often expressed as function of

$$R_d = \frac{\text{thickness absorber}}{\text{thickness active media}}$$

e/h ratios for different Uranium calorimeters

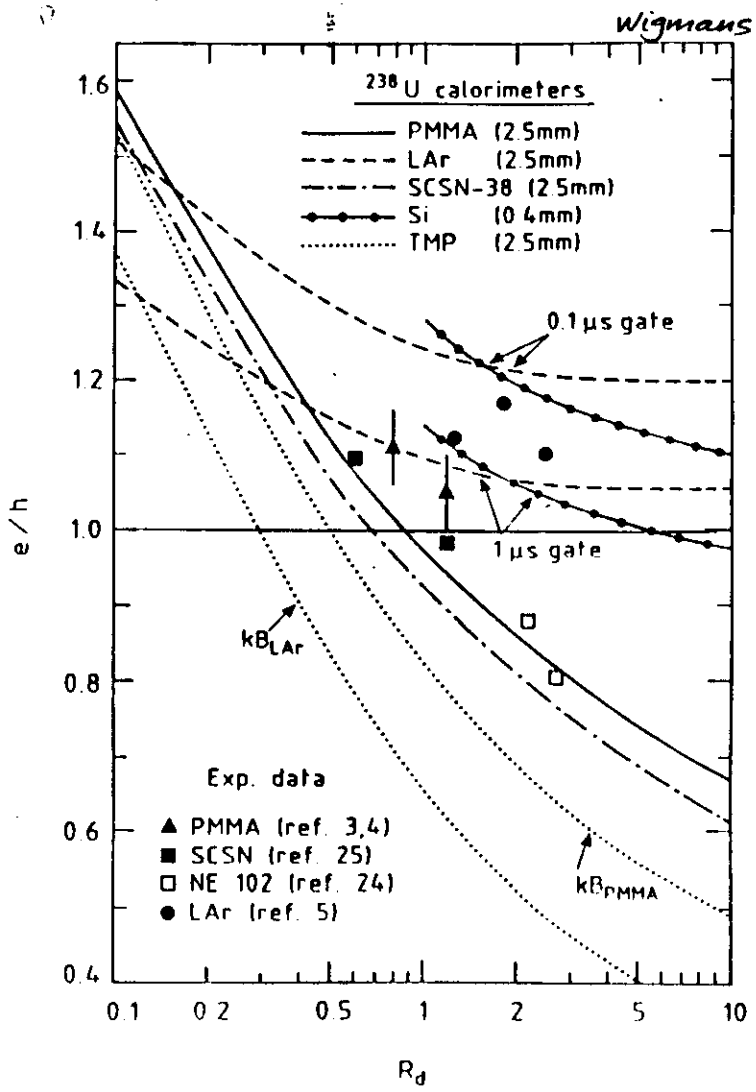

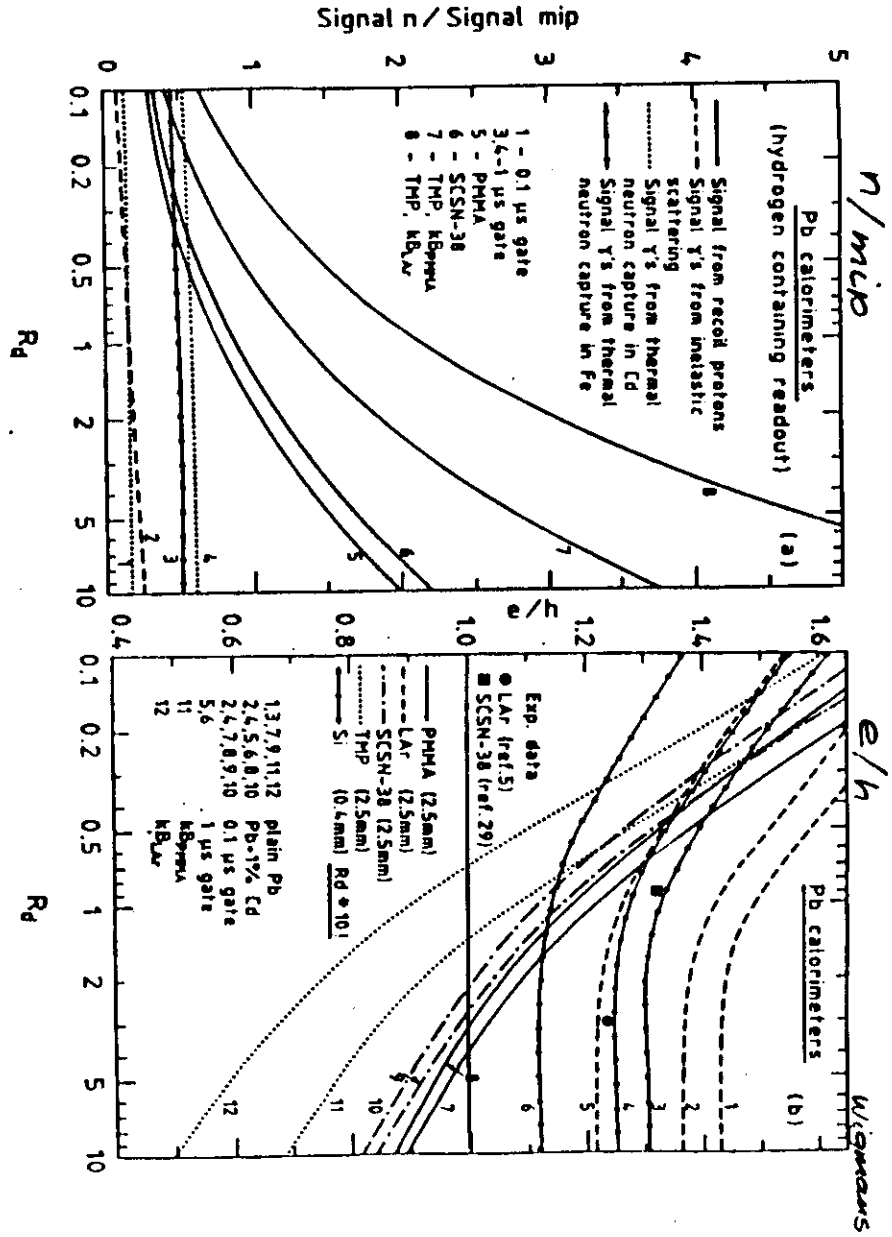

experimental resolutions

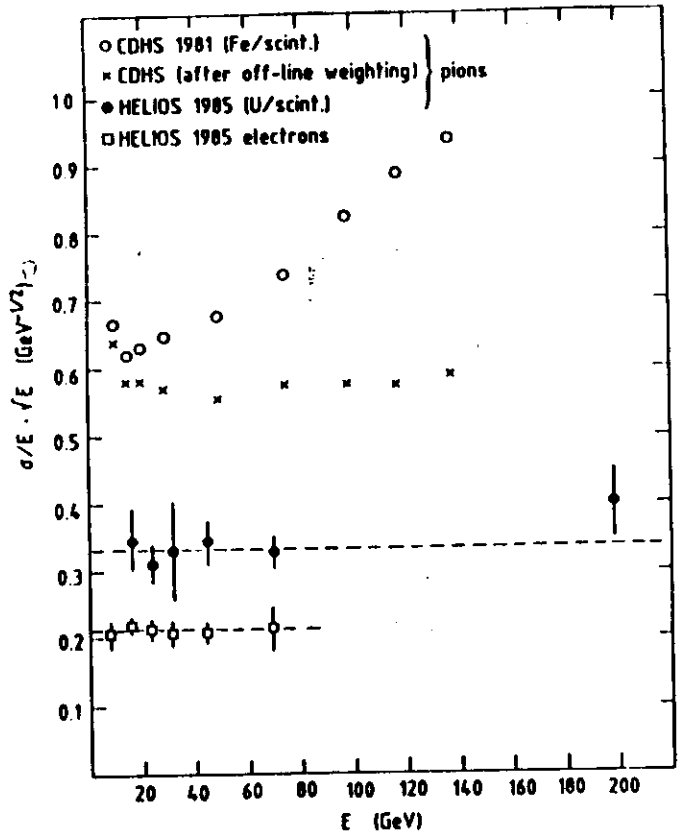

non-compensating

compensating

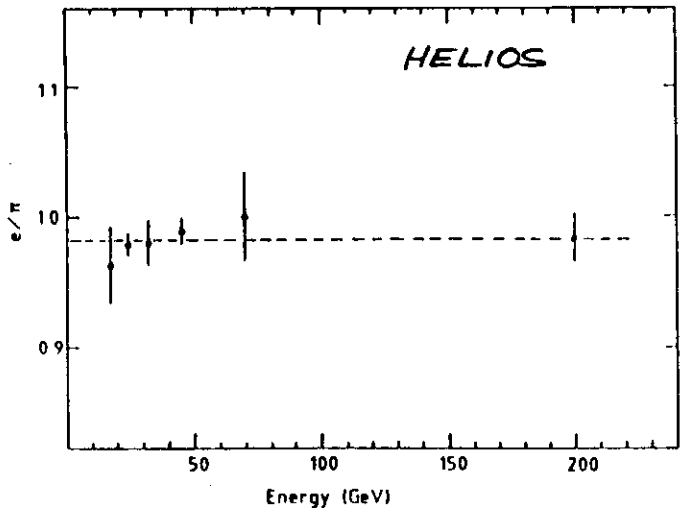

HELIOS

excellent resolution at 3 TeV total energy

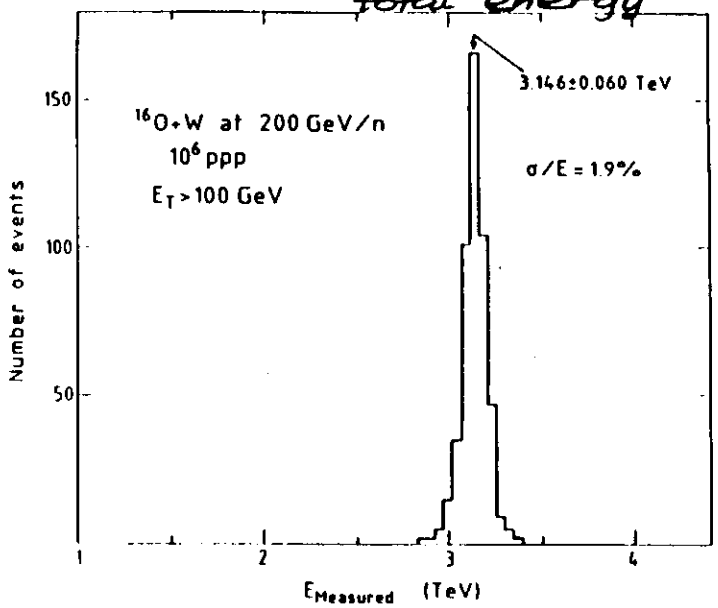

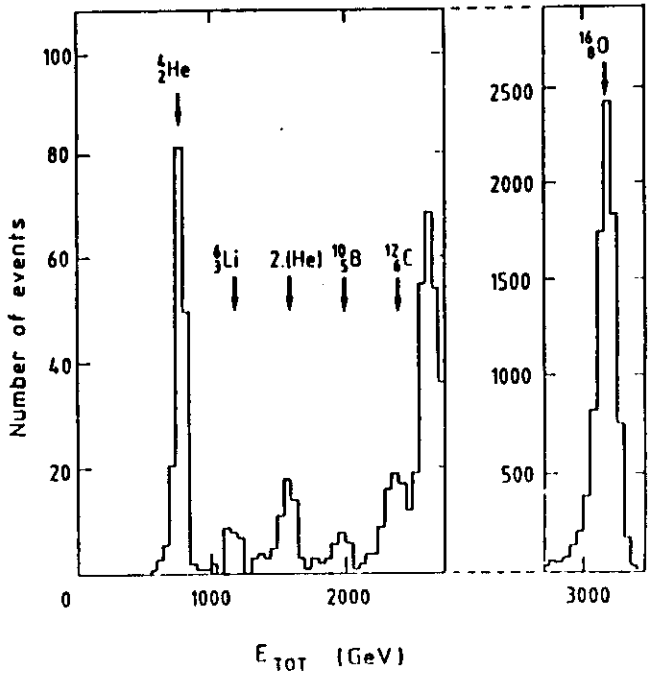

ZEUS

pre-prototype studies

Pb / scintillator calorimeter

1 cm Pb

0.25 cm scintillator

$e/h = 1.05 \pm 0.04$

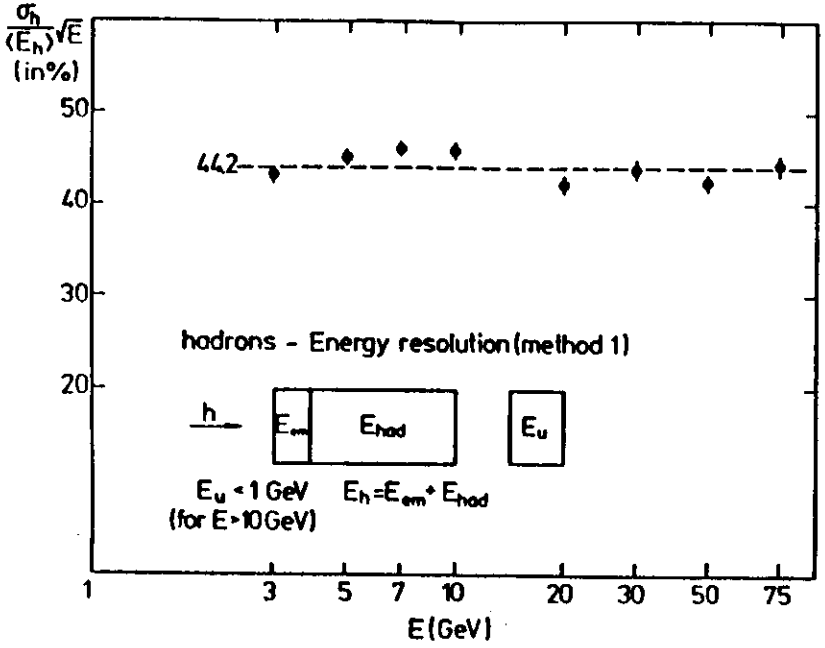

The resolution of hadronic calorimeters has a large contribution from the intrinsic resolution and from the deviation from e/h = 1.

The sampling fluctuations are typically

$$\sigma_{E/E} \approx 0.09 \sqrt{\Delta E/E}$$

ΔE energy lost by a charged particle in one sampling layer

The intrinsic fluctuations are

$$\sigma_{E/E} \approx 0.20 / \sqrt{E} \quad \text{(compensation)}$$

$$\approx 0.50 / \sqrt{E} \quad \text{(no compensation)}$$

Further contribution can come from instrumental effects and incomplete shower containment.

Sampling fluctuations

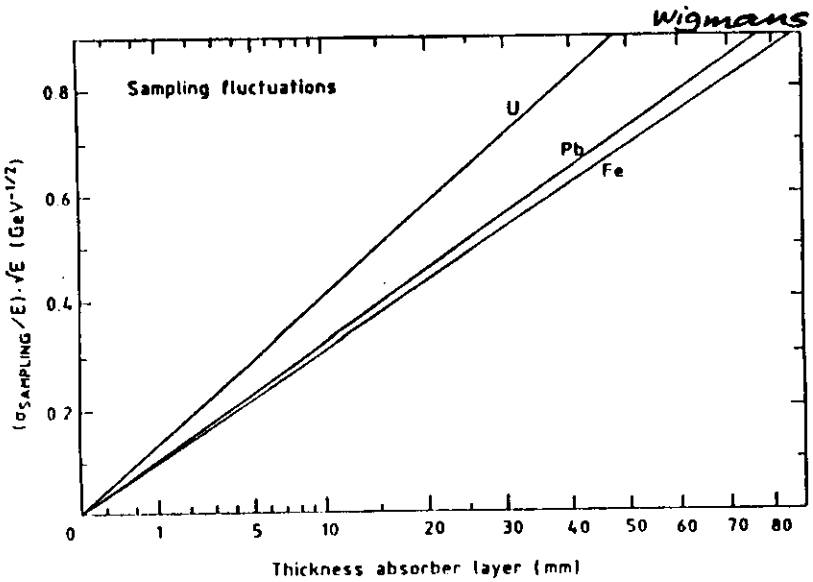

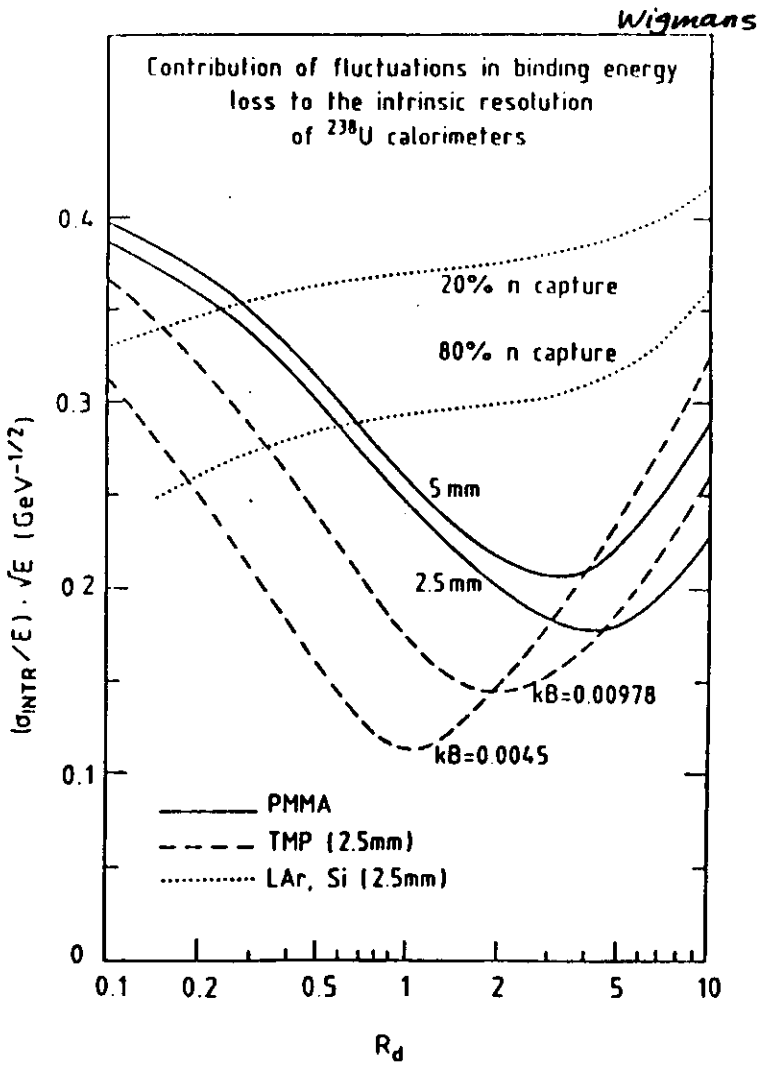

Expected total resolution for Pb / 2.5 mm PMMA scintillator calorimeters

Expected resolution for the Pb / scintillating fibre R+D calorimeter

1 mm ϕ fibres

$R_d \propto 4$

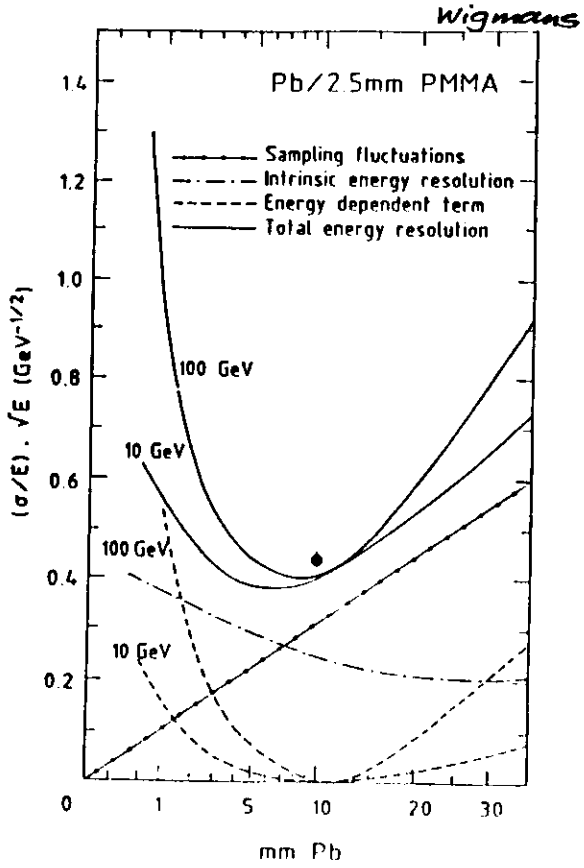

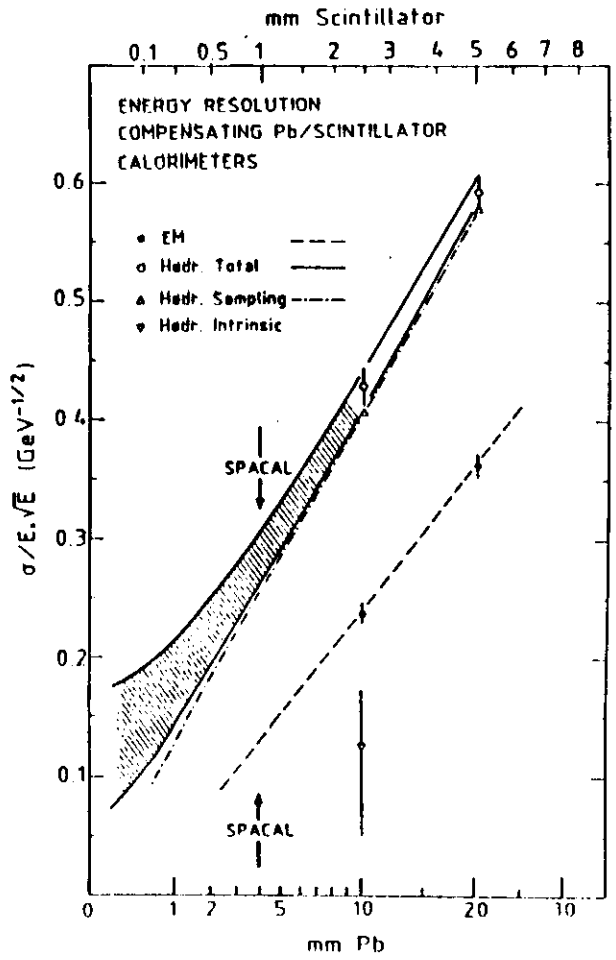

Some typical hadron calorimeter performances of collider experiments:

A — UA2 Pb and Fe/scintillator

B — UA1 proto. U/TMP followed by Fe/scintillator $54\%/\sqrt{E} \oplus 8\%$

C — DØ U/LAr $48\%/\sqrt{E} \oplus 5\%$

D — H1 Pb and Fe/LAr with weighting $45\%/\sqrt{E} \oplus 2\%$

E — ZEUS U/scintillator $35\%/\sqrt{E} \oplus 2\%$

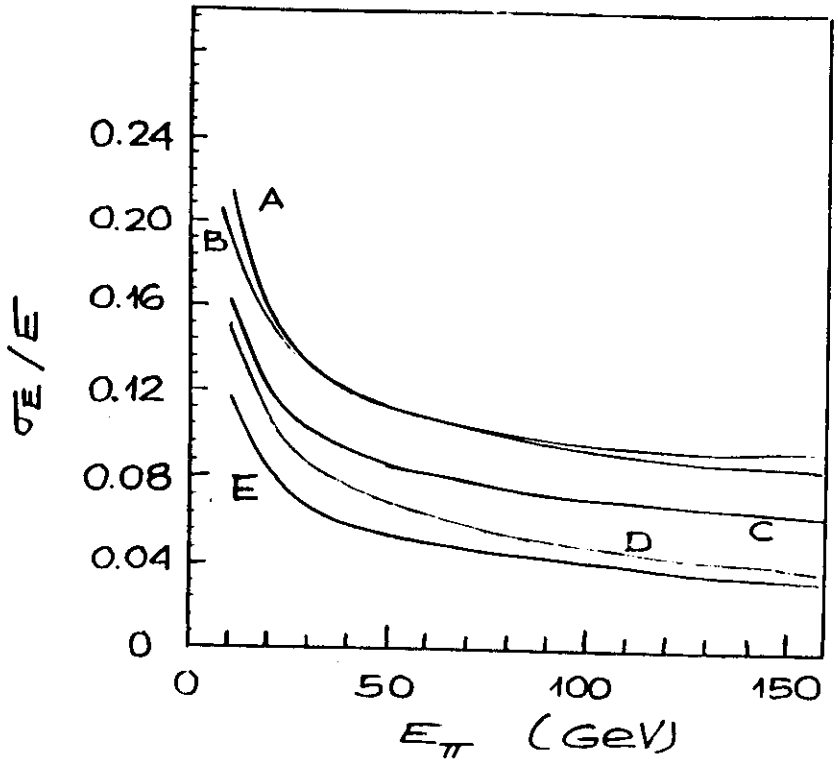

VI CALIBRATION ISSUES

Resolution and linearity are not the only important aspects for the performance of a calorimeter in a real experiment.

- One needs to know the absolute energy scale, namely the equivalence of an observed charge signal (pC) to the incident particle energy (GeV)
  → calibration constant

- This calibration constant needs to be known for each cell of the calorimeter.
  In an ideal case all cells have the same constant.

- The resolution of a physics signal (for example $Z \rightarrow e^+e^-$ or $W \rightarrow$ jet + jet) will depend also on the fluctuations of the calibration for each cell.

- Furthermore for a real experiment the calibration has to be known typically over long periods of serveral years.

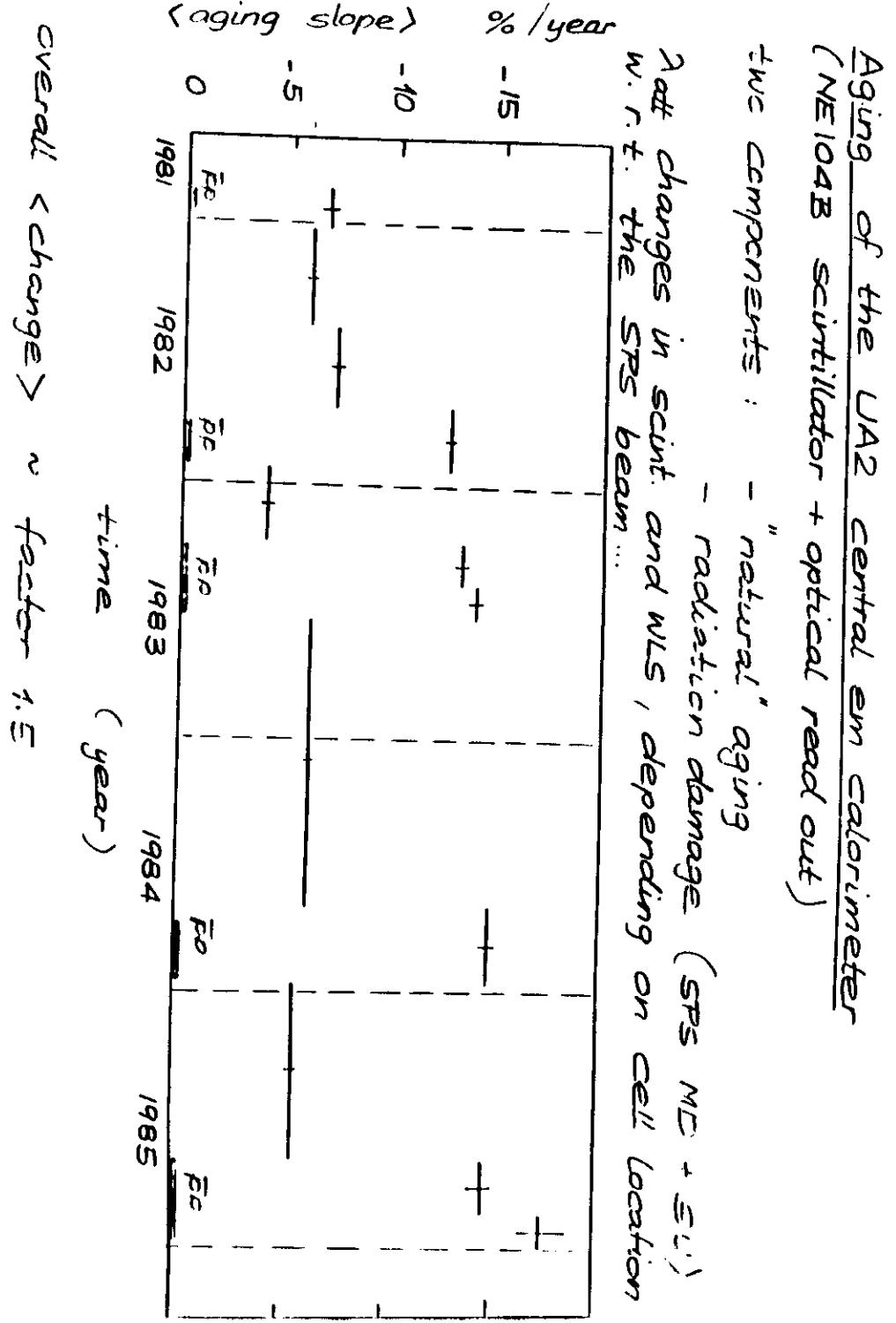

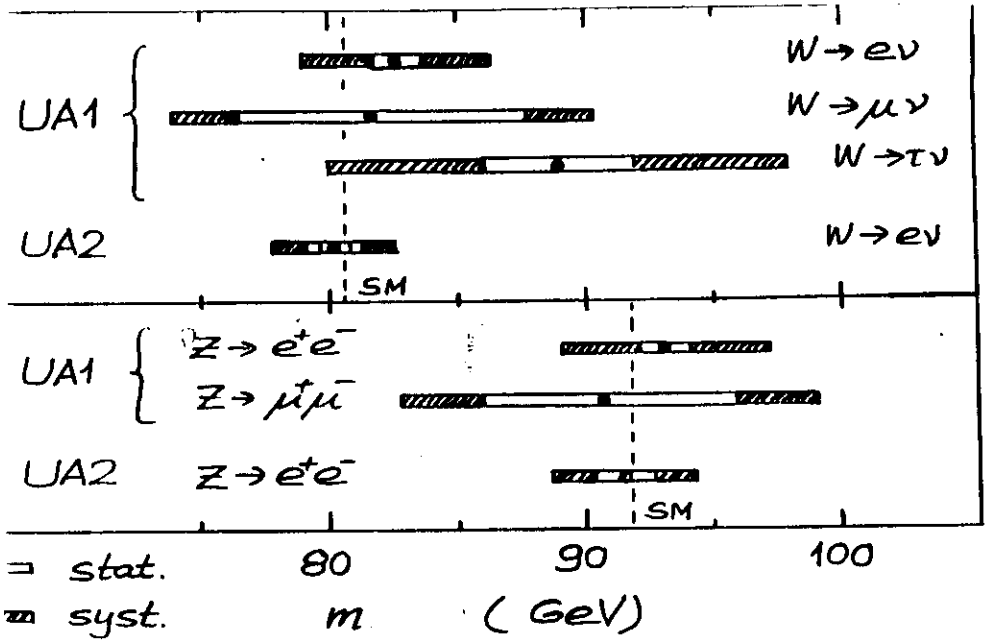

errors are (almost) dominated already by systematics → calorimeter calibration

example:

UA2 recalibration in test beam of 4 modules (of 24) after 4-5 years at the collider

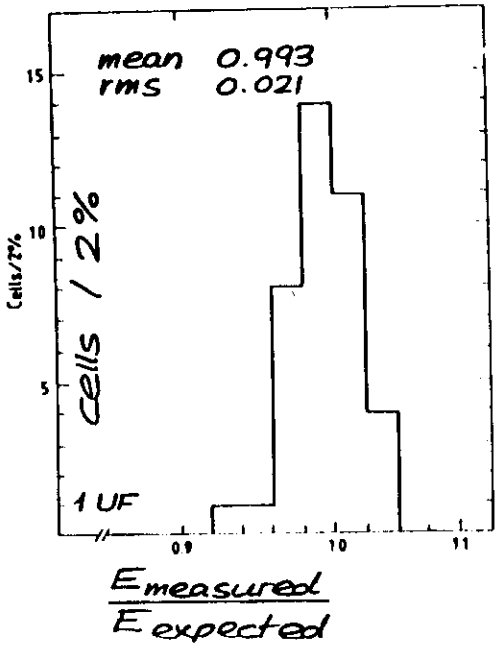

Methods of initial calibrations :

- **Test beam with known particle energy for all calorimeter. Best method, but maybe not practical for future calorimeters with very large amount of cells. Very difficult / impossible for calorimeters which are not modular (example LAr devices) examples : UA2, ZEUS in order to reach an absolute calibration ≈ 1%.**

- **Test beam with known particle energy for sample modules. Extrapolating to other modules by**
  - **radioactive sources (example U noise in U/scintillator calorimeters**
  - **material control (measuring absorber and active layer thickness, controlling liquid purely and response with calibrated test chambers, relying on an absolutely known dE/dx response in Silicon, ...)**

- Using known physics signals ($\pi^0 \rightarrow \gamma\gamma$, $Z \rightarrow e^+e^-$ ...) is difficult at hadron colliders.
  $e^+e^- \rightarrow e^+e^-$ has been used at e^+e^- storage rings.

Checks of the calibration for a running experiment

- radioactive sources
- charge injection systems
- light flasher systems
- average energy distributions in unbiassed data
- muon signals
- transverse energy balance of jet-jet events (hadron colliders) or e-jet events (HERA)

Two comments on the calibration in a test beam for calorimeters with longitudinal samples.

- Often the first samples are used for (and called) em calorimetry and are calibrated with electrons.

  In most cases a finer sampling is used for this em part to obtain a good resolution for electrons.

  If e/h # 1 this calibration differs from the one which has to be used for hadrons. This is typically the case for mixed calorimeters with Pb absorber plates for the em part and Fe absorber plates for the hadronic part.

  The best resolution for hadrons is therefore not always obtained from the direct sum of the signals from the different longitudinal samples. Relative global calibration constants may be required for these samples.

- In order to calibrated longitudinal samples in a calorimeter muons are used because they deposite energy that can be fitted more easily (Landau peak) than the broad distributions from a partial hadron shower.

  In this case it is important to take into account that μ/mip is energy dependent.

ZEUS test calorimeter Pb/scint.

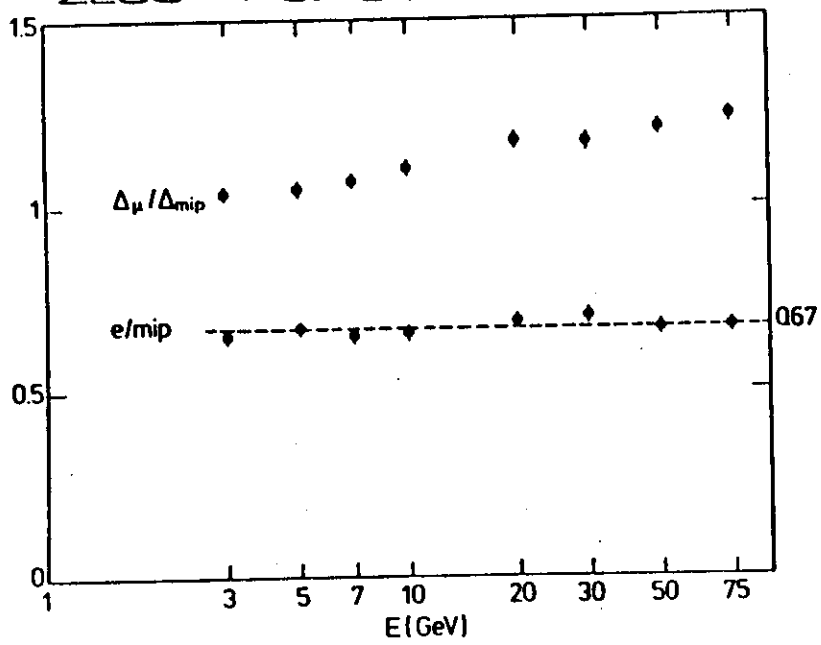

muon signals at various energies in the HELIOS U/scintillator calorimeter.

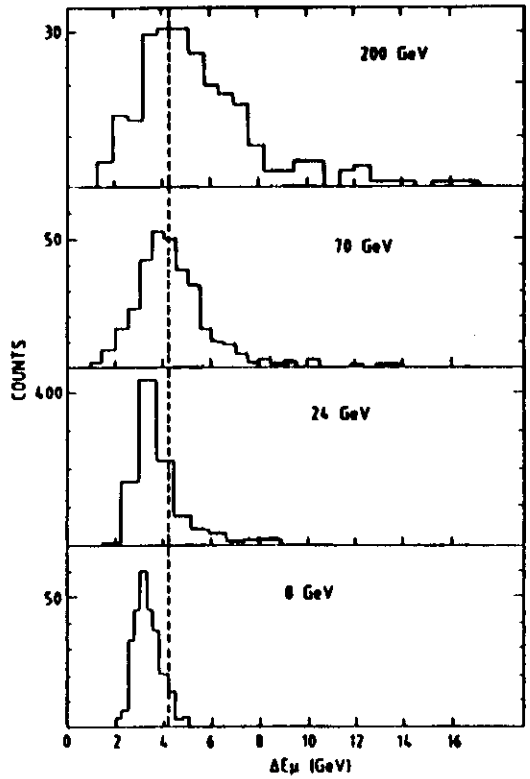

VII JET CALORIMETRY AND MISSING TRANSVERSE ENERGY MEASUREMENTS

Jets consists of many particles with various energies. Large fluctuations occur in the $\pi^0/\pi^\pm$ composition. Also very low energy particles contribute in a very significant way to the total jet energy.

Compensation (e/h = 1) is again the best tool to have the best jet energy resolution.

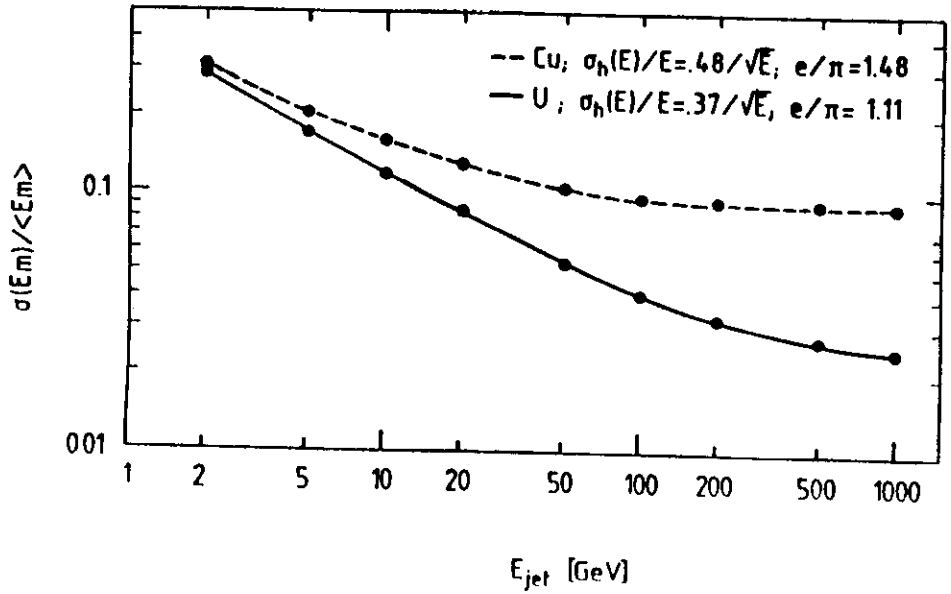

low energy particle contribution to $W^\pm \to$ jet + jet

$\bar{p}p \to W^\pm$
$\hookrightarrow$ jet + jet
$\sqrt{s} = 630$ GeV

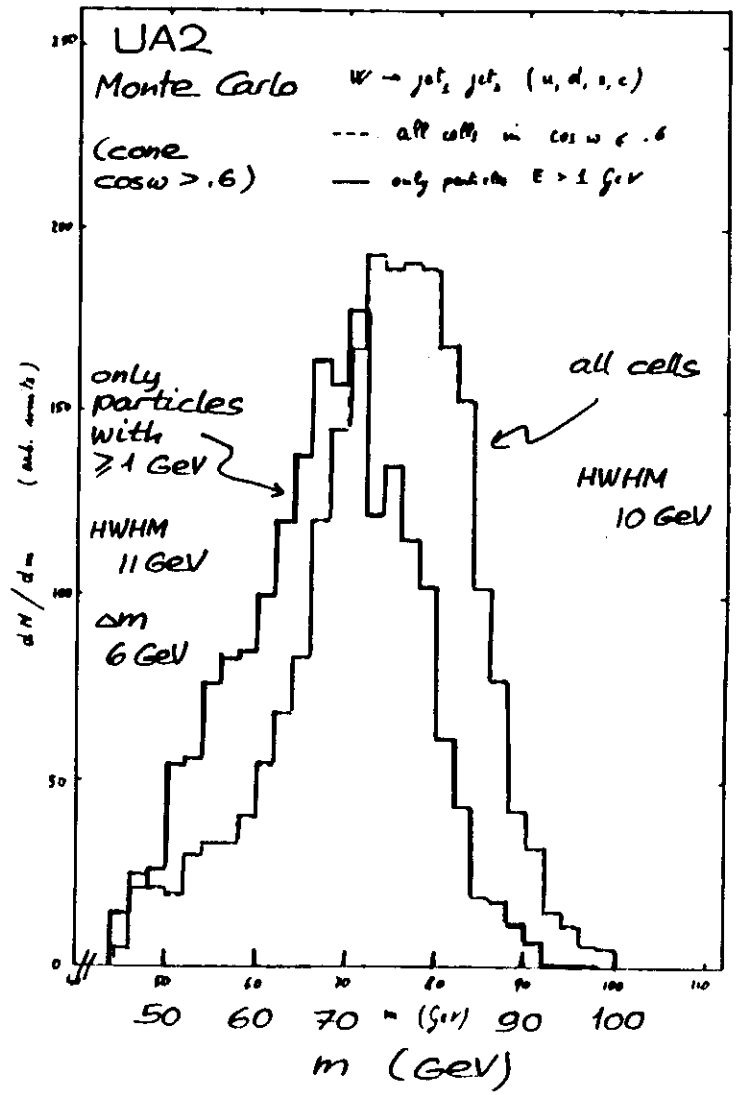

Present collider experiments (UA1, UA2, CDF) have realized that systematic errors on jet energy scales depend strongly on the knowledge of the calorimeter response to very low energy jet fragments.

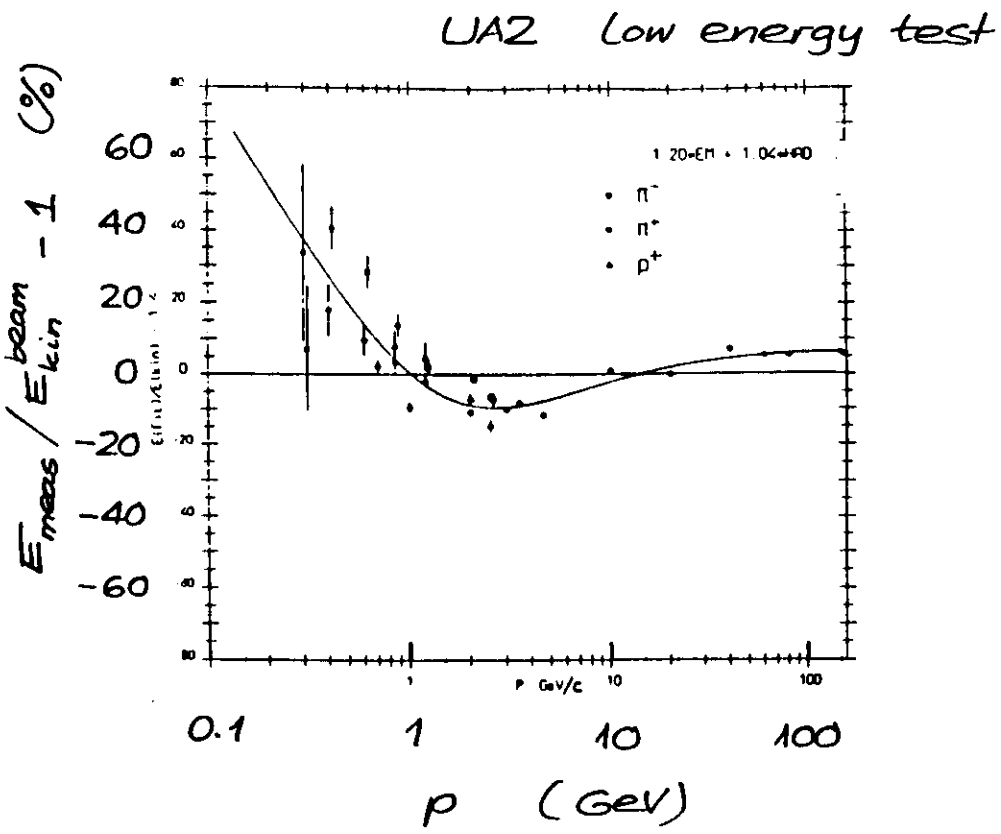

Missing transverse energy measurements are an important tool to search for new physics processes (see introduction).

The main factors which determine the performance of a collider experiment calorimeter in this respect are :

- angular coverage with respect to the beam
- full azimuthal coverage
- minimal cracks between calorimeter cells or modules (non-pointing cracks)
- energy resolution
- shower containment

In addition the experiment should have a muon detection system to eliminate events where the missing transverse energy in the calorimeter is due to muons.

2 - jet events; $p_T^{jet} > 25$ GeV, $20^\circ < \vartheta < 160^\circ$

(larger p_T's are more central...)

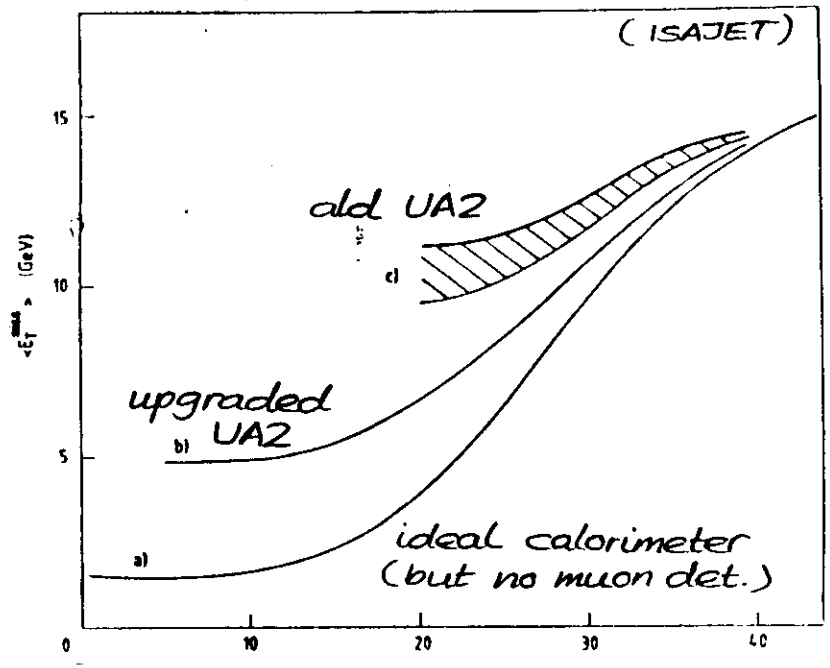

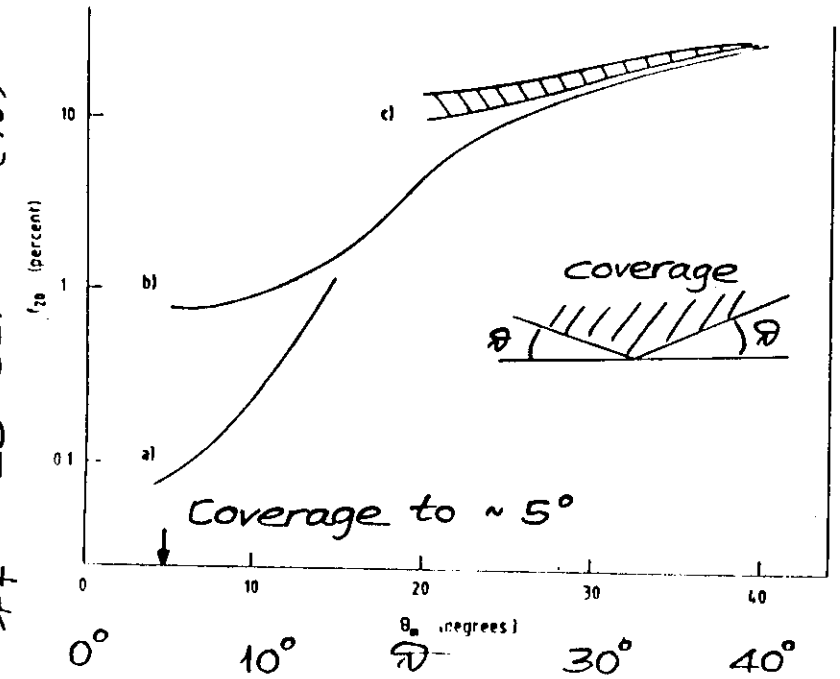

$\not{p}_T$ resolution

(the best of the present collider experiments)

$$\frac{dn}{d\not{p}_T^2} = \frac{1}{\Delta^2} e^{-(\not{p}_T/\Delta)^2}$$

$$\Delta = 0.82 \, (\Sigma E_T)^{0.43}$$

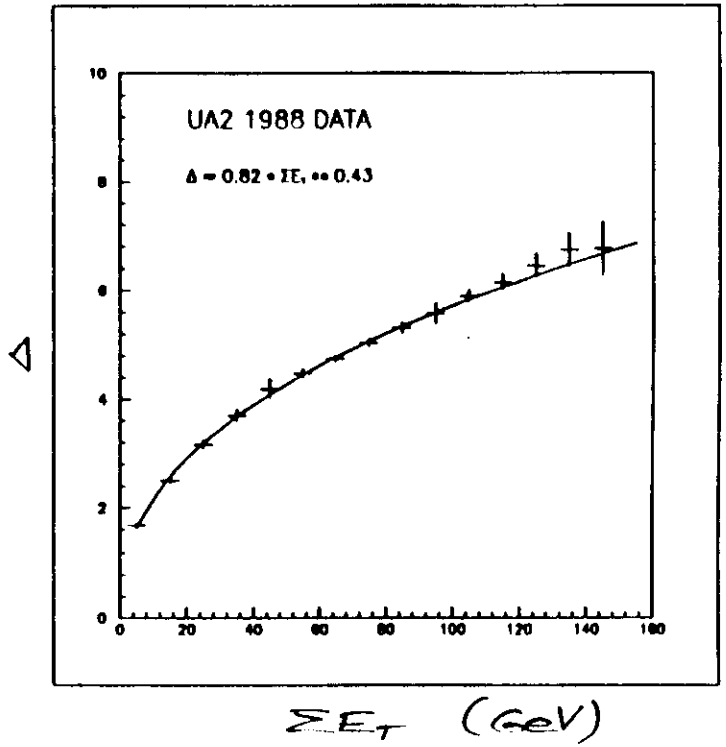

$\bar{p}p$ $\sqrt{s}$ = 630 GeV UA2

both components have Gaussian distributions

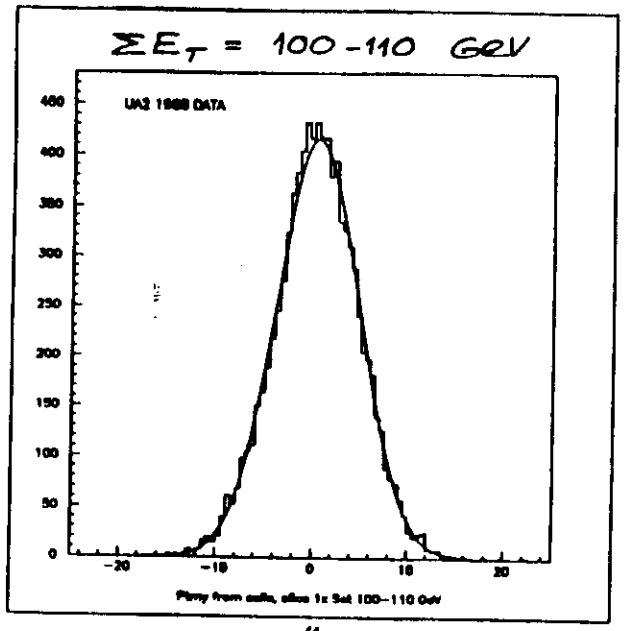

dn/dp_T^2

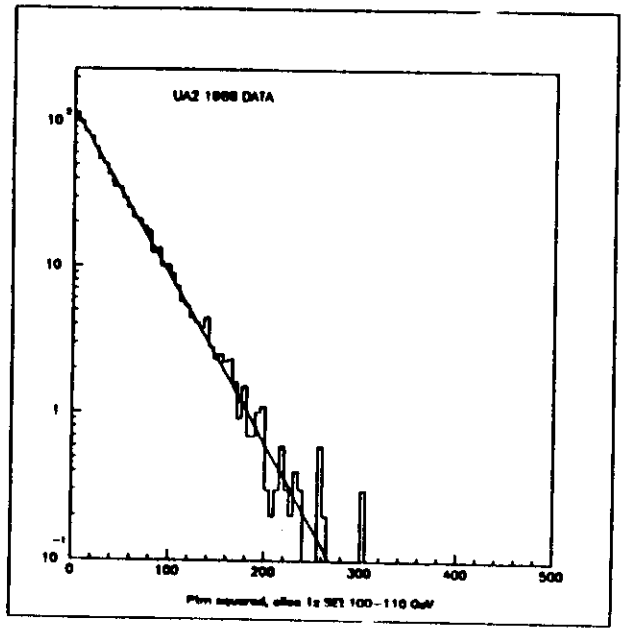

Parameters for a jet calorimeter

resolution

- **best performance (σ_E/E with no constant term and good linearity) is obtained with a compendating calorimeter with e/h = 1**
- **good calibration needed**

granularity

- **high transverse granularity for the front part (ρ_M) for electrons and larger transverse granularity (λ) for the hadronic part**
- **minimal cracks over full solid angle**
- **longitudinal segmentation governed by e/π separation requirements**

depth

- **deep calorimeters ($\approx$ 10 λ for 1 TeV jets) are required to get best resolution and to eliminate fake $\not{p}_T$ events due to late shower fluctuations**
- **economical solution is to have typically 2/3 of the depth covered with a high resolution calorimeter and the rest by a cheaper backing calorimeter combined with muon detection**

VIII CALORIMETERS IN PRESENT AND FUTURE COLLIDERS

The following examples will be briefly described :

$p\bar{p}$ CERN	:	UA1, UA2
$p\bar{p}$ FNAL	:	CDF, D0
HERA DESY	:	H1, ZEUS

Some challanges for future high energy high luminosity hadron colliders

UA1 upgrade

TMP - Uranium calorimeter ($\sim 2.5\lambda$) backed-up with the old Fe-scintillator calorimeter

a)

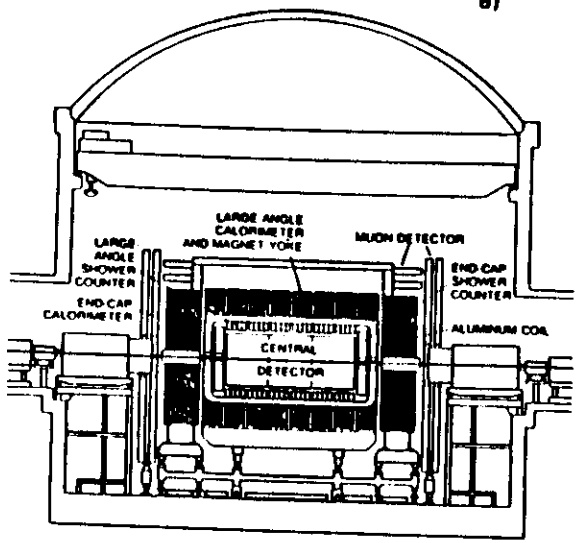

b)

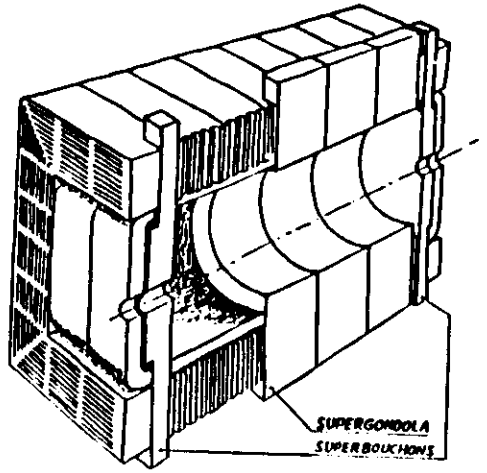

UA2 upgrade

Pb and Fe / scintillator

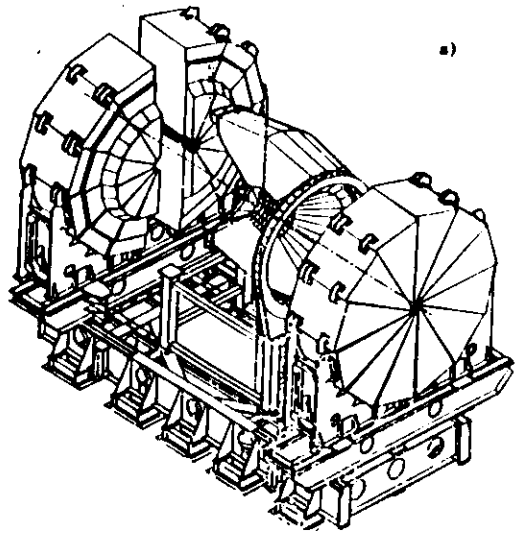

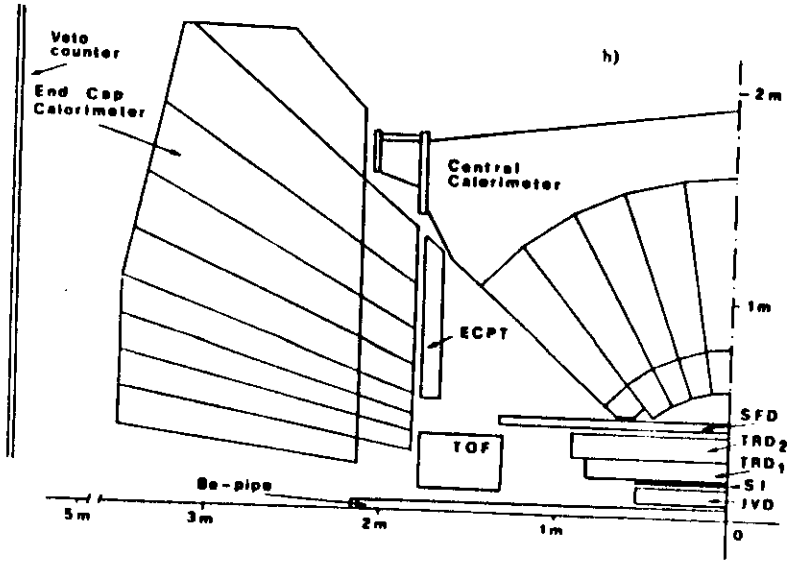

CDF

complete detector to study the general features of $\bar{p}p$ collisions at 2 TeV

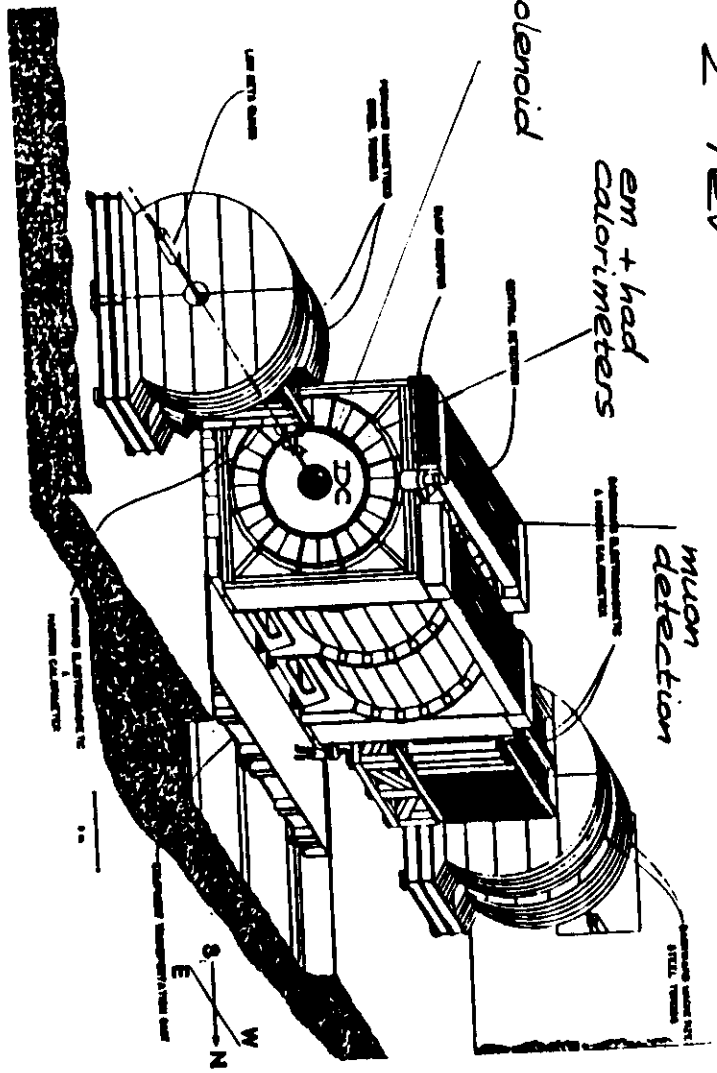

DØ

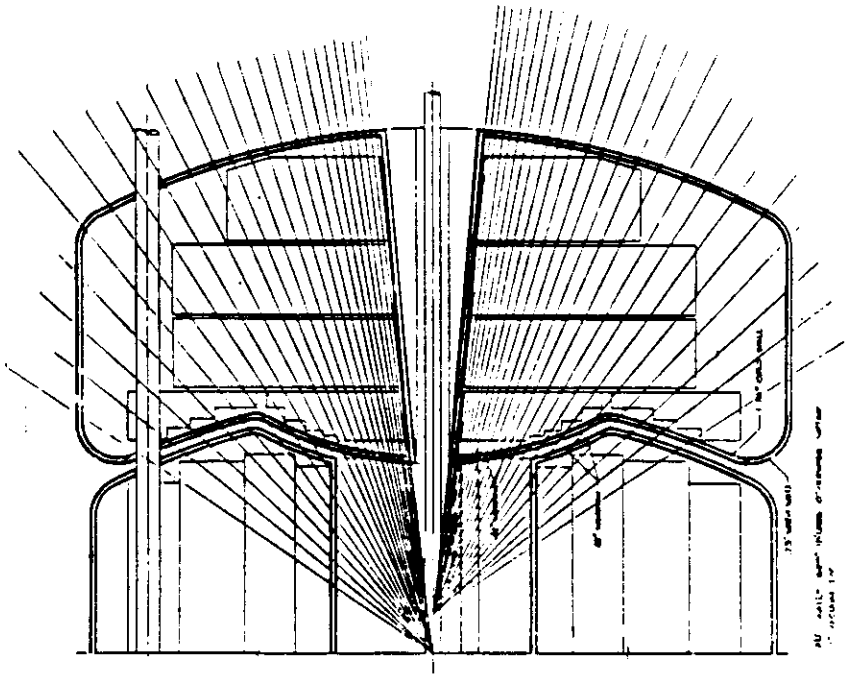

DØ major emphasis on excellent
- calorimetry (em+had energy, granularity ..)
- electron/pion separation (TRD)

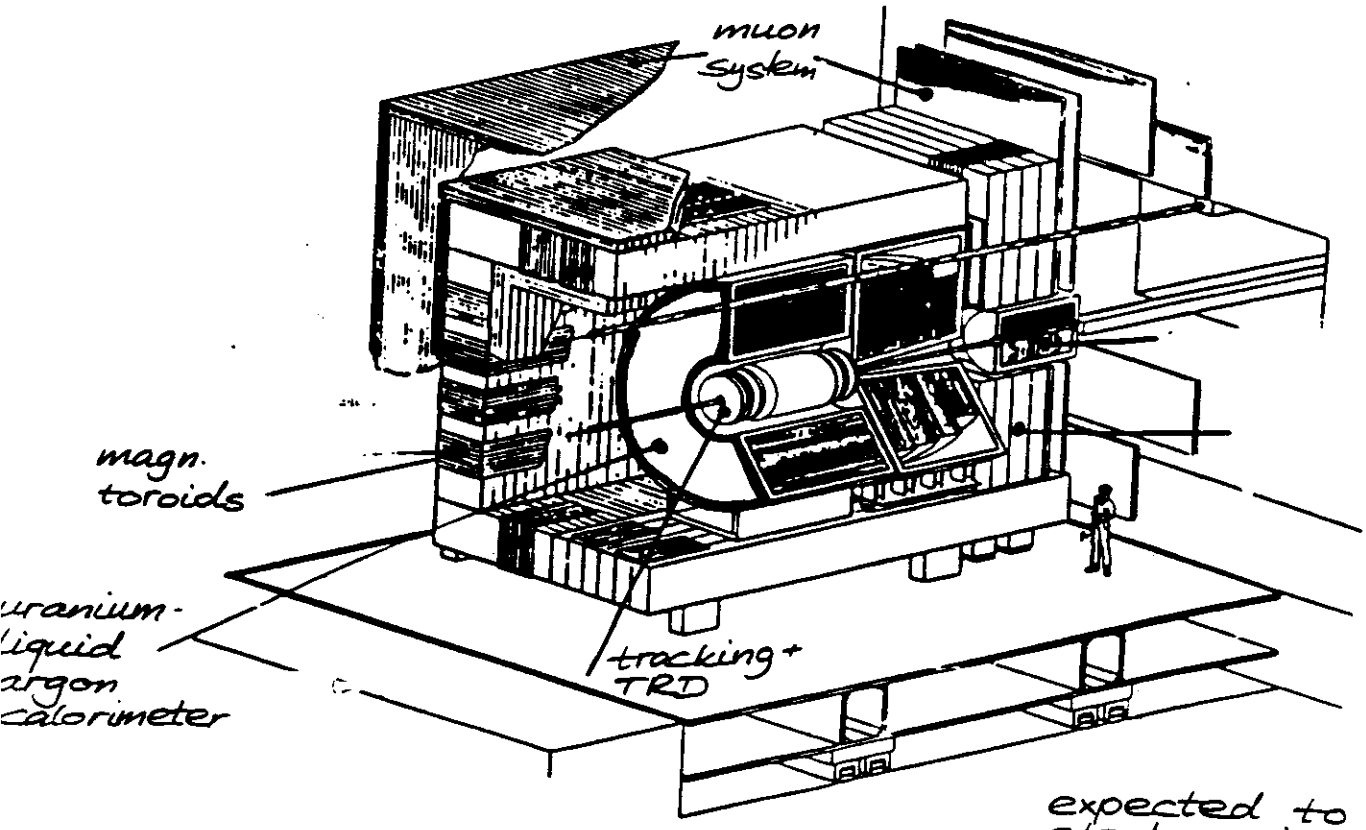

expected to start up in the coming years

DØ

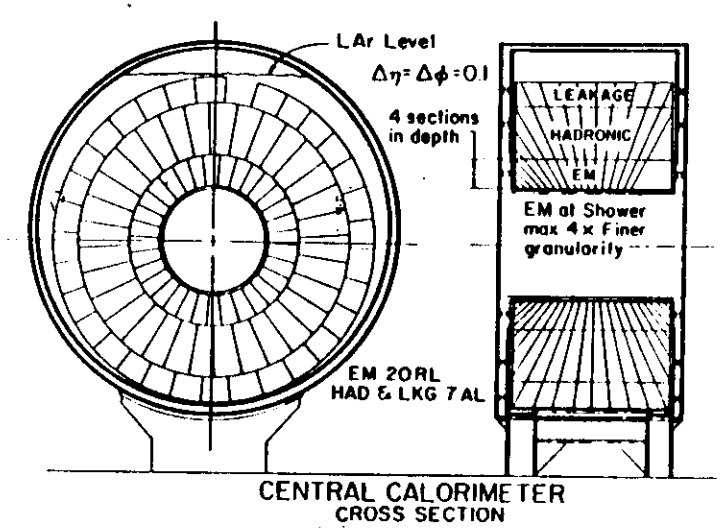

CENTRAL CALORIMETER
CROSS SECTION

END CAP CALORIMETER

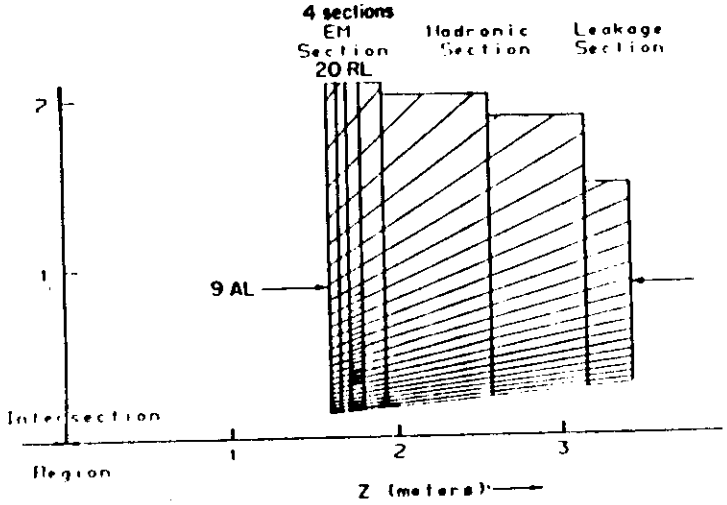

The H1 detector

Calorimetry
- liquid argon with Pb and Fe plates high granularity 45000 channels
- Fe + LST backing calorimeter

Charged particle tracking
- two jet chambers interleaved with two z chambers and MWPC in the central part
- radial and planar drift chambers, MWPCs and TRD radiators in the forward region

Field
- large superconducting solenoid outside LA calorimeter, 1.2 T
- $\sigma(p)/p = 0.003\,p$

Iron yoke
- 2000 t 7.5 cm Fe plates instrumented LST

Muon detector
- three layers of muon chambers in the barrel
- forward muon spectrometer

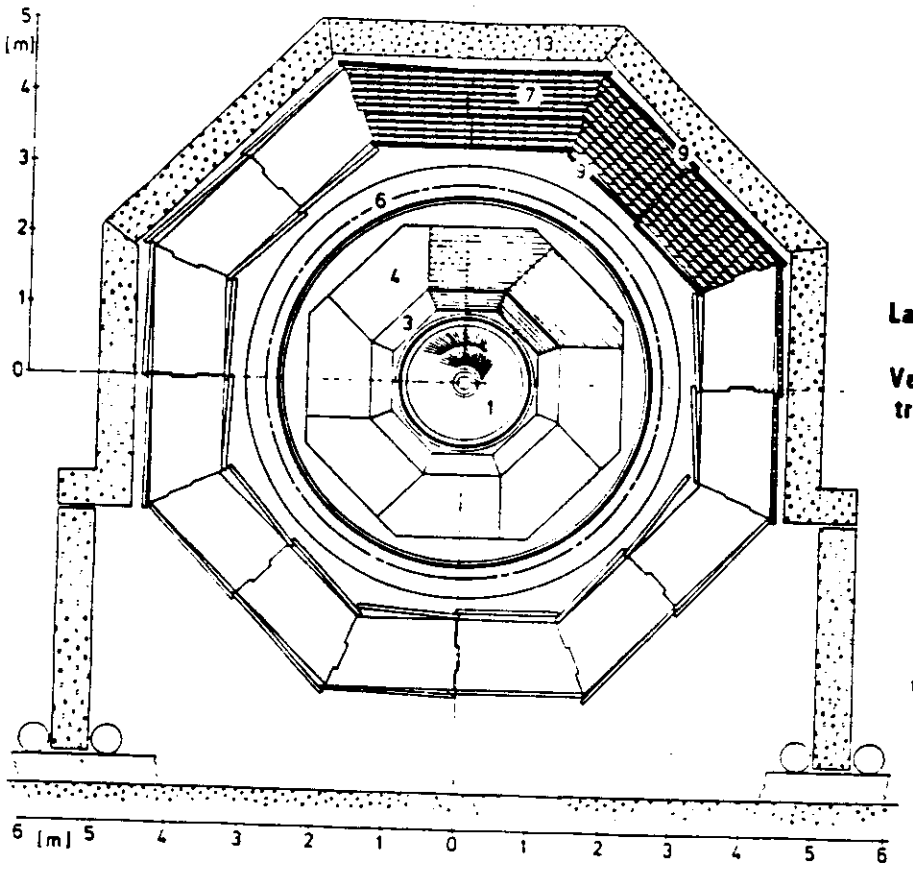

Layout of the H 1 detector

Vertical cut transversal to the beam

1 CENTRAL TRACKING
3 ELECTR. LIQU. AR. CALORIM.
4 HADR. LIQU. AR. CALORIM.
6 COIL
7 INSTRUM. IRON
9 MUON CHAMBERS
13 CONCRETE

Pb and Fe / LAr

H1

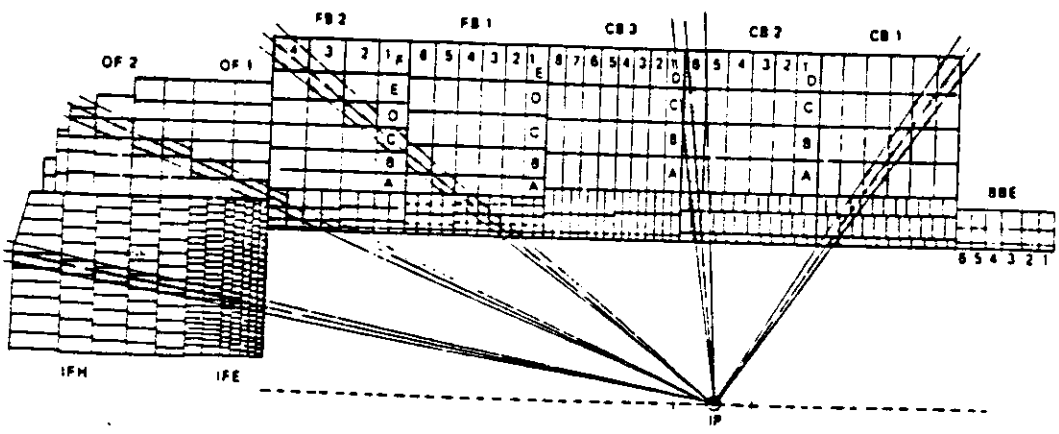

calorimeter stacks and segmentation

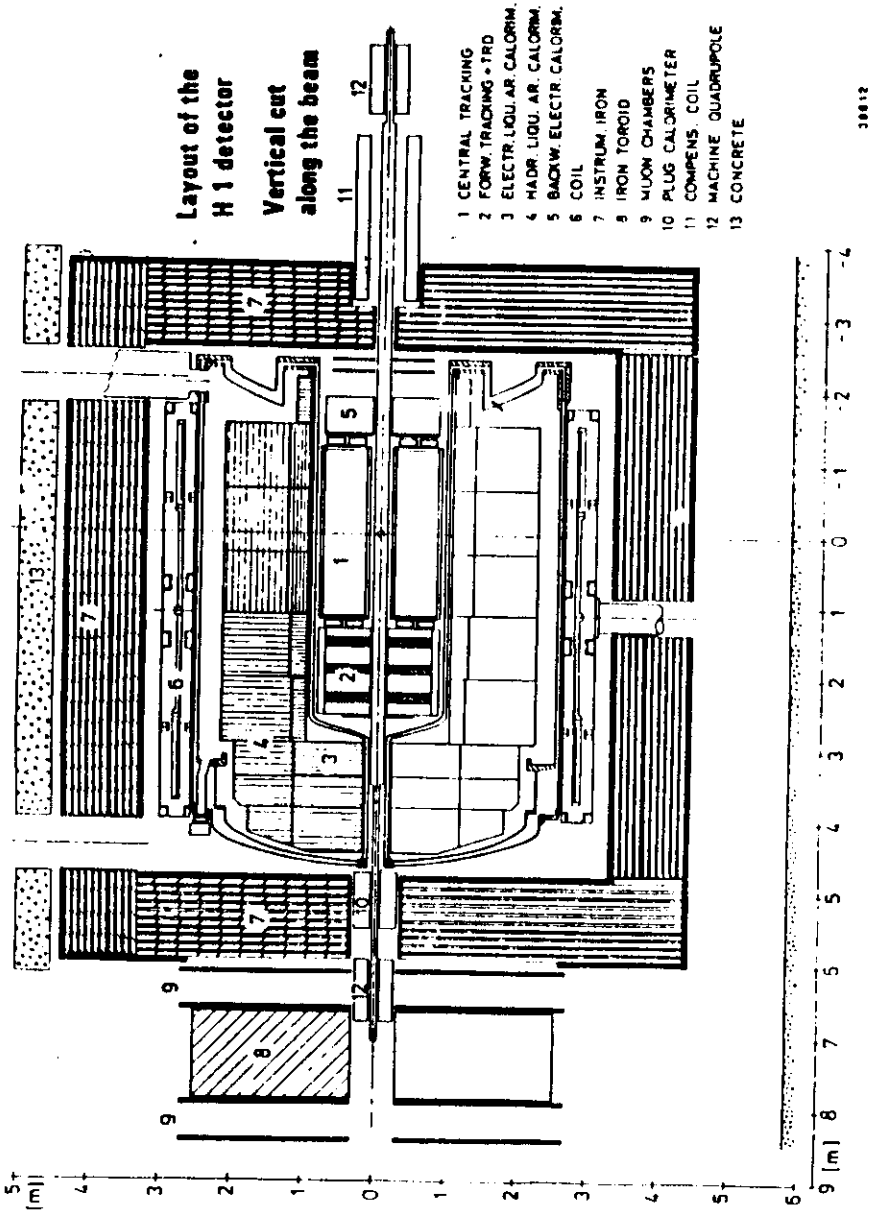

The ZEUS detector

Calorimetry

- compensating DU-scintillator calorimeter, towers 5×20 cm^2 em and 20×20 cm^2 had., 13 000 PMs
- Silicon pads at 3 - 6 X_0 (50 m^2, 50 000 pads) to enhance e-π separation
- Fe + LST backing calorimeter

Charged particle tracking

- central "vector" drift chamber
- planar drift chambers + TRD in the forward region

Field

- (small) superconducting solenoid inside calorimeter, 1.8 T
- $\sigma(p)/p = 0.002\,p$

Iron yoke

- 2000 t 7.5 cm Fe plates
- magnetized by copper coils

Muon detectors

- proportional tube chambers and LST chambers inside and around the yoke
- forward spectrometers

Proton spectrometer

- Roman pots in the out-going p direction

The luminosity will be measured in both experiments with detectors for the reaction $ep \rightarrow ep\gamma$.

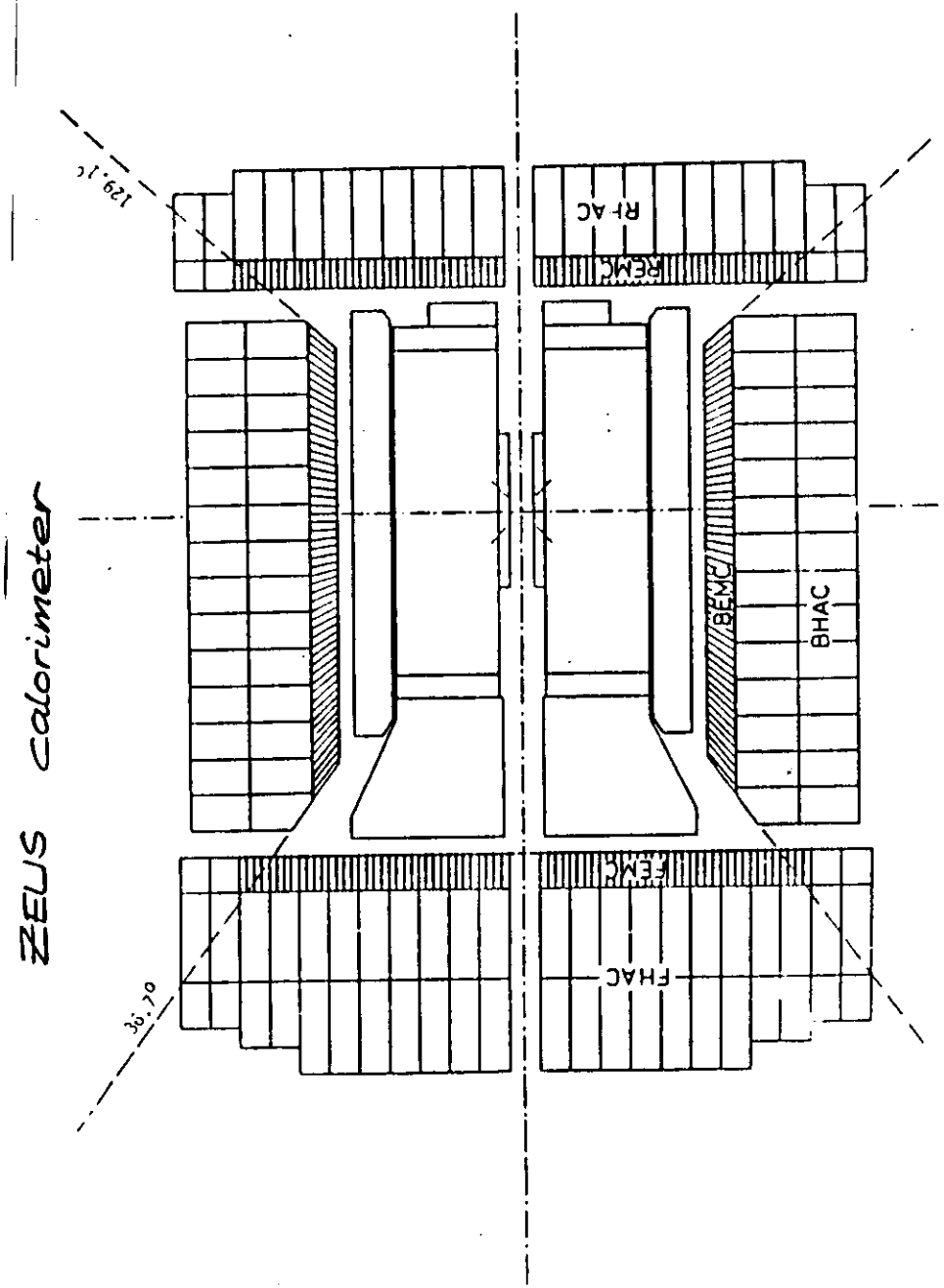

Fig. 5.3.1 The high resolution calorimeter

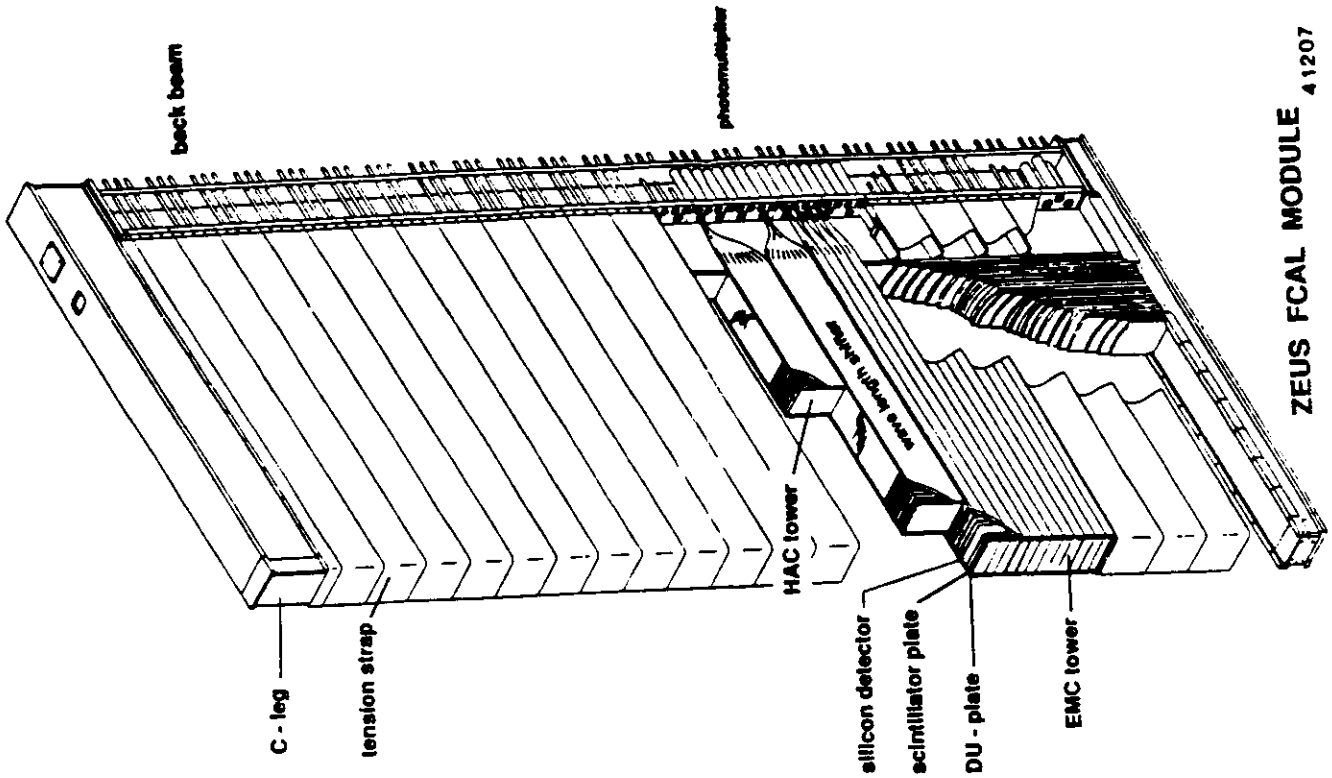

containment in the ZEUS calorimeter

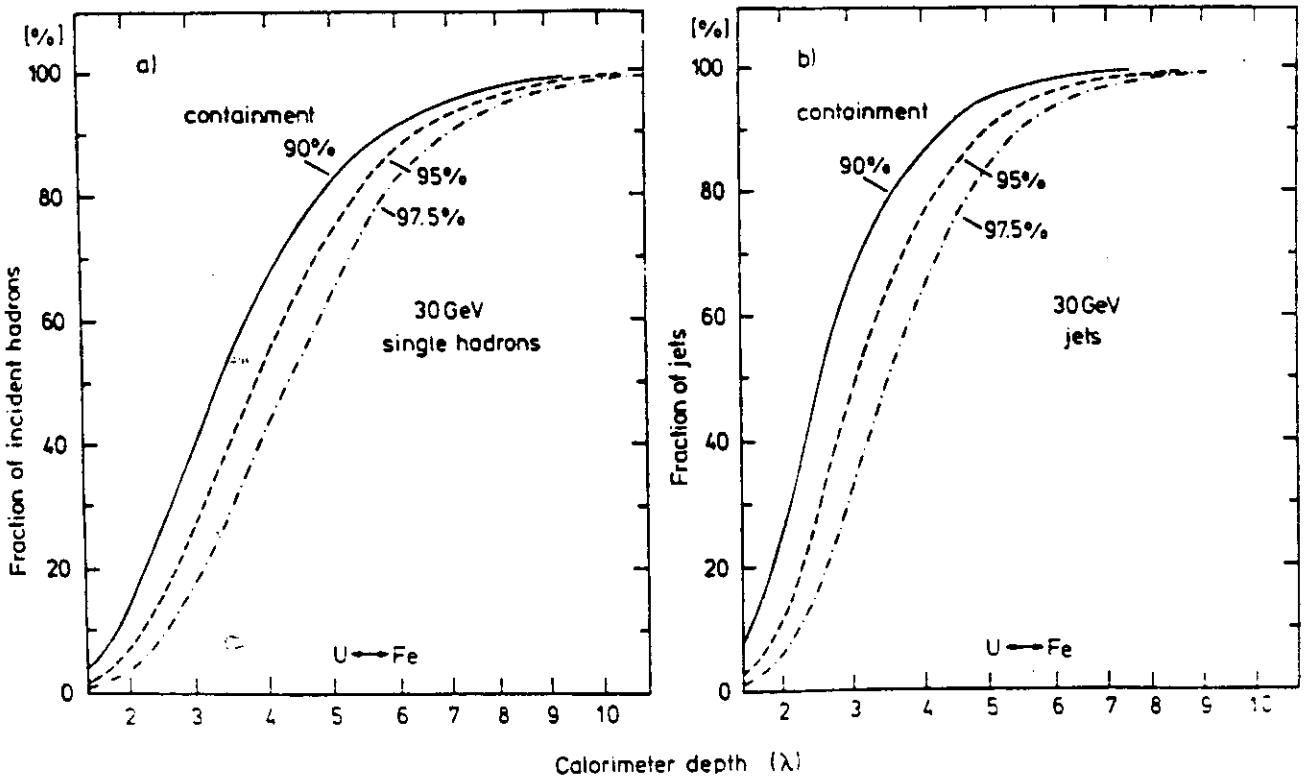

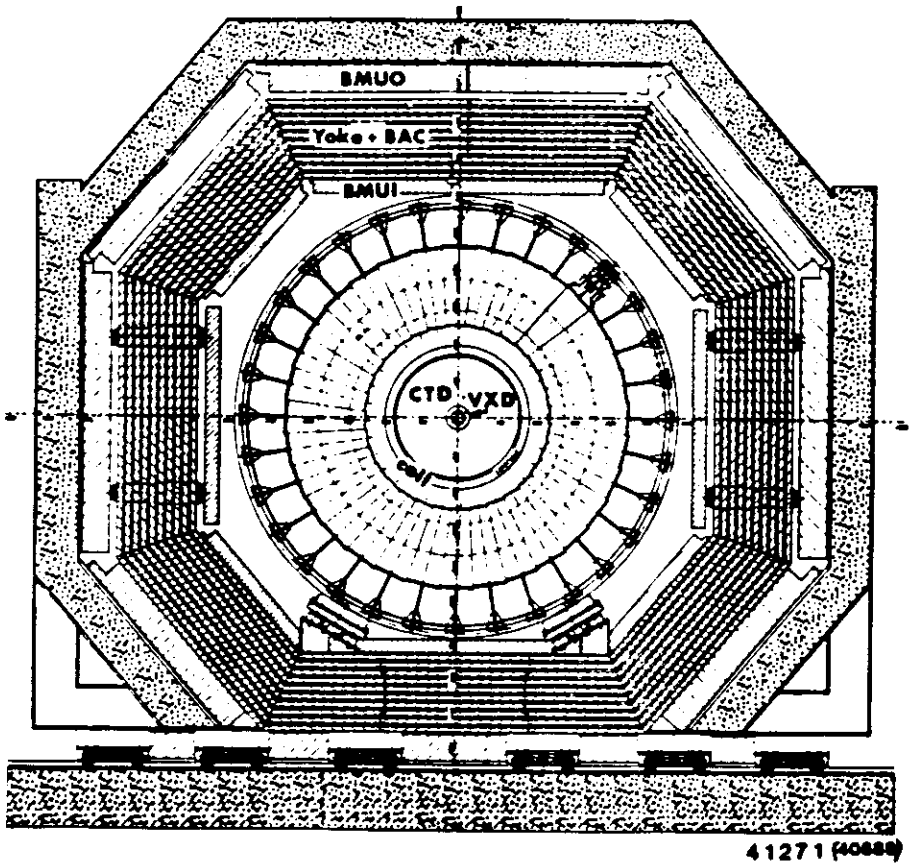

41271 (40688)

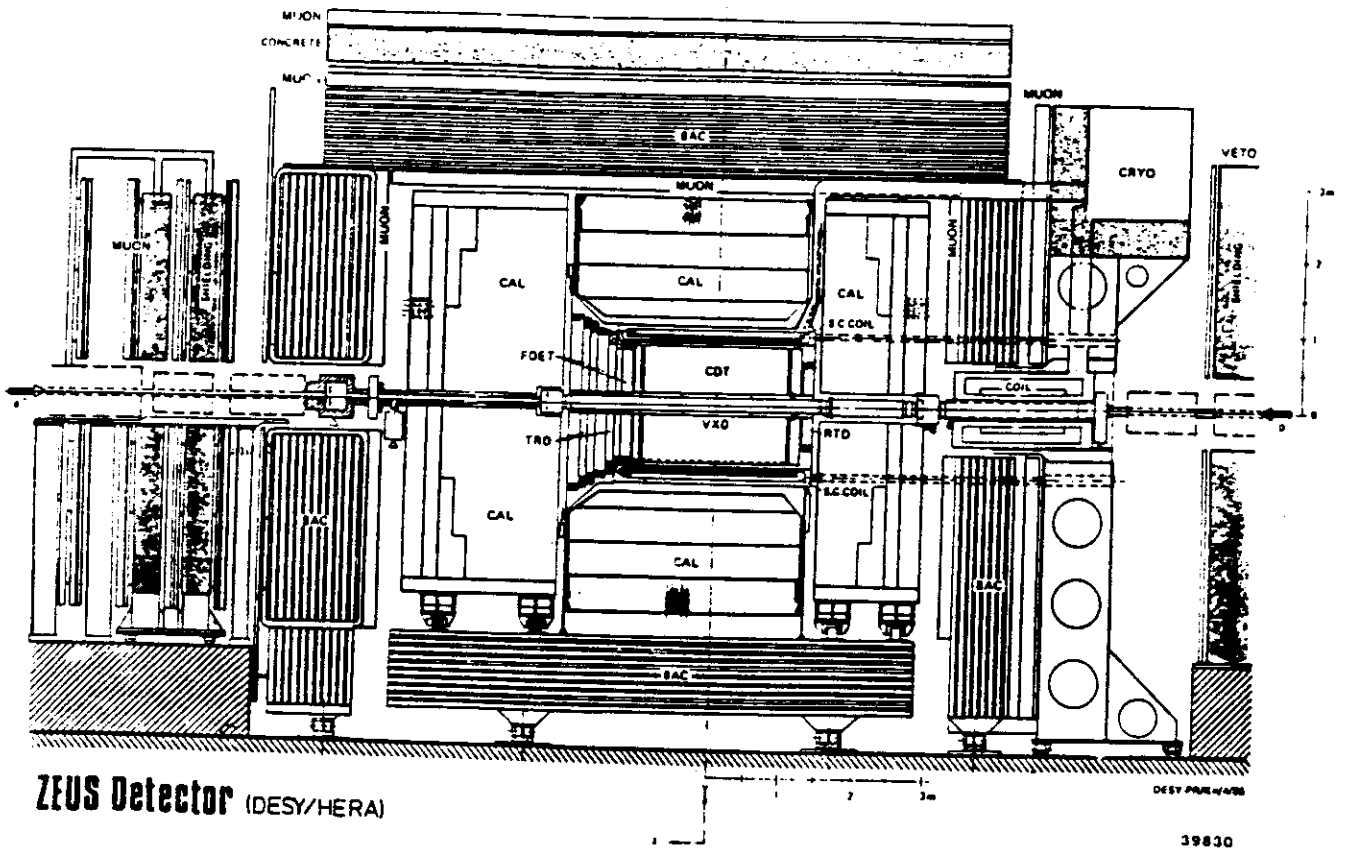

ZEUS Detector (DESY/HERA)

39830

future Machine projects

Hadron colliders

- Large Hadron Collider (LHC) in the LEP tunnel pp $\sqrt{s} = 16$ TeV
- Superconducting Super Collider (SSC) pp $\sqrt{s} = 40$ TeV
- UNK $\bar{p}p$ up to $\sqrt{s} = 6$ TeV

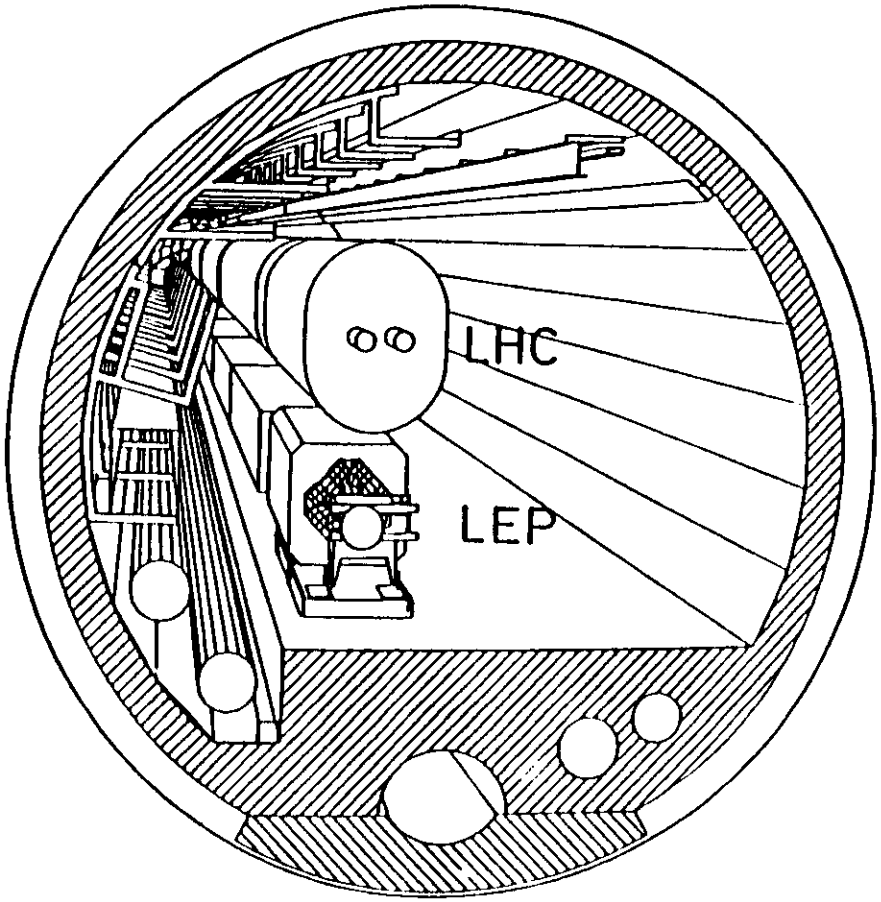

LHC in the LEP tunnel

main parameters of LHC

the LHC machine parameters are such that even higher luminosities could be reached:

- $1.8 \cdot 10^{34}\ cm^{-2}s^{-1}$ with bunch crossings every $\Delta = 15$ ns
- or even more extreme $5 \cdot 10^{34}\ cm^{-2}s^{-1}$, $\Delta = 5$ ns

Nominal LHC p-p performance

Number of bunches	3564
Bunch spacing	25 ns
Number of interaction points	4
β values at crossing points	1 m
Normalized emittance $4\pi\gamma\sigma^2/\beta$	5π μm
r.m.s. beam radius	12.11 μm
Full bunch length ($4\sigma_s$)	0.31 m
Full crossing angle (ϕ)	96 μrad
Maximum energy	8000 TeV
Circulating current	164.3 mA
Particles/bunch	2.56×10^{10}
Beam-beam tune shift	2.5×10^{-3}
Stored beam energy	116.88 MJ
Luminosity	$1.42 \times 10^{33}\ cm^{-2}s^{-1}$
Luminosity/collision	$3.55 \times 10^{25}\ cm^{-2}$
$\langle n \rangle$ at Γ = 100 mb	3.55

Experimental challenges of detectors at future hadron colliders

Two major points (among others, as examples)

① high luminosities are needed to reach the low cross-section levels expected for many processes

typical LHC parameters anticipated are

bunch spacing		25 ns
$\mathcal{L}$ ($cm^{-2}s^{-1}$)	4.1×10^{32}	$-\ 1.6\times10^{33}$
$\mathcal{L}$/bunch crossing	1×10^{25}	$-\ 3.9\times10^{25}$
⟨number of interactions per bunch crossing⟩	1	− 4

(with σ = 100 mb)

this imposes strong constraints on detector designs (radiation hardness, rate capability, triggering .....), most of the present detector types will not be adequate.

interaction rates at hadron colliders compared to e^+e^- machines

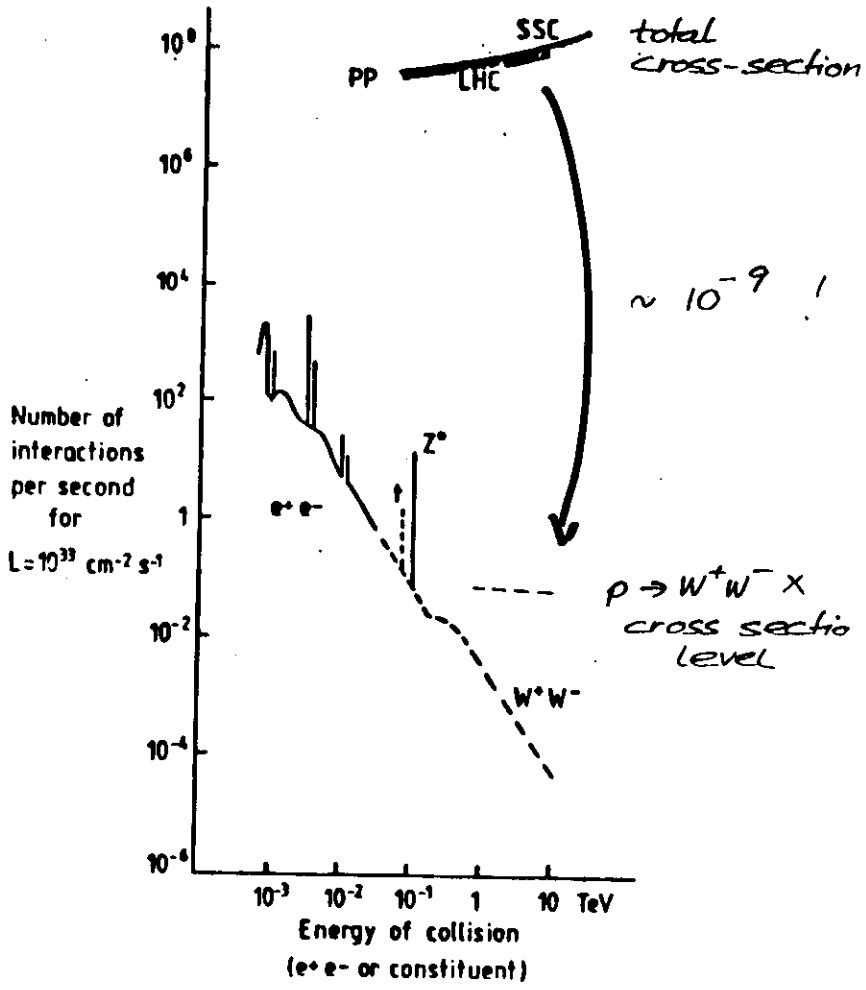

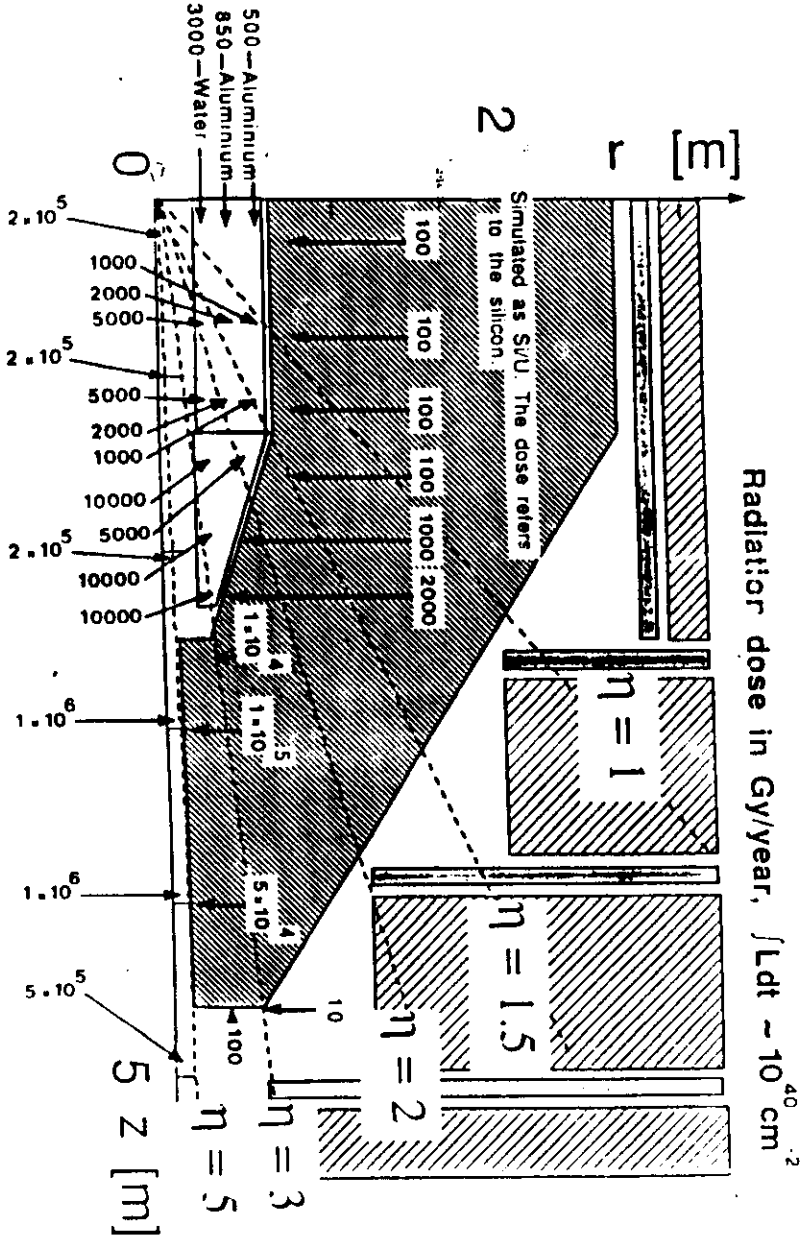

(1 Gy = 100 Rad)

(2) Calorimetry will be a crucial tool at future hadron colliders even more than now.

main requirements are

- radiation hardness
- absolute energy calibration
- rate capability
- sufficiently precise fast signals to provide first level triggering
- optimal hadron jet resolution at higher level triggers and offline physics analysis

...

Pulse shapes from the calorimeter (as an example)

[The situation is even more difficult for slow calorimeters]

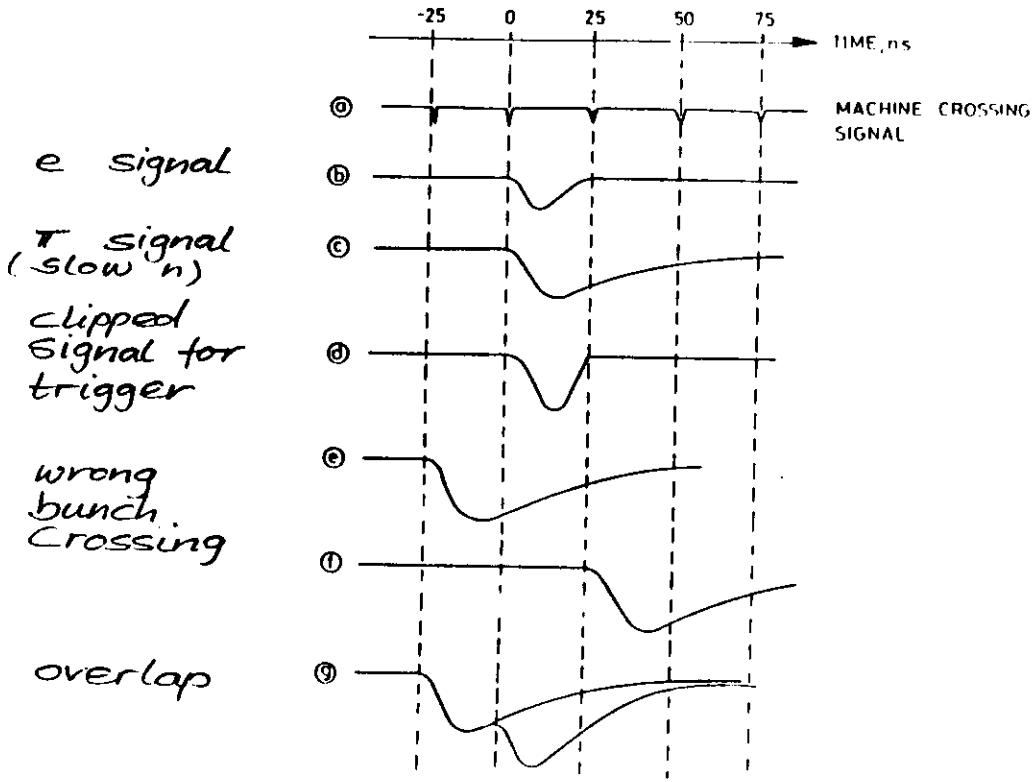

First-level fixed cluser size analog trigger for high-$\mathcal{L}$ LHC

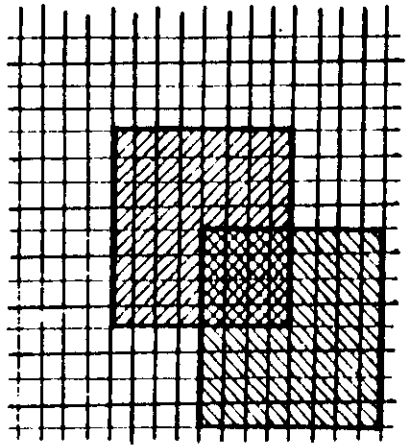

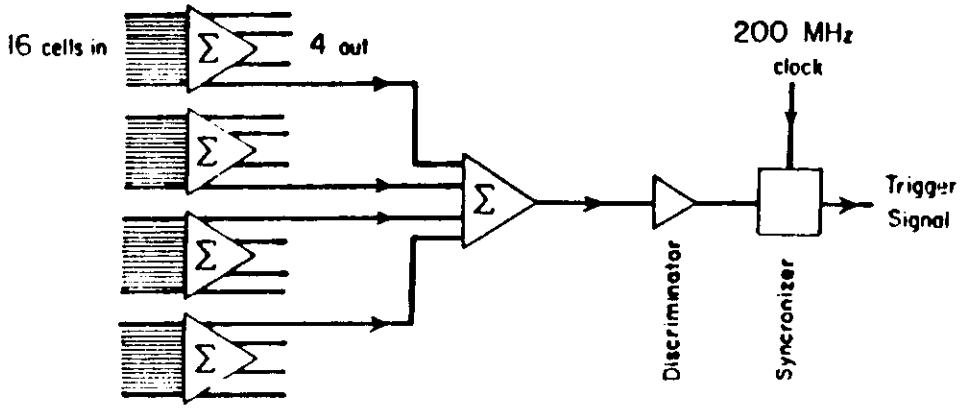

Schematic layout of a second-level trigger

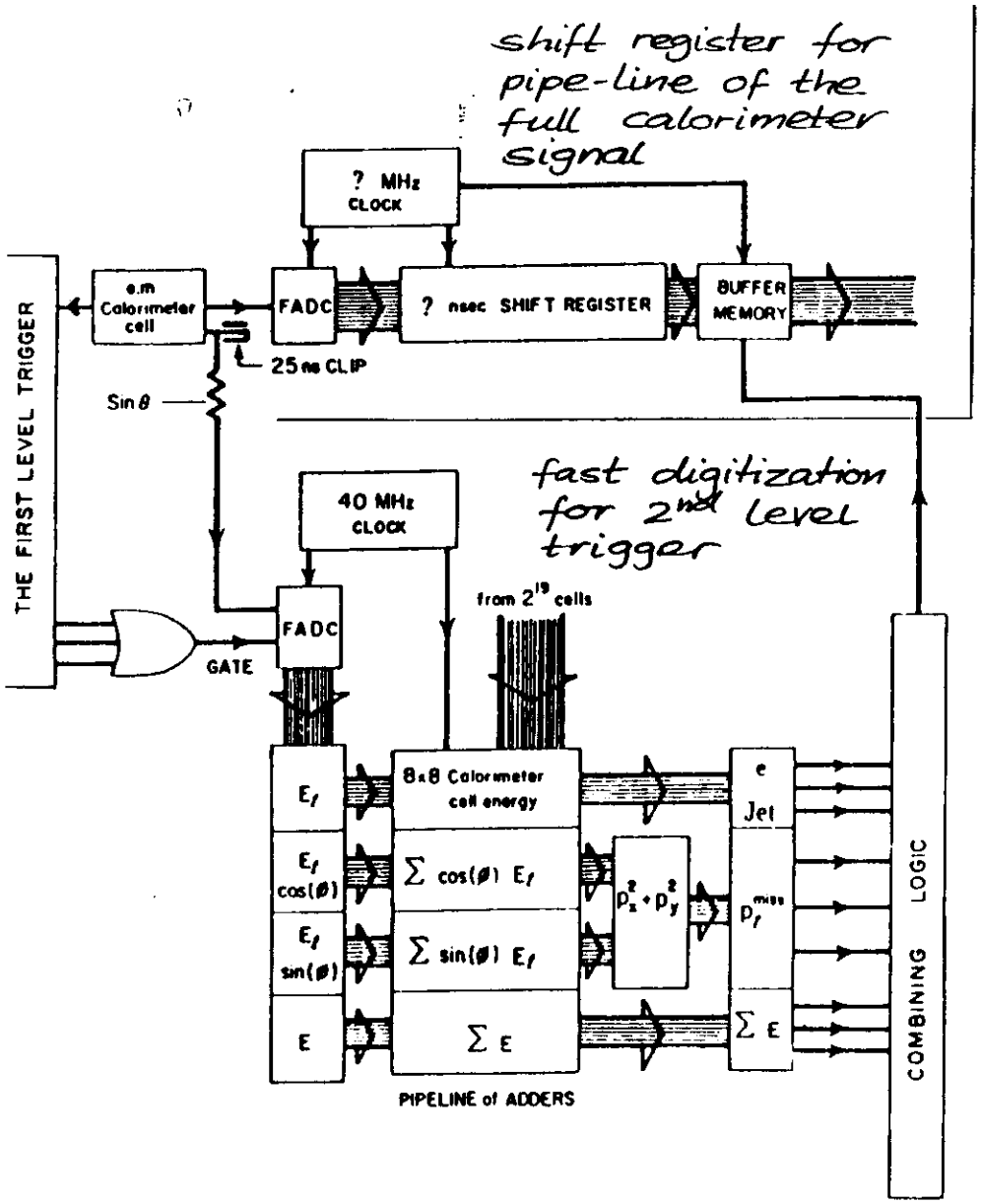

LHC 1 jet calorimeter

$\Delta\phi \times \Delta\eta = 5^\circ \times 0.1$ for $-3 < \eta < 3$

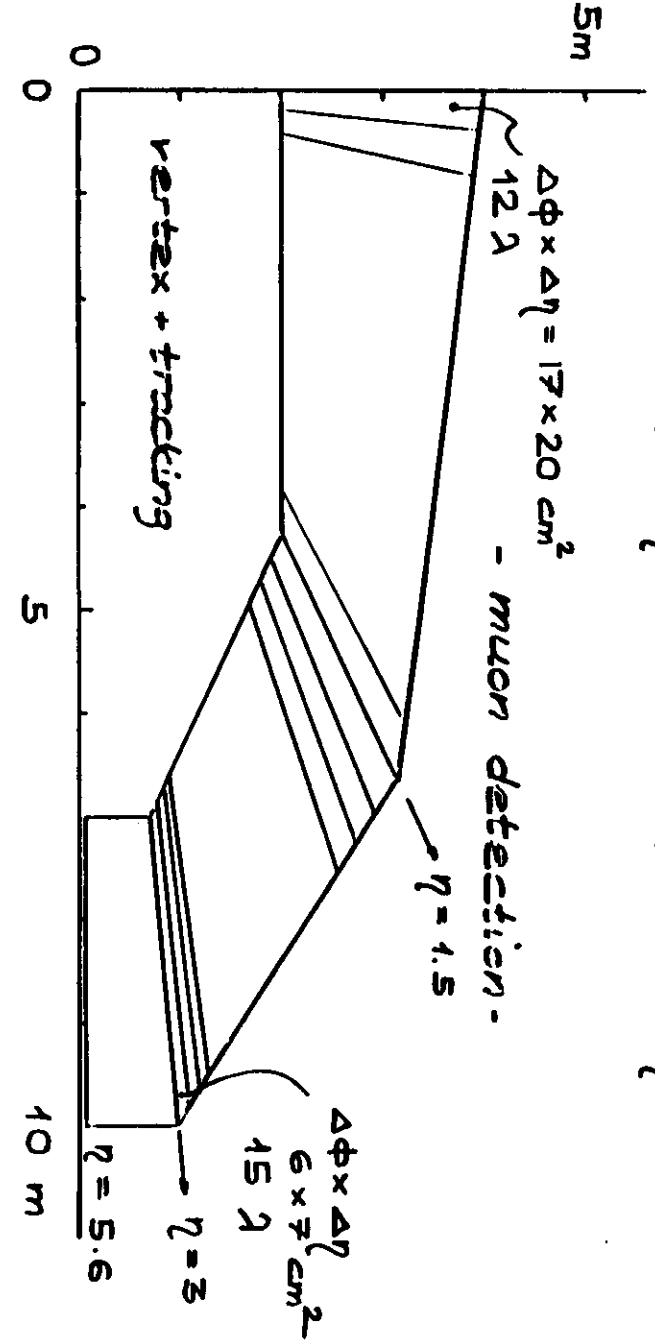

Possible lay-out for a compact non-magnetic high-$\mathcal{L}$ LHC detector to measure

- jets
- isolated electrons
- muons